

CONTENTS

Editorial	1
Climate profile of Bulgaria in the period 1988-2016 and brief climatic assessment of 2017 <i>T. Marinova, K. Malcheva, L. Bocheva, L. Trifonova</i>	2
Cold waves on the territory of Bulgaria in the period 1952-2011 <i>K. Malcheva</i>	16
Cold season tornadoes in Bulgaria – brief analysis <i>L. Bocheva and B. Markova</i>	32
On the relationship between atmospheric and soil drought in some agricultural regions of South Bulgaria <i>V. Georgieva, St. Radeva, V. Kazandviev</i>	42
Numerical study of meso-scale circulation specifics in the Sofia region under different large-scale conditions <i>E. Egova, R. Dimitrova, V. Danchovski</i>	54
The Operative System ProData – Part One: Current Stage and Recent Improvements <i>H. Chervenkov, V. Spiridonov, E. Artinyan, P. Neytchev, K. Slavov, M. Stoyanova</i>	73
Applicability of Gaussian dispersion models for accidental releases in urban environment – results of the “Michelstadt” test case in COST Action ES1006 <i>A. Petrov, J. Valente, K. Baumann-Stantzer, E. Batchvarova</i>	87
<i>In remembrance</i>	
In remembrance of George Djolov	103

ISSN 0861-0762

Bulgarian Journal of Meteorology & Hydrology

Volume 22, 2017, number 3-4

BULGARIAN JOURNAL OF Meteorology & Hydrology

Volume 22, 2017, number 3-4

ISSN 0861-0762 (Print)

ISSN 2535-0595 (Online)

AIMS AND SCOPE: The *Bulgarian Journal of Meteorology and Hydrology (BJMH)* is published by the National Institute of Meteorology and Hydrology at the Bulgarian Academy of Sciences (NIMH-BAS). The purpose of the journal is to disseminate the latest achievements in meteorology, hydrology and related scientific fields. *BJMH* publishes original research and review papers, technical and conference reports, book reviews, short research communications, chronicles and news. Papers from Bulgarian and foreign authors are equally welcome.

BJMH addresses research related to meteorology; climatology; hydrology; oceanography; numerical modeling; agricultural, urban, coastal and mountain meteorology; experimental meteorology, atmospheric boundary layer and air pollution studies; ecology, early warning systems, water resources research, etc.

EDITORIAL BOARD

BATCHVAROVA E. – Editor-in-Chief
SPASSOVA T. – Executive Editor

TOPIC EDITORS

ALEXANDROV V. (meteorology) SPIRIDONOV V. (weather forecast)
NINOV P. (hydrology) BALABANOVA S. (hydrological forecast)

ADVISORY BOARD

ANDREEV V.	Bulgaria	LEITL B.	Germany
ARBOGAST P.	France	MILOSHEV N.	Bulgaria
ATANASSOV D.	Bulgaria	NEYKOV N.	Bulgaria
BAUMANN-STENZEL K.	Austria	NIAGOLOV I.	Bulgaria
BURNAZKI E.	Bulgaria	NOVITSKY M.	Russia
DIMITROVA R.	Bulgaria	ORLANDINI S.	Italy
GEORGIEVA V.	Bulgaria	RACHEV N.	Bulgaria
GEORGIEVA E.	Bulgaria	RODRIGUES E.	Spain
GRYNING S.-E.	Denmark	SLAWINSKI C.	Poland
KARAGIOZOVA Tz.	Bulgaria	SYRAKOV D.	Bulgaria
KORTCHEVA A.	Bulgaria	TRINI CASTELLI S.	Italy

EDITORIAL OFFICE

National Institute of Meteorology and
Hydrology



66 Tsarigradsko shose blvd
1784 Sofia, BULGARIA
BJMH@meteo.bg

PUBLISHER: NIMH – BAS

PRINT HOUSE: Bolid-ins

PREPRINT: Vladimirov E.

BULGARIAN JOURNAL OF METEOROLOGY AND HYDROLOGY

ISSN 0861-0762 (print)

ISSN 2535-0595 (online)

GENERAL GUIDELINES FOR AUTHORS

Authors are encouraged to submit original research papers, short scientific communications, book reviews, etc. in the area of meteorology, hydrology and related fields.

Language: Papers are accepted in English, American spelling for issues 1 to 4. For issue 5, published in Bulgarian language, all papers should have titles, abstracts, figure captions and table titles in both Bulgarian and English.

Page size and margins: Page size has to be 16.5 x 23.5 cm. All materials should fit within the following margins: 2.00 cm from the top and bottom, 1.5 cm from the left and right.

Structure: Manuscript should be structured as follows: title; authors names; authors affiliations; abstract; keywords; main text; acknowledgements; appendices; references.

Title: Title should be in 14pt Times New Roman (TNR) font, bold, centered on the page, in sentence case style.

Authors: Full names of all the authors should be in 11pt TNR, bold and centered on the page. The e-mail address of the corresponding author should be given in the footnote.

Affiliations: Affiliations and postal addresses should be in 11pt TNR, italic, centered on the page.

Abstracts and Keywords: Abstracts should not exceed 500 words. Keywords should be maximum 5. Both should be written in 10pt TNR, justified, with spacing 18pt before and 6pt after, with 1 cm left and right indent.

Body text: Text should be in 11pt TNR, justified, with single line space. Main sections should be numbered, written in 11pt TNR bold capital letters, left aligned, with spacing 18pt before and 6pt after. Sub-sections should be numbered correspondingly, in 11pt TNR bold, sentence case style, left aligned, with spacing 18pt before and 6pt after. First paragraph of the text after section's title is with 0 cm left indent, while the first line of the following paragraphs starts with 0.5 cm left indent.

Units: Authors should follow SI units. Units are not italicized.

Figures/Images: Figures should be placed in the body text as close as possible to the reference. They should be numbered, with captions in 10pt TNR, placed below them and centered. Color or black figures should be designed in an appropriate format according to the page size and margins, so that to be well visible when printed. Raster images should be not less 300 dpi in the natural size.

Tables: Tables should be placed in the body text as close as possible to the reference. They should be numbered separately from the figures, with captions in 10pt TNR, placed above them and left aligned. Tables should not be too bulky.

Citations and references: Citations within the text should be placed in parentheses with the author's last name and year separated by a comma. The "et al." construction should be used for citations with three or more authors. Ex: (Petrov, 2016), (Petrov&Ivanov, 2016), (Ivanova et al., 2016). If the authors' names are included in the sentence, only the year should be placed in parentheses. Ex: ...as stated in Petrov (2016). Multiple references should be listed alphabetically and separated by semicolons. Ex: (Agov, 2000; Botev, 2016; Cacic et al., 1999). References should be in 10pt TNR, left hanging by 0.5 cm. They should be completed in the following style: (a) for journal articles - author(s), year in parentheses, paper title, journal name, volume, inclusive page numbers; (b) for books - author(s), year in parentheses, title, publisher, number of pages; (c) for contribution in a book: author(s), year in parentheses, title of the contribution, In: editor(s), title, publisher, page numbers.

MS Word template of a paper is available at http://meteorology.meteo.bg/global-change/for_authors.html

Submission: Authors are encouraged to submit manuscripts as attachments to the e-mail address of the journal BJMH@meteo.bg.

Copyright form: The Copyright form, available at http://meteorology.meteo.bg/global-change/for_authors.html, should be filled, signed and sent back to the Editor-in-Chief together with the final version of the manuscript.



EDITORIAL

Dear readers,

We have the pleasure to offer you issues 3-4 of volume 22 (2017) of the Bulgarian Journal of Meteorology and Hydrology (BJMH).

Issues 3-4 of volume 22 consist of seven original scientific papers. The first four of them consider different aspects and manifestations of climate peculiarities in Bulgaria (climate profile of the country for the last almost 30-years, cold waves for 60-years period, cold season tornadoes and atmospheric and soil droughts). The fifth one presents a numerical study of airflow forecast over large urban area (Sofia) in complex orography. The sixth paper describes the created at the National Institute of Meteorology and Hydrology operative system ProData which combines in methodologically consistent way all available on hourly basis meteorological, auxiliary and satellite data and produces high-quality gridded time-series of the most significant meteorological variables. The seventh one focuses on the comparison and applicability of several Gaussian dispersion models for accidental releases in urban environment. At last, we express our deep respect and honor for Professor George Djolov, who left us in 2017 at the age of 77.

BJMH publishes online and in print original research and review papers by Bulgarian and foreign authors. You can find all published issues since 2014 on the website of our journal at <http://meteorology.meteo.bg/global-change/index.html>.

Ekaterina Batchvarova (Chief Editor)
Tatiana Spassova (Executive Editor)



Climate profile of Bulgaria in the period 1988-2016 and brief climatic assessment of 2017

Tania Marinova*, Krastina Malcheva, Lilia Bocheva, Lyubov Trifonova

*National Institute of Meteorology and Hydrology - BAS,
Tsarigradsko shose 66, 1784 Sofia, Bulgaria*

Abstract: With regard to national and international obligations of the National Institute of Meteorology and Hydrology at the Bulgarian Academy of Sciences (NIMH-BAS), climate profile of Bulgaria in the period 1988-2016 as well as brief climatic assessment of 2017 are prepared on the basis of monthly and annual data, provided by the Meteorological database of the NIMH-BAS, for 115 meteorological stations on the territory of Bulgaria and the obtained results are presented.

Keywords: Bulgaria, climate profile, climatic assessment of 2017

1. INTRODUCTION

In accordance with the United Nations Framework Convention on Climate Change, Member States of the Convention are required to provide national communications on a regular basis with information on the process of implementation of the Convention. As a part of the Seventh National Communication on Climate Change of Bulgaria and in view of the requirements of the Ministry of Environment and Water, climate profile of Bulgaria in the period 1988-2016 is prepared at the National Institute of Meteorology and Hydrology at the Bulgarian Academy of Sciences (NIMH-BAS). Also a brief climatic assessment of 2017 is made as a contribution of the NIMH-BAS to the publication „Annual Bulletin on the Climate in WMO Region VI – Europe and Middle East”. The results of the corresponding investigations and more detailed climatic background (as compared with the previous National Communications) are presented in the paper.

* Tania.Marinova@meteo.bg

2. DATA

Monthly and annual data concerning air temperature, precipitation, snow cover and number of days with thunderstorms and hail precipitation, provided by the Meteorological database of the NIMH-BAS, for 115 meteorological stations on the territory of Bulgaria in the period 1961-2017 are used in the study. Data processing is performed by program procedures.

3. CLIMATE PROFILE OF BULGARIA IN THE PERIOD 1988-2016

3.1. Climatic background

Bulgaria has unusually various climate conditions due to the influence of the strongly different continental and Mediterranean climates and diverse landscape. The climate has four distinct seasons and varies with altitude and location. According to the accepted in the NIMH-BAS climate classification, the territory of Bulgaria is divided into two climatic areas (European-Continental and Continental-Mediterranean), four climatic subareas (Moderate-Continental, Transition-Continental, South-Bulgarian and Black-Sea), and twenty-five climatic regions, which include the corresponding coastal and mountainous zones.

Clear expressed seasonality in the intra-annual course of insolation (relevant to the intra-annual alteration of sunshine duration) determines the levels of heat balance and thence the affiliation of the country to the regions of the continent with warmer climate. Because of the distance from the ocean, the Atlantic air masses appear chilled during the cold half year and overheated in the warm half year. Comparatively large and compact area of the Balkan Peninsula advantages the formation of local continental air masses, which during the summer become almost like tropical air, and during the winter – like cold continental air. The short distance to Mediterranean Sea enhances the climate differences between Northern and Southern Bulgaria. The immediate proximity to the Black Sea reinforces some characteristics of atmospheric circulation, mainly in the cold half year, and results in formation of specific sea climate in coastal area (20-40 km). High mountains serve as barriers for the air masses transfer, which predetermines the distribution of precipitation. The Mediterranean cyclones are most frequently observed from November to May/June; they have significant influence over the weather and climate in Southern Bulgaria. The Atlantic cyclones rarely reach the central areas of the Balkan Peninsula but they have influence over the weather and climate in Northern Bulgaria; their frequency is highest from February until June (with a maximum in May). The north-western anticyclones appear most frequently from the middle of spring until the middle of summer and usually cause cold spells in late spring and early summer. The western anticyclones cause warm spells in the winter and cold

spells in the summer. The south-western anticyclones usually bring tropical air masses and the highest temperatures and droughty spells in the period July-September. The arctic anticyclones (moving from north/north-east towards southern continental areas) bring prolonged snowfalls and snowstorms in February and March. The process of formation of local anticyclones in the ridges of north-eastern ones causes the lowest temperatures in Bulgaria.

The sunshine duration reaches the highest average annual value in the southern border part of Struma Valley – 2800 hours. Along the Black Sea coast, in the Thracian Lowland, and Mesta Valley, the annual value of sunshine duration is 2200-2300 hours; in the Danube Plain – 2100 hours. Due to the higher cloudiness and naturally narrowed horizon in the mountains, the sunshine duration decreases to 1900 hours per year. For the non-mountainous parts of Bulgaria, the average annual values of the total solar radiation vary from 4000 MJ/m² to 4700 MJ/m² (up to 5000 MJ/m² in the southern parts of the country). In December as well as in January, the total solar radiation is 3-4% of its annual values. In the summer months (June, July and August) the total solar radiation is about 40-45% of the annual values.

During the winter, the average temperature in January is negative in the Danube Plain (from -2.3°C to about -1°C) and in the higher valleys of the West Central Bulgaria (below minus 2°C), and positive in the Thracian Lowland (0-1.5°C) as well as in the southern parts of Black Sea region (above 3°C). In the mountains, the temperature in January drops with altitude with 0.3-0.4°C per 100 m. The spatial distribution of average seasonal air temperature in the winter is shown on Fig. 1 (left panel).

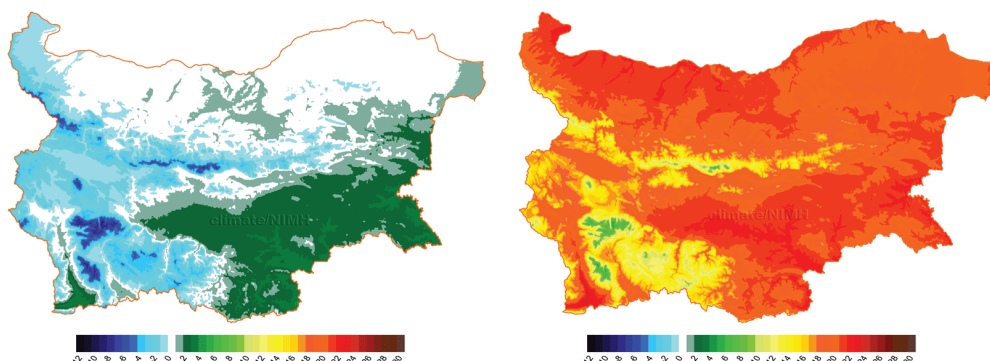


Fig. 1. Air temperature (°C) in the winter (left) and summer (right) during the current climate 1961-1990

In the spring, spells of warm and cold weather succeed each other because of the exchange of air masses from different origin. Foehn winds are often observed in Northern Bulgaria. Thermal differences between northern and southern parts of the country almost disappear except the southernmost parts. The average temperature in April is 10-13°C (greater than 13°C in the southern regions and lower than 10°C in the

valleys). In the mountains, the temperature decreases with the elevation with 0.6-0.7°C per 100 m. Conditions for the onset of spring frost appear during the cold snaps, when the minimum temperatures even in the lowlands fall below 0°C.

During the summer, thermal conditions are dominated by the transformed Atlantic air masses with Azorean origin in the circumstances of intense solar radiation. The temperatures to the north and south of the Balkan Mountains are almost equal. The average temperature for July is 21-24°C in the Danube Plain, and 22-24°C in the Thracian Lowland. The average monthly temperature is around or less than 20°C in the high valleys of the West Central Bulgaria, 22°C in the Black Sea region and above 23°C in the southern regions (24-25°C along the Struma Valley). A marked decrease in the temperature with altitude is observed in the mountains (0.7°C/100 m). The spatial distribution of average seasonal air temperature in the summer is shown on Fig. 1 (right panel).

In the autumn, the transfer of cold air masses from north-west and north-east is registered more frequently. The barrier effect of the Balkan Mountains and southern mountains (Rila-Rhodope region) causes some differences in the climate between northern and southern parts of the country. The values of average monthly temperature in October are lowest in the Danube Plain (11-12°C) as well as in the high valleys of West Central Bulgaria (lower than 11°C). The autumn is warmer in the Thracian Lowland (above 12°C), on the Black Sea coast and in the southernmost regions (13-14°C). In the higher parts of the country the differences are not so obvious in comparison with the spring and summer and the temperature decreases with 0.5°C per 100 m.

Absolute maximum temperatures in the non-mountainous parts of Bulgaria are higher than 40°C (35°C for the Black Sea coast); the set up temperature record is 45.2°C in Sadovo, registered in 1916.

Absolute minimum temperatures range from -20°C to -30°C in the lowlands and from -15°C to -20°C in the coastal zone. The lowest air temperatures aren't measured in the mountains but in the plains. The set up record for absolute minimum air temperature is -38.3°C (Tran, 1947).

The annual course of precipitation is closely related with the peculiarities of atmospheric circulation over the country and strongly differs in the mentioned above climatic areas. Average annual values of precipitation alter from 450-500 mm in the Black Sea region and some parts of the Danube Plain and the Thracian Lowland to 900-1100 mm in the mountainous regions (Fig. 2). In the mountains, the annual amount of precipitation increases linearly with altitude up to 2000 m.

During the winter, in the Moderate-Continental climatic subarea, the precipitation amount is smallest – 18-20% of the annual sum (100-110 mm in the lowland parts and 190-200 mm in the highest parts of the mountains). In the Continental-Mediterranean climatic area, the winter precipitation amount is highest: 150-300 mm. In the spring, the rainfall in the Moderate-Continental subarea increases to 25-27% of the annual amount. More frequently are observed rains of convective type. In the regions with Continental-

The prevailing winds are north-west/west and north-east (in some southern parts of the country). Several regions could be outlined with relation to the average annual wind speed. The first one includes lowland parts, where the average wind speed does not exceed 2 m/s (with maximum in February/March and minimum in September/October). The second region comprises the north-eastern parts of the country and the unsheltered low mountainous regions (up to 1000 m), where the average annual wind speed is 2-4 m/s (with maximum in February-March and minimum in August-September). The third region consists of unsheltered and deforested mountainous regions over 1000 m, where the wind speed exceeds vastly 4 m/s, with an annual maximum in February and minimum in August. Among the local winds, the most characteristic are the breeze (3-5 m/s), mountain-valley winds (3-6 m/s), katabatic winds (Sliven's wind with velocity more than 15 m/s) and foehn winds (10-20 m/s).

3.2. Main climatic characteristics in the period 1988-2016

Since the middle of 1980s, the tendency of the average annual air temperature in Bulgaria is towards warmer climate (Fig. 3). In the period 1988-2016, the average annual air temperature for the lower part of the country (for areas up to 800 m altitude) is increased on average with 0.8°C relative to the climatic normal for the reference period 1961-1990 and ranges between 10.6°C and 13.0°C. The tendency in the long-term variations of the average annual air temperature remains positive. In fact, the annual temperature anomalies are positive from 1997 to now. Moreover, they are equal or exceed 1°C for the all years after 2007 (except 2011). Since the beginning of 21st century, 2015 appears as the warmest year (1.6°C above the climatic normal in the areas up to 800 m altitude); in Northern Bulgaria – 1.8°C above the normal (Fig. 4). Warmest months are November, July and January, with deviations from the monthly normal +3.2°C, +2.7°C and +2.6°C, correspondingly.

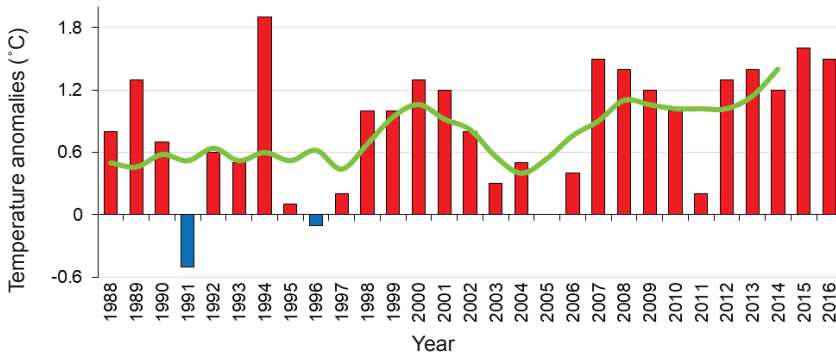


Fig. 3. Anomalies of annual temperature in areas up to 800 m altitude for the period 1988-2016 relative to the period 1961-1990

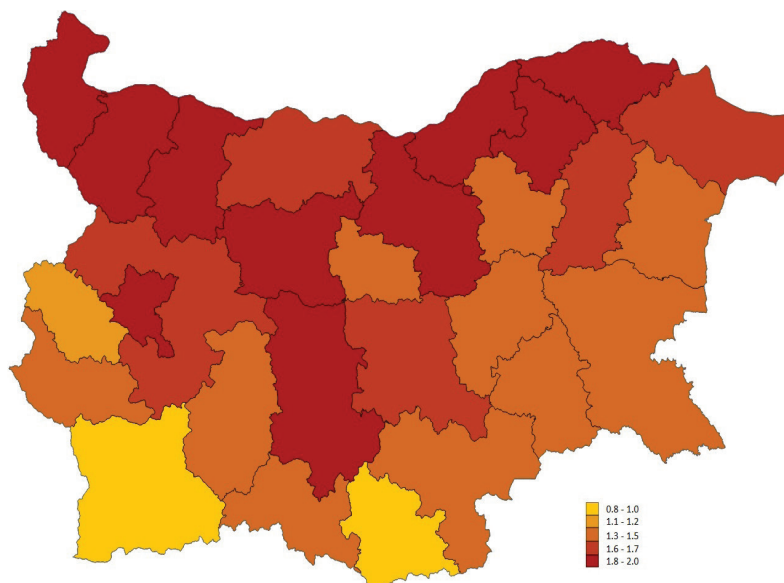


Fig. 4. Deviations of annual average air temperature (°C) in areas up to 800 m altitude for 2015 relative to the climatic normal for the period 1961-1990 (averaging by districts)

Climate in Bulgaria became not only warmer but also drier at the end of the 20th century. During the last decade however, precipitation totals have increased (Fig. 5) but heavy rainfall events caused severe floods damaging various socioeconomic sectors. 2014 is the rainiest year in the whole period 1988-2016 (Fig. 6). The average annual precipitation amount is 1013 mm for the areas up to 800 m altitude that is more than the previous reached maximum of 924 mm in 2005. Most rainy months are September (902% of the monthly normal in Asenovgrad), October (487% in Avren, Varna district) and December (370% in Silistra). In 2014, in the period April-October, have been measured extreme 24-hour rainfall amounts. The largest value of 245 mm (Burgas district) ranks 2014 among the seven years in the period 1988-2014 with extreme 24-hour precipitation above 220 mm.

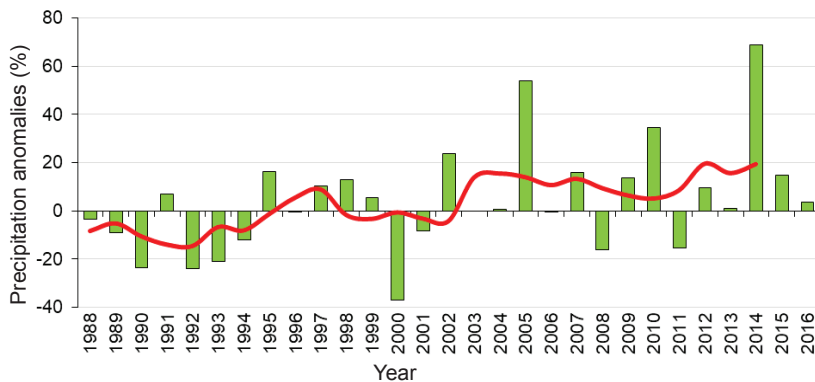


Fig. 5. Anomalies of annual precipitation in areas up to 800 m altitude for the period 1988-2016 relative to the period 1961-1990

During the period 1988-2016 the decreasing trend of the average maximum snow cover depth in the upland areas (800-1800 m altitude) is retained, as in 2014 was reached the lowest value of this indicator – 24 cm. Excluding 2012, the snow cover persistence decreased considerably in the last years (Fig. 7).

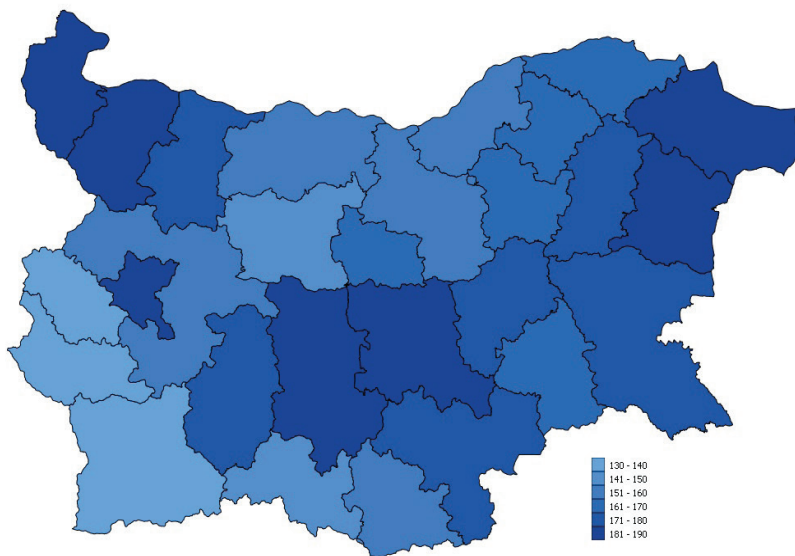


Fig. 6. Deviations of annual precipitation (%) in areas up to 800 m altitude for 2014 relative to the climatic normal for the period 1961-1990 (averaging by districts)

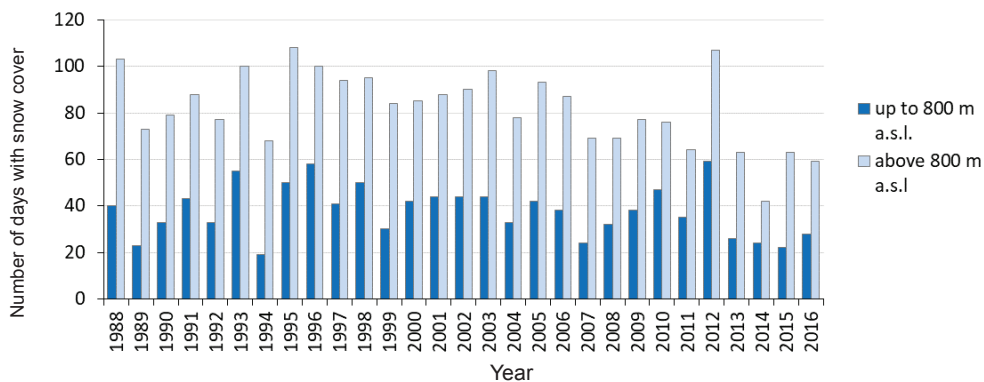


Fig. 7. Snow cover persistence in the period 1988-2016

3.3. Climate change and extreme events

Weather and climate extremes have increased during the last decades, as shown on Fig. 8. In line with the tendency of global warming, one of the basic indicators of winter severity – number of ice days – has diminished with over 25% in all climatic subareas in the period 1971-2010, compared to the period 1931-1970 (Fig. 8a). Since the middle of 1990s, recurrent disastrous situations, mainly related to the development of powerful convective storms, brought to economic losses and human casualties. Especially, in 2014 dangerous weather phenomena of convective origin such as intense heavy rains, thunderstorms, and heavy hails (often accompanied by strong wind gusts) caused human victims and serious damage to agricultural production, infrastructure, and buildings in many areas of the country.

During the period 1991-2014 the intra-annual distribution of number of days with convective precipitation ≥ 60 mm/24h, registered at least in 4 districts shows the increasing trend (Fig.8b). Shift of the maximum in the distribution of heavy rain days connected with thunderstorms during the periods 1991-2002 and 2003-2014 is observed. While during the first period the greatest number of heavy rain days is observed in July, in the second period such type of precipitation more frequently occurred in September and October, where their increase is about 30-100%. Furthermore, increasing in frequency of the heavy rain episodes in all months from June to October (except July), as well as in the cold season months December and March, is observed in the period 2003-2014.

During the period 1991-2014, the annual number of days with convective precipitation ≥ 60 mm/24h has shown a positive tendency in almost all regions of the country. The increasing in the number of convective heavy rain days is statistically significant for North East (NE), South Central (SC) and South West (SW) Bulgaria (Fig. 8c).

In the period 1988-2016, about 75% of all hail events occur during the period April-July (with maximum in May and June), more frequent in western and central south

parts of the country, nearby to the mountains because of the favourable orographic conditions for development of convective processes. The largest number of days with hail precipitation is registered in 2014, followed by 2005. In comparison with the period 1961-1990, the number of days with wide-spread hail precipitation (observed in at least 4 districts) also has increased, reaching maximum value in 2014 (Fig. 8d).

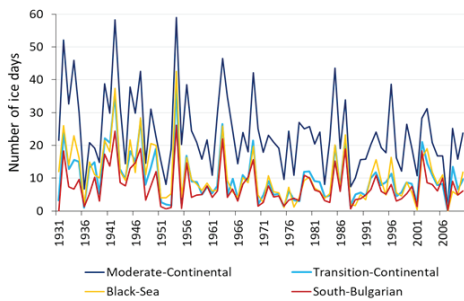


Fig. 8a. Number of ice days (daily $T_{max} < 0^{\circ}C$) during the cold season (November-March)

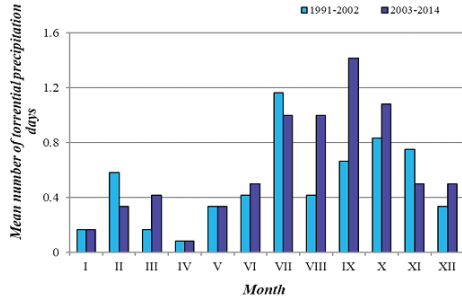


Fig. 8b. Intra-annual distribution of torrential precipitation days

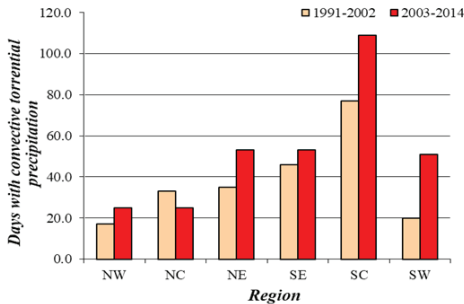


Fig. 8c. Distribution of days with convective heavy rainfall by regions

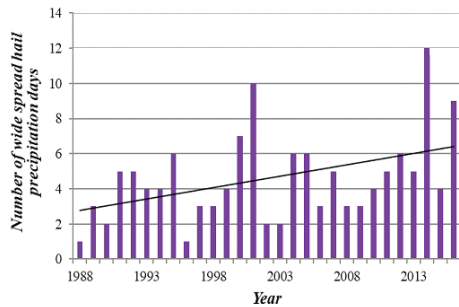


Fig. 8d. Number of wide-spread hail precipitation days

Fig. 8. Changes in the rate of extreme weather events

4. BRIEF CLIMATIC ASSESSMENT OF 2017

In 2017 the mean annual air temperature for the lower parts of Bulgaria (up to 800 m altitude) increased on average with $1.2^{\circ}C$ relative to the climatic normal that arranges the year among the hottest since 1980. According to the deviation from the monthly normal, the warmest month was March ($+1.7^{\circ}C$ to $+5.6^{\circ}C$), followed by December ($+1.3^{\circ}C$ to $+4.6^{\circ}C$) and August ($+0.5^{\circ}C$ to $+3.9^{\circ}C$). The coldest month was January with deviations from $-6.1^{\circ}C$ to $-2.1^{\circ}C$.

Winter season was $-1.2^{\circ}C$ colder than normal, after cold December 2016 (with deviations down to $-2.7^{\circ}C$ in North Bulgaria and $-3.9^{\circ}C$ in South Bulgaria) and 7-day cold spell in January (06-13.01.2017). Minimum temperatures in January 2017 in some

parts of West Bulgaria were close to the absolute minimum possible at least once in 50 years (-26°C in Kyustendil and -27°C in Pernik). The extremely cold weather in January 2017 in Bulgaria was caused by the advection of a pool of cold air from northern Russia to the southwest at the first decade.

Low temperatures come after the heavy snowfall developed over the relatively warm Mediterranean Sea when a compact low pressure system forms in the region. Snow cover held over whole month in many regions. This development was linked to the amplification of a ridge over the north-eastern Atlantic and of a trough downstream. Later the trough formed a cut-off low over south-eastern Europe and prolonged cold spell in Bulgaria till 12-13 January (Fig. 9).

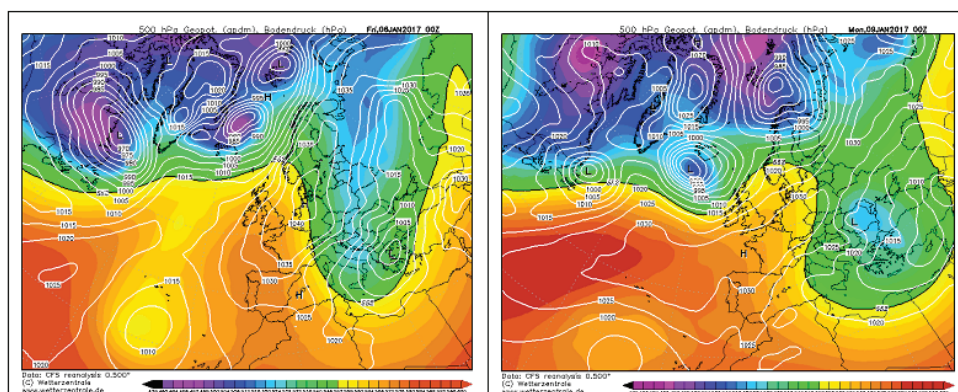


Fig. 9. Sea-level pressure (white contours), height of the 500 hPa surface (colors) on 6 and 9 January 2017. Source: NOAA/NCEP via <http://www.wetterzentrale.de>

Spring was $+1.1^{\circ}\text{C}$ warmer than normal. After warm March, the season continued with slightly negative anomaly in April (-2.5°C to $+1.3^{\circ}\text{C}$) and positive in May (-1°C to $+1.5^{\circ}\text{C}$).

Summer anomalies reached $+4.6^{\circ}\text{C}$ in North Bulgaria in June and $+3.9^{\circ}\text{C}$ in South Bulgaria in August during two severe heat waves: 1) from 20.06 to 2.07.2017 with maximum temperature up to 42.5°C in Sandanski and 43.6°C in Ruse; 2) in the period 30.07-13.08.2017 in South Bulgaria (40.8°C in Sandanski), and from 30.07 to 07.08.2017 in North Bulgaria (40°C in Vidin).

Prolonged heat waves (up to 13 days) are caused by combinations of different synoptic situations. Mainly the heat waves persist from 3-4 day during SW (South-West) advection up to 5-6 days during radiative overheating. During the first part of the period 20.06-02.07.2017 the active frontal zone in the upper air is moved to the north. Positive radiation balance during sunny days in a low-gradient anticyclone field causes radiative overheating and heat wave for 5-6 days. The temperature on 850 hPa over whole Southern Europe during this period increased up to $20-22^{\circ}\text{C}$ (Fig. 10). Gradually the atmospheric circulation was transformed and during the second part of the period

a deep trough over Western Europe in the upper air and low pressure over Northern Europe caused prolonged advection of warm air from SW. The air temperature on 850 hPa additionally is increased up to 24-26°C.

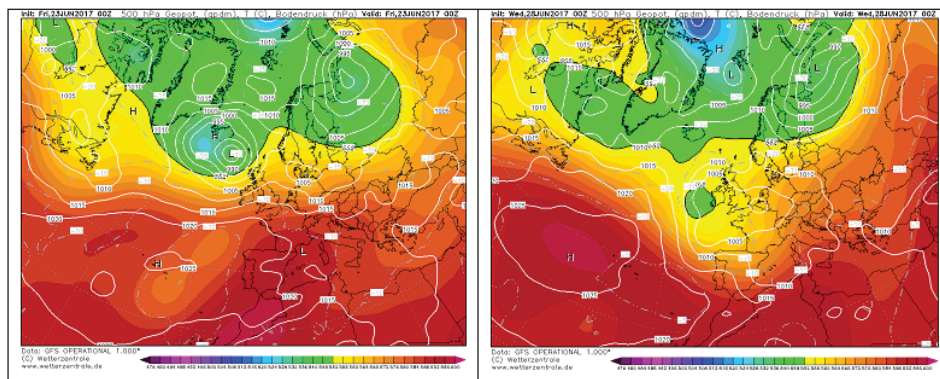


Fig. 10. Sea-level pressure (white contours), height of the 500 hPa surface (colors) on 23 and 28 June 2017. Source: NOAA/NCEP via <http://www.wetterzentrale.de>

Autumn was +1.2°C warmer than normal in North Bulgaria and +0.9°C – in South Bulgaria. December 2017 was warm with deviations of +3.1°C on average in North Bulgaria (+4.6°C in Knezha), and +2.3°C on average in South Bulgaria (+3.6°C in Kotel).

Average annual precipitation in areas up to 800 m altitude was mostly near-normal despite the small parts of South-Central and South-East Bulgaria (with annual totals up to 160% of the 1961-1990 normal). Seasonal precipitation amounts were: 80% of climatic normal in the winter, 108% in the spring, 100% in the summer, and 154% in the autumn. Considerable spatial variability of deviations from monthly normal was registered on the territory of the country. January was not only very cold but also very snowy month with positive precipitation anomalies, especially in East Bulgaria (257% in Omurtag, North-East Bulgaria; 287% in Sredets, South-East Bulgaria). The snow cover reached 1m in Ispirih, North-East Bulgaria. The rainiest month was October with average precipitation about 2.5-3 times more than monthly normal (692% in Karnobat, Burgas district).

The year was marked by a number of extreme weather events (Fig. 11). Severe convective storms, associated with hail and strong winds hit northwestern and northcentral parts of the country on 3 July. In some meteorological stations more than 4 hail-fall events were registered in the time interval 00:00-05:45 local time. In Mezdra and Levski the giant hail stones with size up to 8 cm were observed.

Very warm weather in August led to occurrence of fires in different regions of Bulgaria. The most destructive of them was those nearby Kresna in South-West Bulgaria

in which more than 1300 ha of pine plantations and deciduous stands was destroyed. According to expert analysis more than 50 years will be necessary to restore the forest.

Torrential precipitation with duration more than 30 hours caused local floods in the southeastern parts of Burgas district in September. More than 10 villages were flooded. In Gramatikovo, the 24-hour precipitation amount of 198 mm was measured on 27 September, which was 4 times over the monthly normal.



3 July: Radar image from BAH5 radars

28 August: Fire near Kresna
(Source: Darik.news)

25 October: After heavy rain in Burgas district (Source: BNT 1)

Fig. 11. Notable extreme weather events in 2017

In the end of October, again in Burgas district, a prolonged 20-hour heavy precipitation led to overflowing dams and rivers, local floods, great damages on infrastructure and 4 victims. In Karnobat, 24-hour precipitation amount of 178 mm was measured on 25 October (460% of monthly normal).

REFERENCES

- Bocheva L., P. Simeonov (2015), Spatiotemporal variability of hailstorms for Bulgaria during the period 1961-2010, Proceedings of the 15th International Multidisciplinary Scientific GeoConference SGEM 2015, ISSN 1314-2704, Book4, 1065-1072.
- Bocheva L., Ts. Nikolova, I. Gospodinov, P. Simeonov (2015), Large-scale severe storms in Bulgaria: seasonal distribution and severity, Proceedings of the 15th International Multidisciplinary Scientific GeoConference SGEM, ISSN 1314-2704, Book4, 827-834.
- Ivanov P. (2007), Practical application of wind power in Bulgaria for electricity generation, "Energetika" magazine of National Electric Company, number 1-2, ISSN 0324-1521 (in Bulgarian).
- Malcheva K., H. Chervenkov and T. Marinova (2016), Winter Severity Assessment on the Basis of Measured and Reanalysis Data, Proceedings of the 16th International Multidisciplinary Scientific GeoConference SGEM, 2, 719-726, ISSN: 1314 -2704.
- Malcheva K., L. Trifonova, T. Marinova and H. Chervenkov (2017), Climate assessment of the winter 2016-2017 in Bulgaria, Proceedings of the 17th International Multidisciplinary Scientific Geoconference SGEM, 17, 41, 391-398.

- Nikolova Ts., L. Bocheva, P. Simeonov and T. Marinova (2015), Regional distribution of torrential convective precipitation in Bulgaria, 8th European Conference of Severe Storms (ECSS2015), 14-18 September 2015, Wiener Neustadt, Austria (poster).
- Petkova N., R. Brown, E. Koleva and V. Alexandrov (2005), Snow Cover Changes in Bulgarian Mountainous Regions, 1931-2000, Croatian Meteorological Journal 40: 662-665.
- Sabev L. and S. Stanev (1959), Climatic Dividing into Districts of Bulgaria, Works of the Institute of Hydrology and Meteorology, vol. V, "Nauka i izkustvo", Sofia. (in Bulgarian)
- Stanev S., M. Kyuchukova and S. Lingova Eds. (1991), The Climate of Bulgaria, Publishing house of Bulgarian Academy of Sciences, Sofia (in Bulgarian).
- Trifonova L. (2010), Typical synoptic situations causing dry wind, droughty and hot spells over territory of Bulgaria, Bulgarian Journal of Meteorology and Hydrology (BJMH), Vol. 15, number 3, 32-45.



Cold waves on the territory of Bulgaria in the period 1952-2011

Krastina Malcheva*

*National Institute of Meteorology and Hydrology- BAS,
Tsarigradsko shose 66, 1784 Sofia, Bulgaria*

Abstract: Cold waves are often associated with massive invasions of very cold air over a large area and retention of cold weather with excessive low temperatures. In the study are analyzed the main spatiotemporal characteristics of cold waves in the non-mountainous parts of the country in the period 1952-2011, as well as some peculiarities of different cold wave indicators. The proposed simplified cold wave duration index shows a good performance in the assessment of cold wave events comparable to other wide used indices. The obtained results reveal a high density of cold waves in the periods 1952-1963 and 1984-1996. The number of cold waves relatively increases in November and December in the period 1982-2011. Over 90% of all cold wave events in South Bulgaria and 85% in North Bulgaria are those of single cold waves with duration from 6 to 11 days. The reached values of minimum air temperature fall in the interval (-20°C, -10°C) in more than 55% of cases. The climatic peculiarities of the severe cold waves in 1954, 1956, 1963, 1985 and 1987 that affected the most part of the territory of Bulgaria consist in long duration or high frequency, large negative temperature deviations and very low minimum air temperatures.

Keywords: cold waves, spatiotemporal characteristics, climate indices

1. INTRODUCTION

Cold weather and cold waves/cold spells are associated with a large negative impact on many socio-economic sectors including problems in infrastructure and transportation, increase of urban air pollution, breakdowns of power lines, reduce oil and gas production simultaneously with strongly increase of energy consumption, development of specific diseases, losses in the agricultural sector and tourism (Peterson et al., 2014; Añel et al.,

* krastina.malcheva@meteo.bg

2017). The impact of low temperatures on the human organism is prolonged in time, which complicates the establishment of causal links. While the most immediate effects are frostbite and hypothermia, the lagged effect of cold weather conditions discloses an increase of the risk of mortality and hospitalization from cardiovascular and respiratory diseases (von Klot et al., 2012). Many studies reveal different temperature thresholds below which the mortality rises (Ryti et al., 2016). Monitoring and forecasting of prolonged cold events is an important task, which requires clear criteria to identify a cold wave/cold spell. As mentioned in RCC Node/WMO RA IV Network documents (2016), in a climatically very heterogeneous region like Europe it is difficult to find a uniform definition which is applicable for the whole continent, and thus to compare and analyze large-scale events. The used definitions of cold waves (based on fixed threshold temperatures, temperature anomalies, percentiles, human adaption capability) correspond to local climatic conditions and some sector-specific requirements. A consistent characterization of cold wave events still lacks not only in Europe but in the entire world. After reviewing the existing definitions in publications and operational activities of some weather offices, the WMO TT-DEWCE (Task Team on Definitions of Extreme Weather and Climate Events) has developed guideline for definition and classification of cold waves as a part of the Guidelines on the definition and monitoring of extreme weather and climate events for WMO members (available draft only on <http://www.wmo.int/pages/prog/wcp/ccl/opace/opace2/TT-DEWCE-2-2.php>). A cold wave is defined as: A marked and unusual cold weather characterized by a sharp and significant drop of air temperatures near the surface (maximum, minimum and daily average) over a large area and persisting below certain thresholds for at least two consecutive days during the cold season, typically associated with invasion of very cold air caused by a polar or high latitude air-mass displacement to lower latitudes, or in some cases associated with or enforced by long radiative cooling during a blocking and clear sky atmospheric circulation. The thresholds for a cold wave are determined by the rate at which the temperature falls, and the minimum to which it falls. This minimum temperature is dependent on the geographical region and time of year. Thresholds can be an absolute value or percentiles. Four indispensable characteristics of cold wave must be computed and evaluated: 1) magnitude (based on an index or a set of indices measuring the temperature drop below certain thresholds); 2) duration (the persistence of a cold wave based on recording its starting time and ending time); 3) severity integrates the magnitude and the persistence of cold wave; 4) extent is computed to inform on the geographical area affected and the widespread aspect of the cold wave.

It is important to note, that the Guidelines don't suggest as obligatory the use of relative thresholds from the statistical distribution of air temperature designed to produce comparable results for different geographical locations. So the choice of indicators may be influenced by their application, for example, the use of indices with fixed threshold can be more appropriate in many applications for impact assessment and risk management.

A thorough study of the cold waves in Bulgaria in terms of climate indices is still not done. In the recent years has published climatic analyses of the winters of 2012 and 2017 (Gocheva&Malcheva, 2014; Malcheva et al., 2017), as well as an assessment of winter severity in the different climatic subareas in Bulgaria in the period 1931-2010 on the basis of six climatic indices (Malcheva et al., 2016). The purpose of the presented here study is to give a general picture of this phenomenon on the territory of the country, as well as some peculiarities of various cold wave indicators. The period 1952-2011 was chosen for two reasons: the significant increase of the number of stations in the national meteorological network in 1950s years and availability of analysis of more severe winters after 2011 (as stated above).

2. DATA AND METHODS

All available daily data of minimum air temperature in the cold half-year (October-March) from the stations of the NIMH-BAS (National Institute of Meteorology and Hydrology at the Bulgarian Academy of Sciences) meteorological network in the non-mountainous parts of the country are checked for gaps, errors and inhomogeneity in the reference period 1961-1990, as well as for prolonged interruptions throughout the period from October 1951 to March 2011. Quality control was facilitated by the built-in procedures in the software package ClimPACT2 (Herold, 2015). Four homogeneity tests – RHtestsV4 (Wang&Feng, 2013), as well SNHT-double, Buishand (or Cumulative deviations) test, and Mann-Whitney-Pettitt test, the last three included in AnClim software (Štěpánek, 2008), were applied on the time series of monthly or yearly average minimum air temperature. The software package RHtestsV4 can be used to detect multiple change-points in data series that may have zero-trend or a linear trend throughout the whole period of record and first-order autoregressive errors. The test is based on the penalized maximal t-test and the penalized maximal F-test, which are embedded in a recursive testing algorithm (Wang, 2008). The change-points detection is also possible when a homogenous reference series is not available. In this case, the verification of detected change-points by another test is a good strategy, especially when metadata is insufficient or not available. Alexandersson (1995) formulated a version of SNHT (Standard Normal Homogeneity Test) for the double shift of the mean level in time series. The double break test is useful for dividing long time series into shorter periods. Cumulative deviations from the mean are often used in the analysis of homogeneity. The test, based on the rescaled adjusted partial sums of deviations, is suitable to detect sudden changes in the mean. Two test statistics are used: Q is efficient in detecting a single shift in the mean; R is more sensitive to two opposite shifts in the mean (Buishand, 1982). Mann-Whitney-Pettitt test is a rank-based test for detecting the change in the median of series with an unknown time of change. According to Pettitt (1979), the test is considered to be powerful relative to Wilcoxon-Mann-Whitney test and sensitive to all possible conditions resulting in a stochastic ordering. The example

of outcomes of homogeneity testing is shown on fig. 1. All stations with incomplete reference period or confirmed by at least two tests and metadata inhomogeneity, or missing data in more than two consecutive cold seasons outside reference period are rejected. So from the available meteorological stations are selected 20, representative for different climatic conditions and relatively evenly distributed in North Bulgaria (NBG) and South Bulgaria (SBG), taking into account the barrier effect of Balkan Mountains on the atmospheric circulation in the cold half-year (fig. 2).

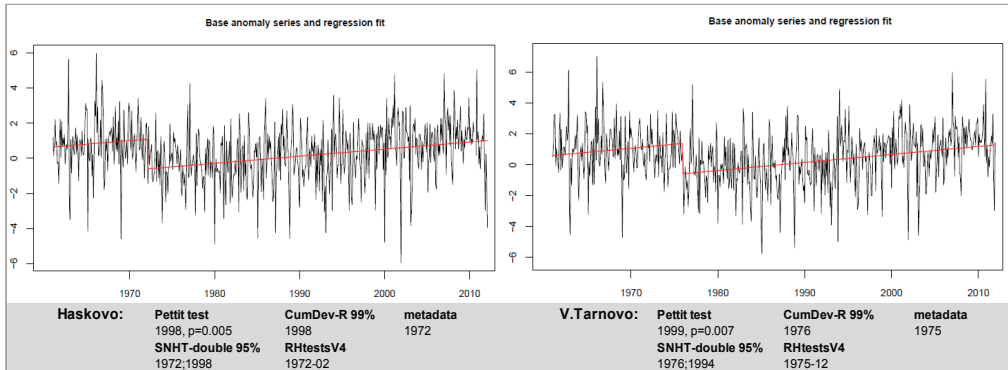


Fig. 1. Example of homogeneity testing and verification

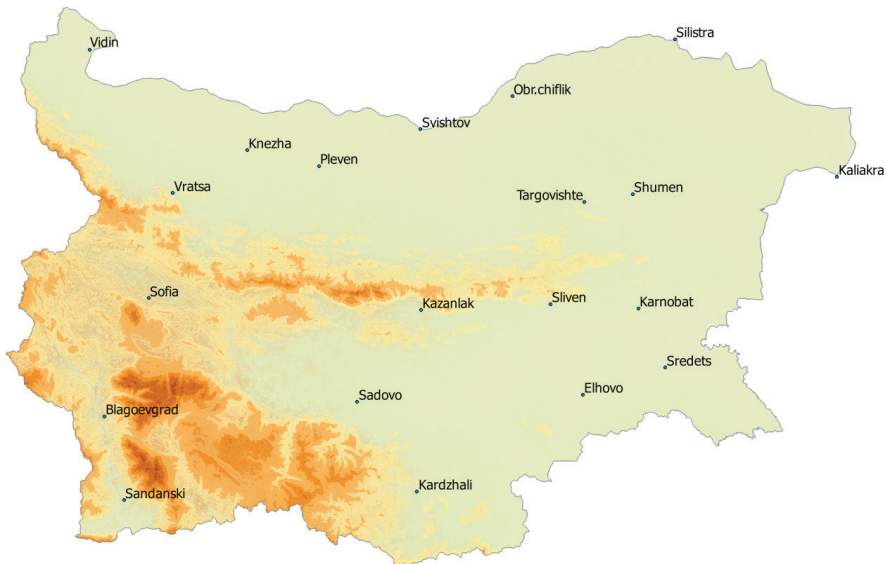


Fig. 2. Meteorological stations of the NIMH-BAS network used in the study

Several climatic indices suitable for evaluating of cold wave/cold spell duration, described in Table 1, can be calculated automatically by commonly available software applications. The computation of other basic characteristics, as magnitude and severity, is not supported.

Table 1 Cold wave duration indices included in different software applications

STARDEX	<i>tncwd</i>	Cold Wave Duration	Let T_{nij} be the daily minimum temperature at day i of period j and let T_{ninorm} be the calendar day mean calculated for a 5 day window centred on each calendar day during a specified period. Then counted is the number of days per period where, in intervals of at least 6 consecutive days: $T_{nij} < T_{ninorm} - 5$	days
RCLimDex ECA&D	CSDI	Cold-spell duration index	Let T_{nij} be the daily minimum temperature at day i of period j and let $T_{Nin 10}$ be the calendar day 10th percentile calculated for a 5-day window centred on each calendar day in the 1961-1990 period. Then counted is the number of days per period where, in intervals of at least 6 consecutive days: $T_{nij} < T_{Nin 10}$	days
ClimPACT2	CSDIn	User-defined CSDI	Annual number of days with at least n consecutive days when $TN < 10$ th percentile where $n \geq 2$	days
	$nTXbnTNb$	User-defined consecutive number of cold days and nights	Annual number of n consecutive days where both $TX < 5$ th percentile and $TN < 5$ th percentile where $10 \geq n \geq 2$	number of events

Similar to the wide accepted definition of heat wave duration (Frich et al. 2002), the cold wave duration index (*tncwd*) in the European project STARDEX (Statistical and Regional Downscaling of Extremes) was defined as a period with at least six consecutive days where daily minimum temperature was lesser than 5°C below 1961-1990 mean daily minimum temperature. The freely available software (STARDEX, 2004) performs the calculation of seasonal and annual values of cold wave duration index.

The main task of European Climate Assessment & Data (ECA&D) project is to analyze the climate of WMO region VI and trends in climatic extremes observed at meteorological stations (Klein Tank et al., 2002). A core set of 26 indices (including indices for cold-related events) follows the definitions recommended by the CCI/CLIVAR/JCOMM Expert Team on Climate Change Detection and Indices (ETCCDI) so that the performed calculations are identical with those in the RCLimDex software package (<http://etccdi.pacificclimate.org>).

ClimPACT2 software is based on RCLimDex but with some more flexibility (Alexander, 2015). The software package is designed to provide a user-friendly Graphical User Interface (GUI) to compute the 34 core indices (including cold spell indicators) recommended by the WMO/CCI/ET CRSCI (Expert Team on Climate Risk and Sector-specific Climate Indices).

All described above software applications, however, provide only annual or seasonal values of duration indices. The more flexible is ECA&D computational procedure but only calculated results on the basis of shared data from a limited number of stations are accessible. Generally, the analysis of individual cold wave events into a cold season

(October-March) is impossible. Also, it should be taken in mind the peculiarities of “yearly” indices noted in Zhang et al. (2011): As the threshold changes within the year, cold spells or heat waves that are defined as daily temperatures away from those thresholds are defined in a relative sense. This latter approach means, for example, that a location could experience what would be classified as a heat wave in the middle of winter. In that context, the indices in Table 1 will sum all cold spells outside the cold half of the year.

In this study CSDI is calculated for the cold half-year by automated procedures in Excel environment, strictly following the methodology of ECA&D (Project team ECA&D, 2013). The results have been verified for several stations available through ECA&D-site (<http://www.ecad.eu/indicesextremes/index.php>), as for the most of them CSDI is calculated for cold half-year in the period from October 1960 to March 2005 (Table 2). For the obviously unreliable values in the ECA&D output files (CSDI value <6, marked in red in the table), the deviations weren’t calculated. A few cases of discrepancies are due, probably, to the revisions and corrections made in the meteorological database of NIMH-BAS in the last years.

Table 2 Deviation of computed values of CSDI for cold half-year in this study (grey columns) from those available through ECA&D-site

YEAR	Vidin		Knezha		Obr. chiflik		Sadovo		Sliven		Sandanski		Kardzhali		Sofia	
	ECA&D	This study dev.	ECA&D	This study dev.	ECA&D	This study dev.	ECA&D	This study dev.	ECA&D	This study dev.	ECA&D	This study dev.	ECA&D	This study dev.	ECA&D	This study dev.
1961	0	0	0	0	0	0	0	0	0	0	0	0	0	0	0	0
1962	0	0	0	0	6	0	6	1	9	0	6	0	0	0	6	0
1963	7	1	22	0	27	2	22	4	11	7	11	0	11	0	20	1
1964	0	0	0	0	0	0	0	0	0	0	0	0	0	0	0	0
1965	0	0	0	0	0	0	6	0	7	0	6	0	0	0	0	0
1966	6	0	0	0	0	0	0	0	0	0	0	0	6	0	0	0
1967	0	0	6	-6	7	-1	0	0	0	0	7	0	0	0	0	0
1968	0	0	0	0	8	0	0	0	0	0	0	0	0	0	0	0
1969	7	0	0	0	7	0	0	0	0	0	0	0	0	0	0	0
1970	0	0	0	0	0	0	0	0	0	0	0	0	0	0	0	0
1971	0	0	0	0	0	0	0	0	0	0	0	0	0	0	0	0
1972	6	0	0	0	0	0	7	-7	14	0	0	0	6	0	6	0
1973	0	0	1	0	0	0	1	0	0	0	7	0	1	0	0	0
1974	6	0	0	0	18	-4	3	0	12	0	6	0	6	0	6	0
1975	0	0	0	0	0	0	0	0	0	0	0	0	0	0	0	0
1976	6	0	8	0	17	-4	0	0	0	0	0	0	0	0	0	0
1977	0	0	0	m.d.			0	0	0	0	0	0	0	0	0	0
1978	9	0	8	m.d.			1	0	1	0	0	0	0	6	0	0
1979	6	0	7	0	0	0	7	0	9	0	0	0	6	0	0	0
1980	0	0	0	0	0	0	0	0	0	0	0	0	0	0	0	0
1981	0	0	0	0	0	0	0	0	0	0	0	0	0	0	0	0
1982	0	0	0	0	0	0	0	0	0	0	0	0	6	0	0	0
1983	15	0	14	0	9	0	14	0	0	0	6	0	7	0	7	0
1984	9	0	9	0	9	0	0	0	6	0	0	0	0	0	0	0
1985	14	-2	12	0	14	0	7	0	14	0	15	0	7	0	12	0
1986	0	0	0	0	0	0	6	0	0	0	0	0	0	0	0	0
1987	14	0	14	0	14	0	20	-3	15	0	23	0	14	0	17	0
1988	0	0	0	0	0	0	0	0	6	-6	0	0	0	0	0	0
1989	0	0	9	0	11	-1	16	0	0	0	13	0	5	0	14	0
1990	15	0	19	-2	8	-1	16	0	6	0	6	0	15	0	10	0
1991	0	0	6	0	6	0	6	0	0	0	6	0	6	0	6	0
1992	0	0	0	0	0	0	0	0	7	0	6	0	6	0	0	0
1993	6	2	6	4	6	0	9	0	10	0	8	0	14	0	13	0
1994	0	0	6	-6	12	0	0	0	0	0	0	0	0	0	0	0
1995	0	0	0	0	0	0	0	0	0	0	0	0	0	0	0	0
1996	0	0	0	0	15	0	0	0	7	0	7	0	19	0	7	0
1997	0	0	0	0	0	0	0	0	0	0	0	0	0	0	0	0
1998	0	0	7	0	0	0	0	0	0	0	6	0	11	0	0	0
1999	6	0	18	0	0	0	0	0	0	0	7	0	8	0	8	0
2000	0	0	0	0	0	0	0	0	0	0	14	-8	8	0	0	0
2001	0	0	0	0	3	0	0	0	0	0	0	0	0	0	0	0
2002	0	0	6	0	23	0	13	0	12	0	20	1	6	0	7	0
2003	0	0	0	0	16	-1	0	0	13	0	0	0	6	0	0	0
2004	0	0	0	0	0	0	0	0	0	0	6	0	0	0	0	0
2005	9	0	m.d.		m.d.		m.d.		7	0	7	-1	8	-1	m.d.	

Radinovic&Curic (2014) define as a representative measure for cold weather the negative departure of minimum daily temperature from the monthly normal as well as the inter-diurnal variability of minimum temperature. The thresholds are derived from the corresponding frequency distribution in a given month during the reference climate period 1961-1990 as one (below normal), two (well below normal) and three (extraordinarily below normal) times the standard deviation. The authors recommend the use of such type of thresholds in cases of incomplete and imprecise daily meteorological information that in practice can improve the quality of weather reports and weather forecasts.

On fig. 3 are presented some basic statistical characteristics of time series used in the study for the reference period 1961-1990.

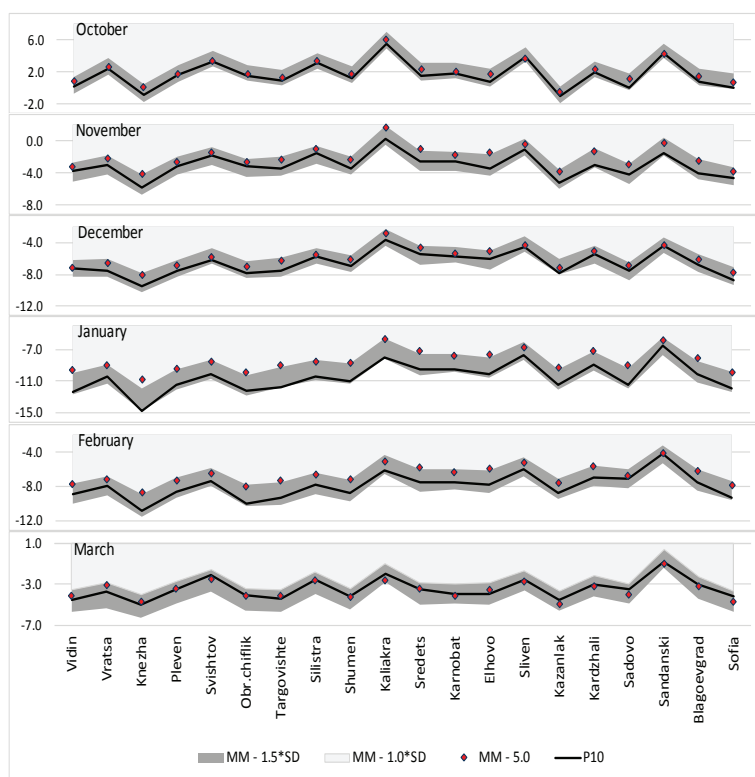


Fig. 3. Basic statistical characteristics of minimum air temperature for the reference period 1961-1990 (SD = standard deviation; MM = monthly normal; P10 = 10th percentile)

As the daily temperature statistics vary around the monthly ones, CSDI and *tn cwd* could be determined as moderate extremes, according to the defined in Radinovic&Curic (2014) temperature thresholds. Obviously, *tn cwd* could “catch out” all cold events on the border of the natural variability of minimum temperature, mainly in January and

February. This is a major disadvantage of *tncwd* as a robust climate signal. As illustrated on fig. 4 in the case of cold waves in Knezha in 1954, CSDI detects a 12-day cold wave (01-12.02.1954), while *tncwd* detects two cold waves (6 days in the period 24-29.01.1954 and 23 days in period 31.01-22.02.1954), or total 29 days. It is interesting to note that the use of fixed threshold (MM-5.0 on the fig. 4) for identifying cold wave events returns an intermediate value of 19 days (6 days in the period 24-29.01.1954 and 13 days in period 01-13.02.1954) but detects another 6-day cold wave in the period 11-16.01.1954 (total 25 days).

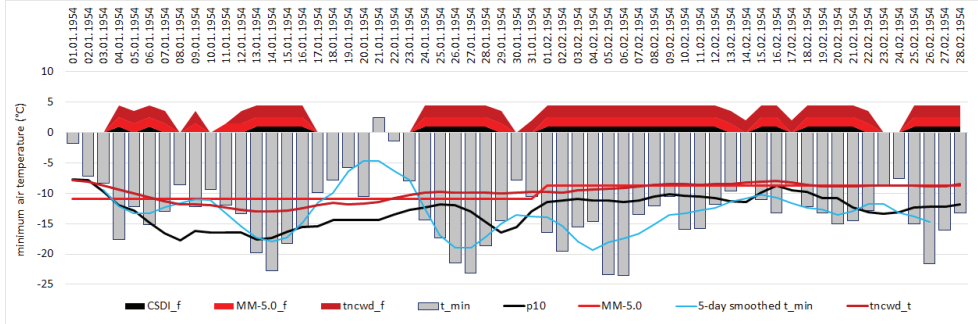


Fig. 4. A case of cold wave events in Knezha in 1954 (MM = monthly normal of minimum air temperature; t_{min} = daily minimum temperature; flags CSDI_f, tncwd_f and MM-5.0_f $\neq 0$, if t_{min} is below the defined thresholds: p10 = daily 10th percentile in the period 1961-1990, tncwd_t = 5°C below daily mean minimum temperature in the period 1961-1990, MM-5.0 = 5°C below monthly normal).

The described case of overestimating of the cold wave duration by *tncwd* compared to the simplified version that uses fixed monthly thresholds is no exception. It is reasonable to assess the applicability of the simplified index, considering the gaps and inhomogeneity in daily minimum temperature data, as well the lack of reliable homogenized time series, which does not allow the calculation of indices with relative thresholds for a number of meteorological stations. The modified index *tncwd_m* is defined similarly to *tncwd* (see Table 1) but instead of the smoothed daily data are used monthly normals for determining of fixed monthly thresholds:

$$T_{mm} = T_{mm_min_norm} - 5,$$

where $T_{mm_min_norm}$ (°C) is the monthly 1961-1990 normal of the minimum air temperature for each of months in the cold half-year (i.e. $mm = \{Oct, Nov, Dec, Jan, Feb, Mar\}$).

The frequency distribution of absolute differences between annual values of *tncwd* (as STARDEX outcomes) and calculated annual values of *tncwd_m* showed very high consistency for all stations in the study period: in over 65% of cases, the differences are ± 1 day; in about 15% of cases was observed a complete mismatch in the detection of the single 6 or 7-day cold waves (fig. 5).

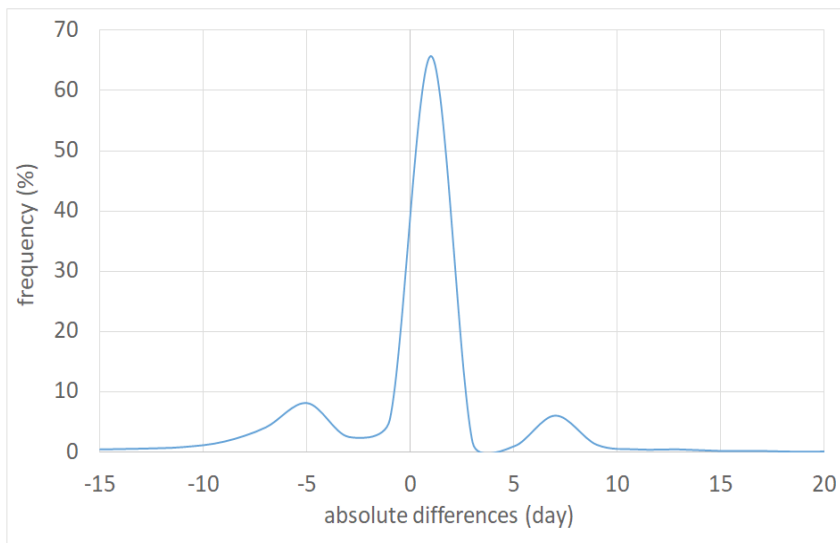


Fig. 5. Frequency distribution of absolute differences between annual values of *tncwd* and *tncwd_m* calculated over all stations in the considered period; on the abscissa are shown upper bin boundaries

Generally, *tncwd* no outperforms substantially the modified index in the assessment of cold wave events. That's why the further study is focused on the analysis and comparison of CSDI and *tncwd_m* in the period from October 1951 to March 2011, both calculated for the cold half-year. All mentioned below periods include the whole cold season (e.g. 1982-2011 should be read as October 1981 - March 2011).

3. RESULTS AND DISCUSSION

Frequency distribution of the number of days in the cold half-year included in cold waves shows very similar results for CSDI and *tncwd_m*. About 60% of cases are those of single events with duration between 6 and 9 days that substantiates the studied indices as moderate extremes (fig. 6).

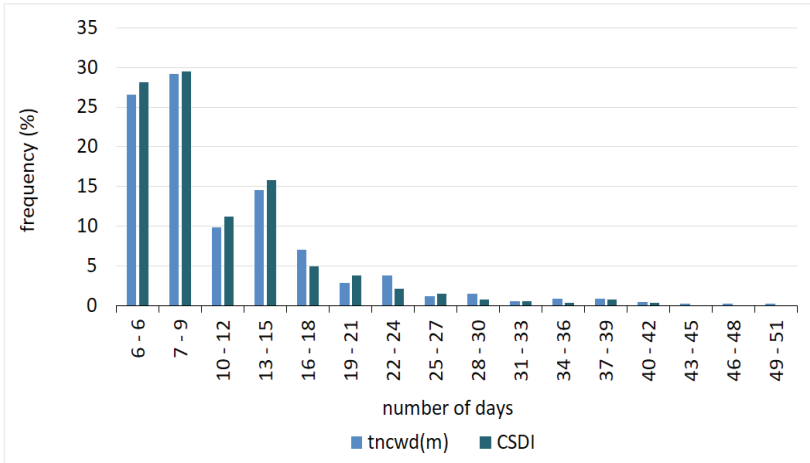


Fig. 6. Frequency distribution of the number of days in the cold half-year included in cold waves in the period 1952-2011

A simple approach to outlining the most extreme events in the spatiotemporal analysis is min-max normalization of obtained results by using the formula:

$$\bar{x}_i = \frac{(x_i - x_{\min})}{(x_{\max} - x_{\min})} \times 10,$$

where the deviation of each value of the parameter x_i from the smallest value x_{\min} is divided by the sample range, and the result is multiplied by 10 to obtain a comfortable uniform scale from 0 to 10. The normalized values of CSDI and $tncwd_m$ for all 20 stations over the period 1952-2011 are rounded to the nearest integer for obtaining a clear picture of the cold season severity in degrees from 1 to 10. Moreover, this method permits an additional proofing of $tncwd_m$ applicability by direct comparison of the discrepancies with the scores obtained for CSDI. In over 60% of cases the differences fall in the interval $(-1, +1)$; in about 88% of cases, they are between -2 and $+2$ (fig.7).

The spatiotemporal distribution of normalized values of $tncwd_m$ and CSDI reveals a high density of cold waves in the periods 1952-1963 and 1984-1996 (fig. 8). Indisputably, CSDI is statistically more precise but the results are spatially more heterogeneous compared to $tncwd_m$ outcomes under the same large-scale atmospheric conditions in the most severe winters (1952-1963). Daily percentiles follow the local peculiarities of the minimum air temperature while the respective monthly averages are spatially more coherent.

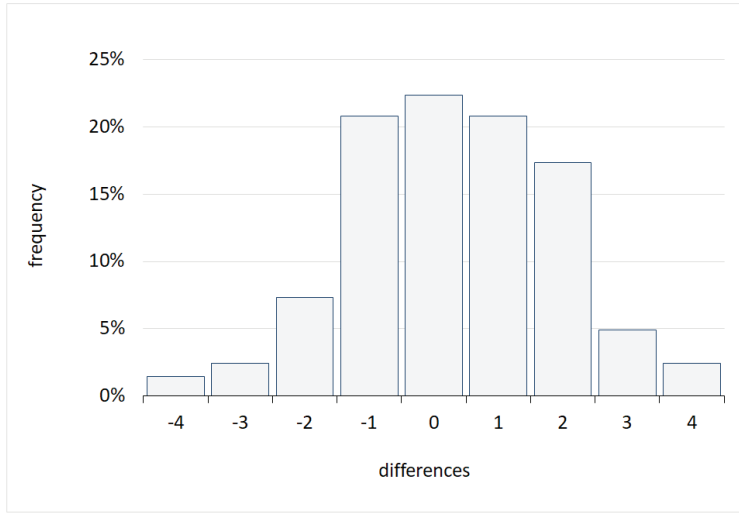


Fig. 7. Frequency distribution of differences between normalized values of *tncwd_m* and CSDI

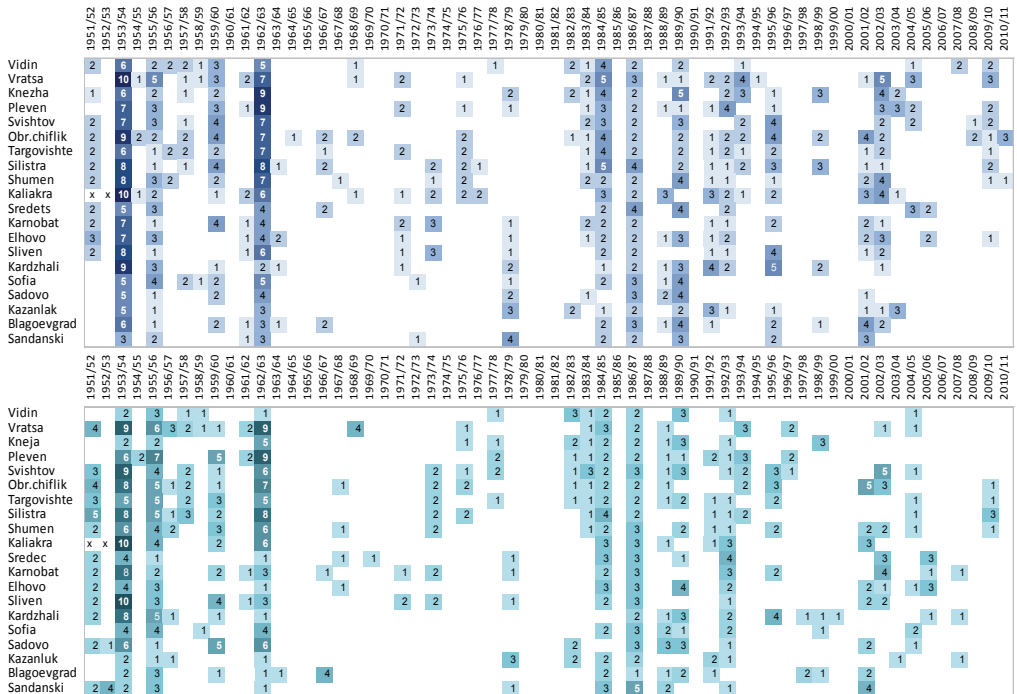


Fig. 8. Spatiotemporal distribution of normalized values of *tncwd_m* (upper panel), and CSDI (lower panel)

The distribution of cold wave events by decades (comprising 10 cold seasons) shows variability without clear tendency, outlining the first one as more severe, especially in South Bulgaria (fig. 9).

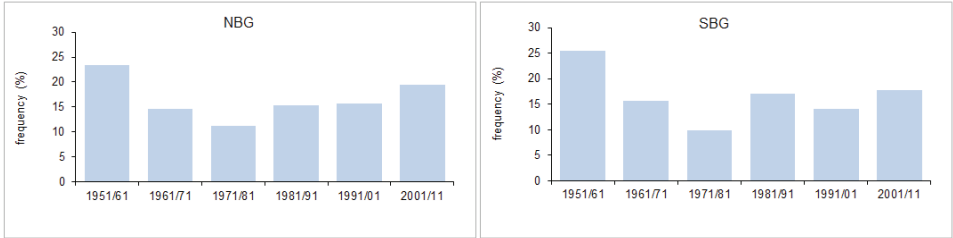


Fig. 9. Distribution of cold wave events by decades in the considered period

Monthly distribution of CSDI and *tncwd_m* cold wave events in the period 1952-2011 are generally similar (the largest difference is about 5%). Most frequently cold waves occur in February, and most rare – in October. Since 1982, the number of CSDI cold waves relatively increased with about 15% in November and 8% in January, while they practically disappear in October. Inversely, the number of *tncwd_m* cold waves in October retains almost the same but relatively increases with about 20% in December (15% in South Bulgaria) and with about 14% in November (fig. 10).

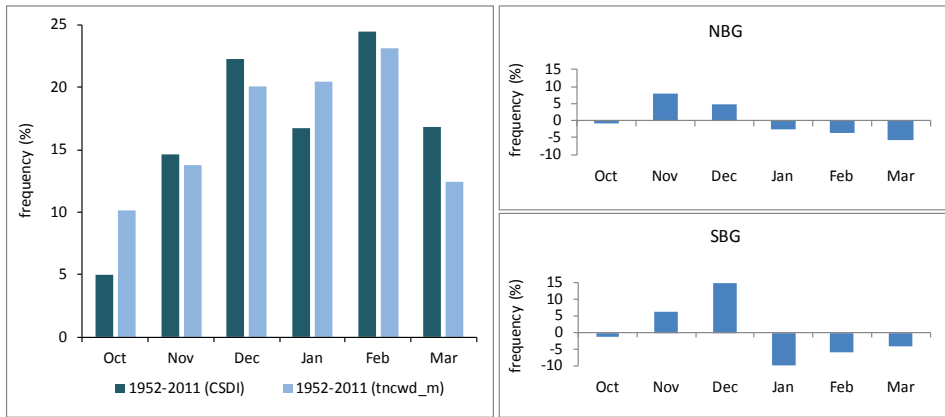


Fig. 10. Monthly distribution (left panel) of cold wave events and relative deviations (two right panels) of *tncwd_m* cold waves in the period 1982-2011 compared to 1952-1981, separately for North and South Bulgaria

In the period 1952-2011, over 90% of cases in SBG and 85% of cases in NBG are those of single cold waves with duration from 6 to 11 days. The maximum cold spell duration is observed in Pleven (1954): 28 days for *tncwd_m* and 22 days for CSDI. The reached values of minimum temperature fall in the interval (-20°C , -10°C) in

about 56% of cases in SBG and in about 64% of cases in NBG. The lowest values are registered in 1956 (below -30°C in Sadovo and Sredec) and 1985 (-29.3°C in Knezha).

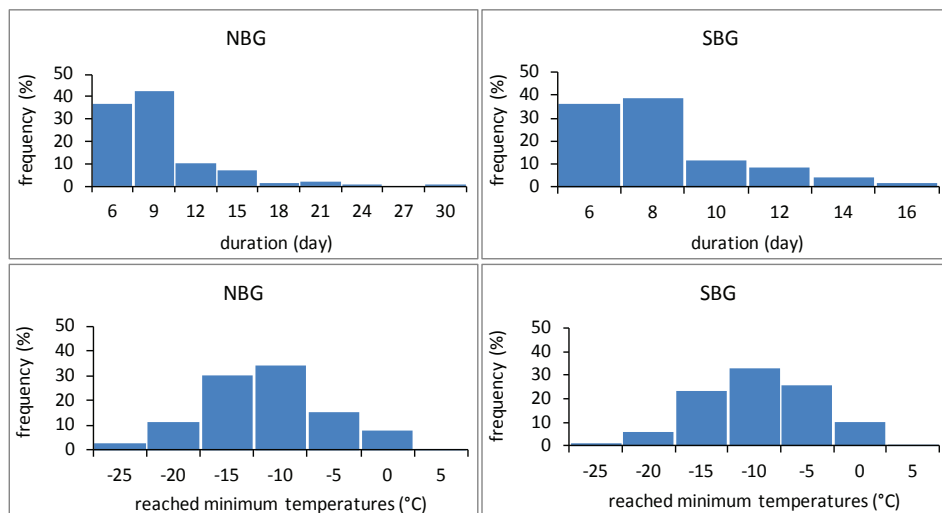


Fig. 11. Frequency distributions of duration of cold wave events and reached minimum temperatures in the period 1952-2011; on the abscissa are shown upper bin boundaries

Following the definition of WMO TT-DEWCE, the cold wave severity can be determined by accumulated negative anomaly from the threshold used to identify the cold wave events. For the purposes of spatial analysis and comparison of the different cold wave characteristics, it is convenient to work with dimensionless parameters. In regard to *tncwd_m*, all cold wave events are weighted to a minimum possible cold wave (i.e. six days with daily deviations from the monthly normal -5.1°C or -30.6°C accumulated anomaly). On the fig. 12 are shown the key features of cold wave events in relative units, spatially averaged for North Bulgaria and South Bulgaria, namely: the maximum severity and duration for each cold season, as well as the frequency defined as the number of events in the cold season. In NBG, it is observed a distinct difference between the sub-periods 1952-1981 and 1982-2011 in the direction of the range decrease for all three characteristics, while in SBG, the maximum values of relative severity and duration were registered in the second sub-period.

The climatic peculiarities of the severe cold waves in 1954, 1956, 1963, 1985 and 1987 that affected the most part of the territory of Bulgaria consists in long duration (above 10 days) or high frequency (up to 5 cases in 1954), large negative temperature deviations (more than $10-12^{\circ}\text{C}$, in particular cases more than 25°C) and very low minimum temperature (in 1954, the reached absolute minimum temperature is at average below -22°C in NBG and below -21°C in SBG).

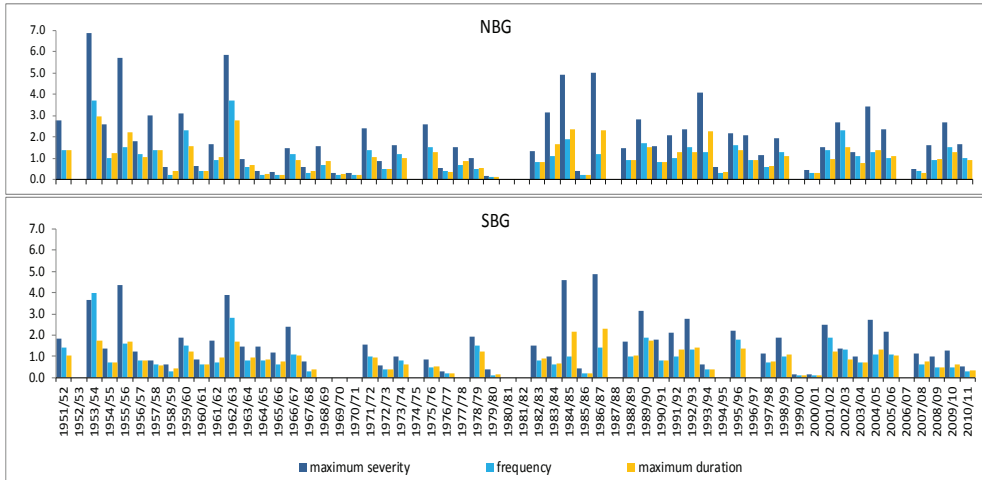


Fig. 12. Long-term variations of the key features of cold wave events in relative units

4. CONCLUDING REMARKS

In the study were analyzed the main spatiotemporal characteristics of cold waves in the non-mountainous parts of the country in the period 1952-2011, as well as some peculiarities of various cold wave indicators. The proposed index *tncwd_m* shows a good performance in the assessment of cold wave events comparable to other wide used indices as CSDI and *tncwd*. The spatiotemporal distribution of normalized values of *tncwd_m* and CSDI reveals a high density of cold waves in the periods 1952-1963 and 1984-1996. Over 90% of all cold wave events in South Bulgaria and 85% in North Bulgaria are those of single cold waves with duration from 6 to 11 days. The reached values of minimum temperature fall in the interval (-20°C , -10°C) in more than 55% of cases. The climatic peculiarities of the severe cold waves in 1954, 1956, 1963, 1985 and 1987 that affected the most part of the territory of Bulgaria consists in long duration or high frequency, large negative temperature deviations and very low minimum temperatures. Since 1982, the number of cold waves relatively increased in November and December.

REFERENCES

Alexander L., (2015), Introduction to the ET-SCI indices, ET SCI workshop, Nadi, Fiji, https://www.wmo.int/pages/prog/wcp/ccl/opace/opace4/meetings/documents/fiji2015/D3-2-Alexander_Intro_to_ETSCI_indices.pdf

- Alexandersson H., (1995), Homogeneity testing, multiple breaks and trends. Proceedings of the Sixth International Meeting on Statistical Climatology, Galway, Ireland, 439-441.
- Añel J., Fernández-González M., Labandeira X., López-Otero X. & de la Torre L., (2017), Impact of Cold Waves and Heat Waves on the Energy Production Sector, *Atmosphere*, 8(11), 209, doi:10.3390/atmos8110209
- Buishand T.A., (1982), Some Methods for Testing the Homogeneity of Rainfall Records, *J. Hydrol.*, 58, 11-27.
- Frich P., Alexander L., Della-Marta P., Gleason B., Haylock M., Tank A. & Peterson T., (2002), Observed coherent changes in climatic extremes during the second half of the twentieth century, *Climate Research*, 19(3), 193-212
- Gocheva A. and K. Malcheva, (2014), The winter of 2012 in Bulgaria compared to 51 previous winters, *Bul. J. Meteo & Hydro* 19/1-2 (2014) 26-32, ISSN 0861-0762
- Herold N., (2015), ClimPACT2-A software tool for calculating climate extremes indices, ET SCI workshop, Nadi, Fiji, https://www.wmo.int/pages/prog/wcp/ccl/opace/opace4/meetings/documents/fiji2015/D2-3-tuesday_stream1.pdf
- Klein Tank AMG, Zwiers FW, Zhang X, (2009), Guideline on analysis of extremes in a changing climate in support of informed decisions for adaptation, *Climate Data and Monitoring, WCDMP-No. 72, WMO-TD No. 1500*, Geneva, Switzerland
- Malcheva K., L. Trifonova, T. Marinova and H. Chervenkov, (2017), Climate assessment of the winter 2016-2017 in Bulgaria, *International Multidisciplinary Scientific Geoconference SGEM, Conference Proceedings*, 17, 41, 391-398, ISBN 978-619-7105-64-3/ ISSN 1314-2704, <https://doi.org/10.5593/sgem2017/41>
- Malcheva K., H. Chervenkov and T. Marinova, (2016), Winter severity assessment on the basis of measured and reanalysis data, *International Multidisciplinary Scientific GeoConference SGEM, Conference Proceedings*, ISBN 978-619-7105-64-3/ ISSN 1314-2704, Book4 Vol. 2, 719-726 pp, DOI: 10.5593/SGEM2016/B42/S19.092
- Peterson T., T. R. Karl, J. P. Kossin, K. E. Kunkel, J. H. Lawrimore, J. R. McMahon, R. S. Vose & X. Yin, (2014), Changes in weather and climate extremes: State of knowledge relevant to air and water quality in the United States, *Journal of the Air & Waste Management Association*, 64:2, 184-197
- Pettitt A.N., (1979), A non-parametric approach to the change-point problem, *App. Statist.*, 28, no. 2: 126-135
- Project team ECA&D, *Algorithm Theoretical Basis Document (ATBD)*, (2013), <http://www.ecad.eu/publications/index.php>
- Radinovic D. and M. Curic, (2014), Measuring scales for daily temperature extremes, precipitation and wind velocity, *Meteorol. Appl.* 21: 61– 65
- RCC Node-CM Product Description Version 1.0, (2016), Heat and Cold Waves, WMO RA IV Network, https://www.dwd.de/EN/ourservices/rcccm/int/descriptions/hkw/01_produktdbeschreibung_hkw_en.pdf?__blob=publicationFile&v
- Ryti, N. R. I., Guo, Y., & Jaakkola, J. J. K., (2016), Global Association of Cold Spells and Adverse Health Effects: A Systematic Review and Meta-Analysis, *Environmental Health Perspectives*, 124(1), 12–22
- STARDEX Diagnostic Extremes Indices Software User Information Version 3.3.1, (2004), https://crudata.uea.ac.uk/projects/stardex/deis/Diagnostic_tool.pdf
- Štěpánek, P. (2008), AnClim - software for time series analysis: Dept. of Geography, Fac. of Natural Sciences, MU, Brno, <http://www.climahom.eu/AnClim.html>

- Vincent, L. A., X. L. Wang, E. J. Milewska, H. Wan, Y. Feng, and V. Swail, (2012), A Second Generation of Homogenized Canadian Monthly Surface Air Temperature for Climate Trend Analysis, *JGR (Atmospheres)*, 117, D18110
- von Klot S., A. Zanobetti and J. Schwartz, (2012), Influenza epidemics, seasonality, and the effects of cold weather on cardiac mortality, *Environmental Health*, 11:74, <http://www.ehjournal.net/content/11/1/74>
- Wang, X. L., (2008), Accounting for autocorrelation in detecting mean-shifts in climate data series using the penalized maximal t or F test, *J. Appl. Meteor. Climatol.*, 47, pp 2423-2444
- Wang, X. L., Feng Y., (2013), RHtestsV4 User Manual, Science and Technology Branch, Environment Canada, <http://etccdi.pacificclimate.org/software.shtml>
- Zhang X., L. Alexander, G.C. Hegerl, Ph. Jones, A.M.G. Klein Tank, Th. C. Peterson, B. Trewin and F.W. Zwiers, (2011), Indices for monitoring changes in extremes based on daily temperature and precipitation data, *WIREs, Clim Change*, 2011, doi: 10.1002/wcc.147, John Wiley & Sons, Ltd.



Cold season tornadoes in Bulgaria – brief analysis

Lilia Bocheva* and Boryana Markova

*National Institute of Meteorology and Hydrology- BAS,
Tsarigradsko shose 66, 1784 Sofia, Bulgaria*

Abstract: From the beginning of 21st century 58 confirmed cases of tornadoes and waterspouts were registered in Bulgaria. In the list of documented tornadoes there are 5 “winter” cases which occurred within the cold half of year: 4 of which in southern Bulgaria and 1 - in northeastern Bulgaria. According to synoptic analysis they were associated with strong thunderstorms which developed along cold fronts introducing cold and moist air masses in Bulgaria after a period of unseasonably warm and dry weather. Some thermodynamic parameters and four instability indices have been calculated. All received values are close to those favorable for development in our country of summer type convective storms.

Keywords: tornado; winter convection; instability indices

1. INTRODUCTION

Tornado is one of the most extreme weather phenomena. Although it is defined as a small-scale convective induced whirl with a width of several tens of meters up to a maximum of 2 km and a lifetime from several minutes to several hours, this type of vortex can cause significant material damages and even loss of life. According to accepted definitions for tornado (Glickman, 2000; Rauhala et al., 2012) “*A tornado is a vortex between a cloud and the land or water surface, in which the connection between the cloud and surface is visible, or the vortex is strong enough to cause at least F0 damage*”. This allows all waterspouts to be included in the definition of a tornado.

In the northern hemisphere, tornadoes occur more often in the spring and much less in the winter, but it is possible to observe them at any time of the year, if the weather conditions are favorable. In Europe (excluding United Kingdom) tornadoes

* lilia.bocheva@meteo.bg

occur mainly in summer (46.9%) and autumn (24.4%). The lowest number of cases was recorded in winter (12.7%) and spring (16.0%). For continental Europe as a whole, the most tornadoes are recorded between May and September and the smallest activity takes place in December, March and April. The monthly distribution of tornadoes reflects the seasonal maximum of thunderstorm frequency over Europe. (Graf, 2008; Antonescu et al., 2016)

Tornadoes occur relatively rarely in Bulgaria compared to other parts of the world. They may often remain unreported when occur in remote and weakly populated mountainous regions of the country or if they leave no significant damage behind. The number of reports of tornado events in Bulgarian from the beginning of 21-century however has significantly increased thanks mainly to the revolutionary development of the information technology. For example, 58 tornadoes and waterspouts have been recorded in Bulgaria since 2001, against only 20 cases for the period 1956-2000 (Simeonov et al., 2013; Bocheva&Simeonov, 2016). The summarized information shows that the maximum frequency of tornadoes in Bulgaria is in warm half of the year between May and August with maximum in June. However, in the list of documented tornadoes there are 5 “winter” cases, all after 2003 year, which occurred within the cold half of year: 4 of them in southern Bulgaria and one - in northeastern Bulgaria. They present a great interest especially taking into account that severe thunderstorms in Bulgaria are not typical phenomena for winter. But recent investigations show that after 1991 frequency of thunderstorms days increased more rapidly during the cold months almost in all regions in the country (Bocheva&Marinova, 2016).

Two of such “winter” tornado cases were analyzed in previous works as a comparison for different types of severe convection and connected with them extreme events such as strong winds, heavy precipitations and hail (Bocheva et al., 2009; Bocheva et al., 2015). The aim of present paper is to summarize and compare all known cases of unusual cold season tornado events in Bulgaria. A serious challenge in this study was a real lack of radar information, because during the cold season the only radar data came from the airports radars, which cover only the short range nearby the main airports in Bulgaria in Sofia and Varna.

2. DATA AND METHOD OF INVESTIGATION

This study identifies the main characteristics of cold season tornadoes in Bulgaria. Data originated from eyewitness reports, site investigations, media news, and reports of the local administration. Press and TV are often the richest source of images of the tornadoes themselves or the damage they have caused. Data from the meteorological data base of National Institute of Meteorology and Hydrology (NIMH) are also included. The analysis of the vertical structure of the atmosphere at the location and the time of occurrence are based on the sounding data from the archives of NIMH. Two of the cases were also verified by using radar images and data: for one of them from the automated

radar system of NIMH (X and S-band AMS-MRL5) based in Gelemenovo and for second – C-band Doppler radar of Bulgarian Air Traffic Services Authority (BULATSA) on Sofia airport. The tornado cases have also been classified by strength according the Fujita scale (Fujita, 1985). The cases have been verified also by means of analysis of the weather patterns based on the NCEP/NCAR Reanalysis (Kalnay et al., 1996), images from GFS (www.wetter3.de) and from EUMETSAT, as well as products from NOAA/ESRL Physical Sciences Division, Boulder Colorado (<http://www.esrl.noaa.gov/psd/>). The sounding data from the national (Sofia) or the closest foreign aerological station (Bucharest) have been used to calculate some thermodynamic parameters and indices of instability at the vicinity of occurrence of the tornadoes. Surface data (pressure, temperature, humidity parameters, wind speed and direction) from the closest synoptic station have been fitted to the lower part of the vertical profile. All computations have been made by the upgraded in 2013 non-adiabatic empirical model developed by Dimiter Syrakov and Petio Simeonov (Simeonov& Syrakov, 1988).

3. RESULTS

3.1. Characteristics of “winter” tornado cases in Bulgaria

The collected database about tornadoes in Bulgaria for the period 2000–2017 has shown the registration of 5 such cases during the cold half of the year after 2003. Cold season tornadoes in Bulgaria presented 12% of all events. For comparison in United Kingdom about 35% occurred in the end of the autumn or winter-time (Holden&Wright, 2004) and in France about 20% of all (Graf, 2008).

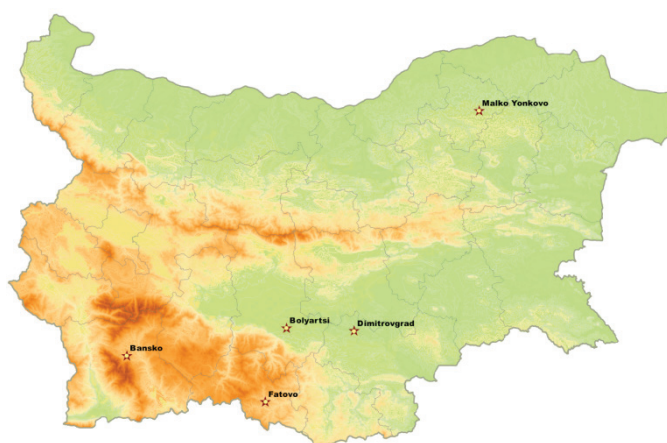


Fig. 1. Distribution of cold season tornadoes in Bulgaria.

Table 1. Main tornadic characteristics for all cold-season tornado cases

Location	Date	Start time UTC	Duration, min	Path length, km	Path width, m	Max wind, m/s	T max, °C	F-scale
Bolyartsi	24.03. 2004	13:30	about 10	0.4	35-130	20	17.6	F1
Fatovo	15.02. 2005	14:35	>30	2÷3	500	30	11.5	F1
Malko Yonkovo	21.03. 2007	13:30-14:00	about 10	*	*	40	17.8	F1
Bansko	02.12. 2010	07:30	10÷20	0.5	20-30	>20	18.0	F0
Dimitrovgrad	08.03. 2016	16:05	15	1	50	>20	17.8	F1

**a)** Broken and fallen radial pines near Fatovo**b)** After a severe storm in Malko Yonkovo**c)** After a tornado in Bansko**d)** After a tornado in Dimitrovgrad**Fig. 2.** Damages after cold season tornado outbreaks

The space distribution of “winter” tornadoes in Bulgaria is presented on Fig.1. The main ground-based characteristics of severe events are presented in Table 1. They have been classified by strength according to the Fujita scale on the base of information from damages reports and surface wind speed data – see Table 1. All cases can be classified as weak (less than or equal to F1) in which group belong about 76% of all tornadoes registered in the country. The available photos of damages after tornadoes are presented on Fig.2. After the tornado has passed, in all cases broken electric poles and damages on roofs of buildings have been reported. The biggest damages are recorded at the tornado

case in the East Rhodopes on 15 February 2005. At least one tornado-like whirl has been observed at the Madan-Rudozem road. Local authorities have reported about a hundred and fifty hectares of pine forest destroyed by wind gust of up to 30 m/s between Fatovo and Tarun (Fig. 2a). The biggest damages in urban environment are registered on 08 March 2016 in Dimitrovgrad where more than 30 roofs of the houses were demolished and many windows and electric poles were broken (Fig. 2d).

3.2. Synoptic and thermodynamic environment

The analyses of synoptic situation in Bulgaria show that the most tornadoes (90%) developed in the context of a cold front system with predominantly meridional extent from southwest to northeast which was associated with a strong air flow in the middle and upper troposphere. The cold-front system should have crossed the country. Such cold fronts are most often associated with a deep upper-level trough to the west of Bulgaria over the Central Mediterranean. When associated with tornadoes although, they appear to be rather stationary for a certain period of time or progress slowly through the country (Simeonov et al., 2013).

The same synoptic features are observed in all 5 cases of cold season tornadoes in Bulgaria. At 500 hPa charts the weather over the country is determined by a deep and slowly moving trough from the north with axes reaching Central Mediterranean (see Fig. 3-7 a). The strong jets from the south-southwest, typical for summer type convective processes, pass over the country. At the surface, Mediterranean cyclones are formed over northern part of the Adriatic Sea 48 hours before tornado and slowly moved eastward over the area. Bulgaria is situated in front of the low pressure area. The warm flows from south spread over the country. In all cases the measured surface air temperatures are with 10-15° C over the typical ones for the season at least 2-3 days before the tornado events. The maximum surface air temperature in tornado days is presented in Table 1. Cold atmospheric fronts connected with Mediterranean cyclones cross the country. After the cold front the temperature on 850 hPa decreased with 5-6 °C in all cases (Fig. 3-7 b).

There are many difficulties when attempting to study the thermodynamics at the vicinity of occurrence of tornadoes. We have only two radar images from quite different meteorological radars – for Bolyartsi from Sofia airport radar (Fig. 3c) and for Dimitrovgrad from NIMH radar (Fig. 7c). According to Fig. 3c the maximum reflectivity of convective clouds over Bolyartsi is about 45dBz (in red). The only available information from Fig. 7c, which presents the software product from Gelemenovo radar, is the existence of the convective clouds with cloud top about 7 km. In addition to lack of radar information, there are only a few sounding profiles available in the region. The NIMH operates only one aerological sounding per day at 12:00 UTC in Sofia. This inhibits the attempts to see the instability factors prior to events occurring before noon for example as is the case in Bansko. For tornado which occurred in morning hours of

02 December 2010 the only available sounding data was from Sofia, because there is no information about Thessaloniki air sounding for this day. Regarding the Dimitrovgrad case, it is impossible to use Sofia sounding data, not because of the distance of 200 km between two towns, but mainly because of the jet from south to north which crossed the central parts of the country and created favorable conditions for severe storm development over Thracian lowland (see Table 2).

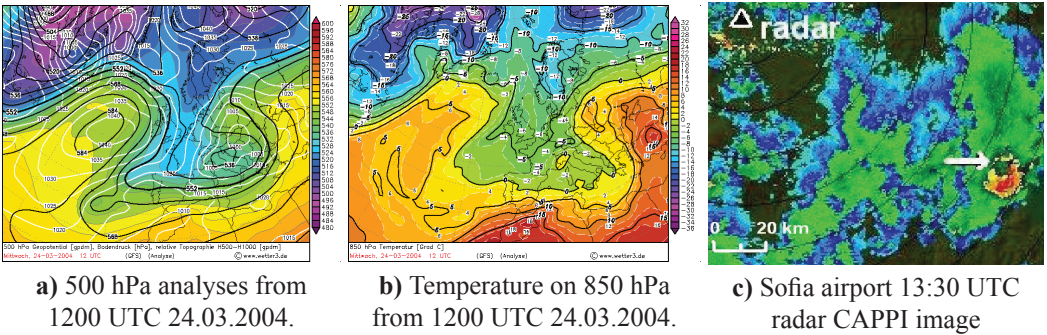


Fig. 3. 24 March 2004 – Bolyartsi tornado outbreak

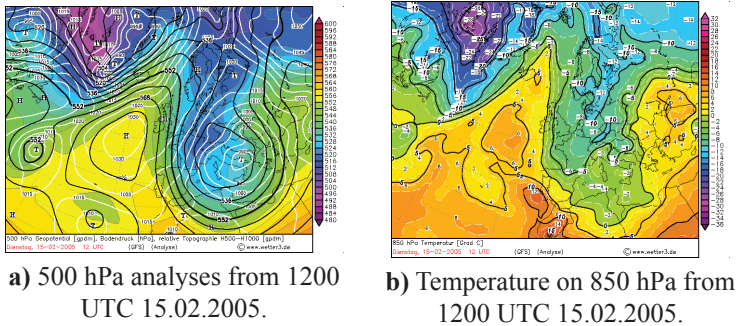


Fig. 4. 15 February 2005 – Fatovo tornado outbreak

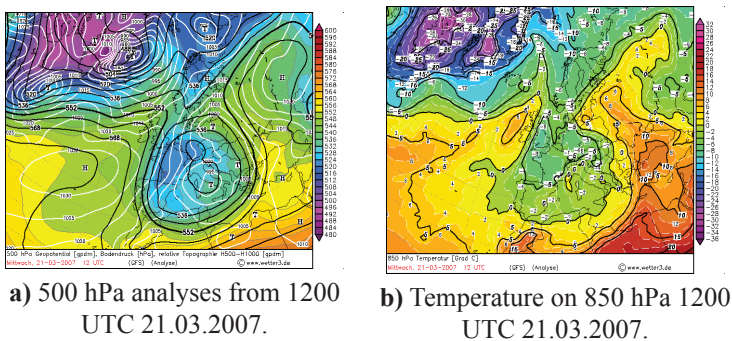


Fig. 5. 21 March 2007 – Malko Yonkovo tornado outbreak

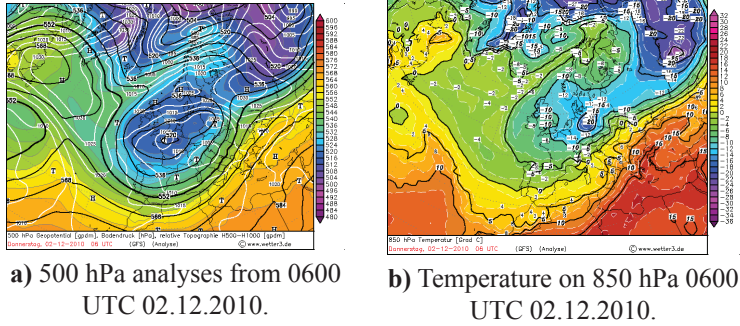


Fig. 6. 02 December 2010 – Bansko tornado outbreak

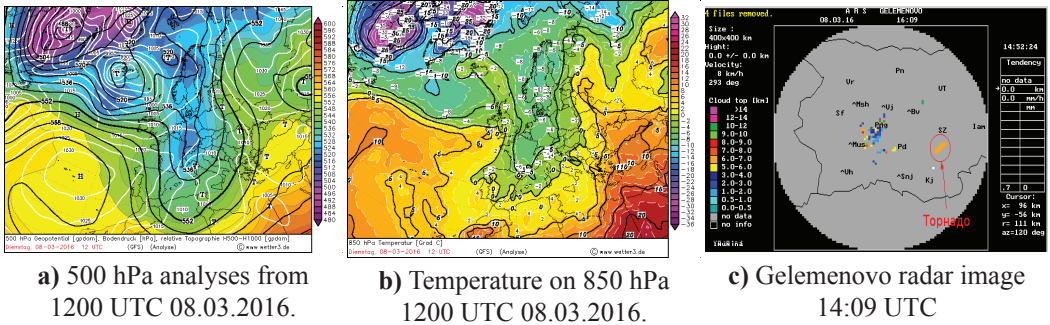


Fig. 7. 08 March 2016 – Dimitrovgrad tornado outbreak

In our case for description of thermodynamic conditions 4 instability indices and 4 parameters are chosen (Table 2). For their calculation the air sounding data from Sofia (for 3 cases in South Bulgaria) and Bucharest (for the case in North Bulgaria) are used as well as data from closest synoptic station in time interval near to tornado occurrence.

Table 2. Instability indices and thermodynamic parameters of the environment of Bulgarian cold-season tornadoes

Location	KI, °C	TT, °C	LI, °C	SWEAT	w_{max} , m/s	Hwmax, m	H_0 , m	Z_{El} , m
Bolyartsi	31.4	61	- 6.6	187	15	5578	2128	8078
Fatovo	14.3	50.4	- 4.3	108	13	4392	2278	9142
Malko Yonkovo	30.8	54.8	- 7.5	385	15	5911	3059	10161
Bansko	33	54.4	- 5.66	385	13	5114	3524	10613
Dimitrovgrad	*	*	*	*	*	*	*	*

Parameters in Table 2:

Four specific indices of instability based on sounding profiles of temperature, humidity and wind in the lower and middle troposphere are:

- **K Index** (George, 1960)

$$KI = (T_{850} - T_{500}) + T_{d850} - (T_{700} - T_{d700}) \quad (1)$$

- **Total Totals Index** (Miller, 1972)

$$TTi = (T_{850} - T_{500}) + (T_{d850} - T_{d500}) \quad (2)$$

where T_{850} , T_{700} , and T_{500} denote temperature at levels 850, 700, and 500 hPa and T_{d850} and T_{d700} denote dew point at levels 850 and 700 hPa.

- **Lifted Index** (Galway, 1956)

$$LI = (T_L - T_{500}) \quad (3)$$

where T_L is the temperature of an adiabatically (dry or wet depending on the level of saturation) ascending air parcel from level 850 hPa to level 500 hPa; T_{500} is the air temperature at level 500 hPa.

- **Severe WEather Threat index (SWEAT)** - Miller (1972)

$$SWEAT = 12T_{d850} + 20(TTi - 49) + 2V_{850} + V_{500} + 125(\sin(dd_{500} - dd_{850}) + 0.2) \quad (4)$$

where TTi is the Total Totals index, V_{850} and V_{500} denote the wind velocity at levels 850 hPa and 500 hPa respectively, and $dd_{500} - dd_{850}$ is the difference between the directions of wind in degrees at the two levels.

- W_{max} – the maximum value of updraft velocity - non-adiabatic empirical model (Simeonov& Syrakov, 1988)
- $H w_{max}$ – the level of maximum value of updraft velocity- non-adiabatic empirical model (Simeonov& Syrakov, 1988)
- H_0 – altitude of 0°C isotherm
- Z_{El} – altitude of Equilibrium level (El)

The calculated high absolute values of indices, presented in Table 2, indicate increased instability. According to other studies (Siedlecki, 2009) values of $KI > 25$, $TT > 49$ and $LI < -4$ indicate conditions favorable for the development of strong thunderstorms with hail and/or tornadoes. The calculated indices for tornado events in Bolyartsi, Malko Yonkovo and Bansko completely satisfy these limits. In Fatovo case KI index is very low, but nevertheless the biggest damages are reported. The explanation of this is in the use of Sofia aerological sounding data for calculation of the index. In 12:00 UTC the cold front passed the Sofia region and the temperature decreased while in the region of Fatovo the situation was quite different.

The SWEAT is close to the one for Greece (Sioutas, 2011) but lower than 400 which was found to be a threshold value for summer tornado storms in the USA (David, 1976). However, the mean values of SWEAT indices obtained in the study are close with the ones estimated for winter months between November and March and close to those for month with the highest tornado frequency in the USA - May (SWEAT_{may} = 253, in David, 1976). The other parameters are also near or above threshold values for strong thunderstorms in the warm half of the year in Bulgaria. The heights of the zero isotherm H_0 (Table 2) are within the limits of typical values (Simeonov et al., 1990) for the development of severe hail thunderstorms during the end of the spring (in May). Regarding the altitude of the Equilibrium level, all calculated values fall within the ranges determined by Boev and Marinov (1984) for the development of convective clouds during the warm half of the year.

CONCLUSION

The intensity analysis indicated that the cold season tornadoes in Bulgaria can be classified as F0–F1 of the Fujita scale which is equivalent to “weak” tornadoes. The analysis of the selected thermodynamic indices and wind parameters showed values comparable to those found in the literature as favorable for development of summer type severe convective storms.

The increased frequency of thunderstorms during the cold half of the year after 1991 (Bocheva&Marinova, 2016), as well as the accompanying severe convective events such as the winter tornadoes presented in this study, show the need for a detailed study of the causes of the occurrence and development of this type of phenomena, using more reliable information from meteorological Doppler radars, satellite data (or products) and other data for the vertical structure of the atmosphere.

REFERENCES

Antonescu B., Schultz D., Lomas F. (2016). Tornadoes in Europe: Synthesis of the Observational Dataset, *Mon. Wea. Rev.*, 144, 2445-2480, DOI: 10.1175/MWR-D-15-0298.1

- Bocheva L., Marinova T., Simeonov P., Gospodinov I. (2009). Variability and trends of extreme precipitation events over Bulgaria (1961 – 2005). *Atmos. Res.*, 93, 490-497.
- Bocheva L., Gospodinov I., Simeonov P. (2015). Comparative analysis of winter and summer tornado cases in Bulgaria. *BJMH*, v.20, 1-2, pp.3-12. (in Bulgarian)
- Bocheva, L., Marinova, T. (2016). Recent trends of thunderstorms over Bulgaria – climatological analysis. *Journal of International Scientific Publications: Ecology and Safety*, 10, ISSN:1314-7234, 136-144
- Bocheva L., Simeonov P. (2016). The tornado cases in Bulgaria from the beginning of 21st century – dabase and analysis. In: *Proceedings of the 3rd Bulgarian National Congress on Physical Sciences*, Sofia, Bulgaria, Sep. 29 - Oct. 02, 2016, S06.16-1-9 [DVD: ISBN 978-954-580-364-2] Heron Press: Sofia (in bulgarian)
- Boev P., Marinov A. (1984) Thermodynamically and spatial-temporal characteristics of severe hail processes over Bulgaria. *Hydr. and Meteor.*, XXXIII, 4, 10-17. (in Bulgarian)
- David Cl. (1976). A study of upper-air parameters at the time of tornadoes. *Mont. Weath. Rev.*, 104, 546-551.
- Galway, J. G. 1956. The lifted index as a predictor of latent instability. *BAMS*, 37, 528–529.
- George J. J. 1960. *Weather Forecasting for Aeronautics*. Academic Press, 673 pp.
- Glickman, T. S., Ed. (2000). *Glossary of Meteorology*. 2nd ed. Amer. Meteor. Soc., 855 pp.
- Graf M. (2008). Synoptical and mesoscale weather situations associated with tornadoes in Europe. Diploma thesis, Institute of Geography, University of Zurich (GIUZ) – published on line.
- Fujita, T.T. (1981). Tornadoes and downbursts in the context of generalized planetary scales. *J. Atmos. Sci.*, 38, 1511-1534.
- Holden J., A. Wright (2004). UK tornado climatology and the development of simple prediction tools. *Q.J.R.Meteorol.Soc.*, 130, 1009-1021.
- Kalnay, E. et al. (1996). The NCEP/NCAR 40-Year Reanalysis Project. *Bull. Amer. Meteor. Soc.*, 77, 437-471.
- Miller, R. C. (1972). Notes on analysis and severe storm forecasting procedures of the Air Force *Global Weather Central. Tech. Rept.* 200(R). Headquarters, Air Weather Service, USAF., 190 pp.
- Siedlecki M (2009). Selected instability indices in Europe. *Theor. Appl. Climatol.* 98, 85-94.
- Simeonov P., Syrakov D. (1988). On some characteristics determining the development of hail processes in Bulgaria. *10th Int.Cloud Phys. Conf.*, August, Bad Homburg, Deutscher Wetterdienst, Offenbach of Main, Germany, vol. II, 576-578.
- Simeonov P., Boev P., Petrov R., Syrakov D., Andreev V. (1988). Problems of Hail Suppression in Bulgaria, Kliment Ohridski University Press, Sofia, 316 pp. (in Bulgarian)
- Simeonov P., Bocheva L., Gospodinov I. (2013). On space-time distribution of tornado events in Bulgaria (1956-2010) with brief analyses of two cases. *Atmos. Res.*, 123, 61-70.
- Sioutas M. (2011). A tornado and waterspout climatology for Greece. *Atmos. Res.* 100, 344-356.
- Rauhala J., Brooks H.E., Schultz D. (2012). Tornado climatology of Finland. *Mon. Wea. Rev.*, 140, 1446-1456.



On the relationship between atmospheric and soil drought in some agricultural regions of South Bulgaria

Veska Georgieva*, Stanislava Radeva, Valentin Kazandjiev

*National Institute of Meteorology and Hydrology – BAS
66 Tsarigradsko shose Blvd., 1784 Sofia*

Abstract: Drought is an extreme event, which affects agriculture. Soil drought occurs when the soil water balance is impaired, which causes the deterioration of the physiological state of the plants and directly affects the yields of the crops. Due to the climatic features of the country, the agricultural lands of South Bulgaria suffer from insufficient humidity during the vegetation period of the main agricultural crops.

High frequency of extreme phenomena, in particular drought, as well as the several droughts observed in the first decade of the 21st century in Bulgaria and different parts of the world, is a premise for extended monitoring. The forecast of the intensity and the probability of drought acquire high importance.

The aim of the study is to investigate the potential in application of atmospheric drought index as a predictor of soil drought in the agricultural regions of Southern Bulgaria.

For this purpose, the Standardized Precipitation Index (SPI) and Soil Moisture Index (SMI) are used in the sense of an indicator of impending soil drought during the vegetation period. Representative dry, normal and wet years were selected. The potential for implementation of SPI as an indicator of imminent soil drought has been assessed.

Keywords: atmospheric and soil moisture, drought, indices

1. INTRODUCTION

Soil drought of varying intensity and duration is a distinctive extreme phenomenon, which determines to a great extent the profitability of the agricultural production in our country. Soil drought can be observed throughout the whole growing season.

The common feature of agrometeorological and meteorological drought is a shortage of precipitation, but agrometeorological drought should be characterized with some additional indicators, such as the difference between potential and actual

* veska.georgieva@meteo.bg

evapotranspiration and soil moisture (Wilhite, D.A., 2000). According to the same author, agrometeorological drought is a result of persistent meteorological one.

Drought monitoring, identification of its intensity and forecasting methods become actual due to increasing frequency of extreme events (IPCC, 2014), in particular drought, as well as drought periods registered in the first decade of 21st century in Bulgaria (Alexandrov, V., 2011) and around the world (Szezypta C. et al, 2012).

As early as the beginning of the last century, attempts have been made to define the concept of drought and ways of identifying it. Common to all types of drought is the fact that they originate from a deficiency of precipitation that result in water shortage. Since the middle of the 20th century precipitation amount is compared to soil water demand and vegetation cover – evapotranspiration (Heim R., 2002). In 1965 W. Palmer published his Palmer drought severity index (PDSI), creating an algorithm for assessing water balance through precipitation and temperature.

Later, McKee, et al., 1993 developed a Standardized Precipitation Index (SPI), which is currently widely used by the global scientific community to characterize moisture conditions for operational needs. To investigate the agricultural drought type, the Crop Moisture Index (CMI), the Palmer Moisture Anomaly Index (Z Index) and the Soil Moisture Anomaly Index (Keyantash J., J. Dracup, 2002) are most widely used.

Each index has both advantages and shortcomings in certain areas, and none of them uses the available water in the soil. The soil moisture index (SMI), developed in the High Plains Regional Climate Centre (HPRCC), determines the drought intensity by evaluating soil water available to plants (Hunt E., et al., 2008) regarding quantity for a given soil type. For the calculation of SMI, the measured soil moisture in agricultural crops is used, which allows to determine the degree of drought for a particular crop.

The aim of the study is to investigate the potential in application of atmospheric drought index as a predictor of soil drought in the agricultural regions of Southern Bulgaria.

2. MATERIAL AND METHODS

Areas of interest are the agricultural regions in Southern Bulgaria, covering the Thracian Lowland and Southeastern Bulgaria. Daily data for precipitation, ten-day data from soil moisture measurements for the period 1981-2010 at 8 stations (Fig. 1), and hydrological characteristics for representative soils were used.

Soil moisture is measured by the gravimetric method, according to the methodology of the National Institute of Meteorology and Hydrology (NIMH). Measurements are conducted every ten days at depths from 10 cm to 1 m during the growth season. For this investigation we used measured soil moisture under winter wheat for 0-30 cm, 0-50 cm and 0-100 cm soil layers during vegetation season (IV-IX).

According to the climatic zoning of the country, the agricultural land in the area of interest falls into two climatic areas - Moderate Continental and Continental-

Mediterranean. The precipitation regimes in these two climatic areas are different - in the first continental area (maximum is during the summer and the minimum is in the winter), in the second climatic area – maximum is in the winter and the minimum in the summer.

The main soil types on the region are Cinnamonic (typical and leached) – Sliven, Haskovo, Svilengrad, Plovdiv, Pazardhik and Vertisols (typical and leached) –Karnobat и Chirpan.

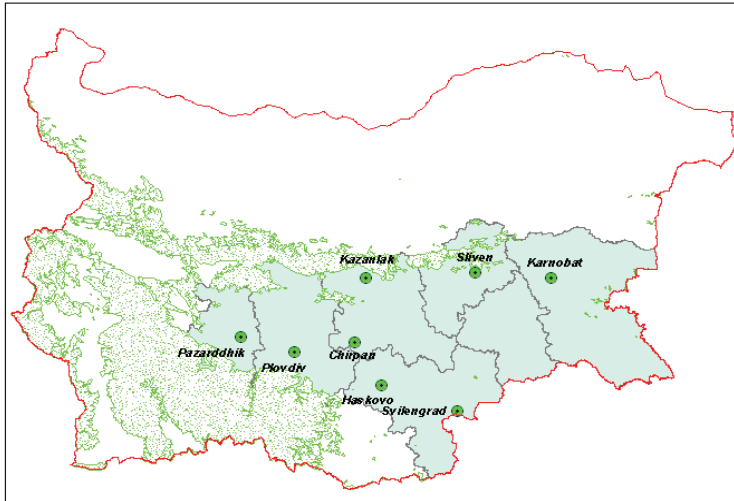


Fig. 1. Area of investigation and location of stations.

The Standardized Precipitation Index (SPI) is widely used to assess atmospheric drought. SPI is a tool which was developed primarily for defining and monitoring drought. It enables analysts to determine the rarity of a drought at a given time scale (temporal resolution) of interest for any rainfall station with historic data. It can also be used to determine periods of anomalously wet events. The SPI is not a drought prediction tool. Mathematically, the SPI is based on the cumulative probability of a given rainfall event occurring at a station. The historic rainfall data of the station is fitted to a gamma distribution, as the gamma distribution has been found to fit the precipitation distribution quite well.

The relative simplicity of the calculations, as well as the few required input data, only a quantity of precipitation, makes it a universal index of assessing moisture conditions. Its application in operational practice is significant. SPI is calculated daily for a 10 day time scale.

Table 1 Drought classification by SPI value and corresponding event probabilities

SPI value	Classification	Cumulative probability (%)
2.00 or more	Extremely wet	2.3
1.50 to 1.99	Very wet	0.4
1.00 to 1.49	Moderately wet	9.2
0 to 0.99	Mildly wet	34.1
0 to -0.99	Mild drought	34.1
-1 to -1.49	Moderate drought	9.2
-1.50 to -1.99	Severe drought	4.4
-2.00 or less	Extreme drought	2.3

The soil moisture index (SMI) classifies the land by measuring or modeling soil moisture values using the following formula:

$$SMI = \frac{5 * (SM - WP)}{(FC - WP)} - 5$$

where: **SM**- Soil Moisture (cm³/cm³); **WP**-Wilting Point (cm³/cm³) and **FC**- Field Capacity (cm³/cm³).

SMI characterizes soil drought from normal to extreme, with the degree of drought increasing when the index decreases (Table 2).

Table 2 Classification of drought events according to SMI

Drought conditions	SMI
Less intense	0–1 or more
Moderate	–2 to –1
High intense	–3 to –2
Severe	–4 to –3
Extreme	–5 or less

3. RESULTS AND DISCUSSION

Agrometeorological dry spell and drought of varying intensity were recorded in 14 of the first 15 years of the 21st century. Dry spell and drought are recorded during each of the months of the vegetation period. In April, soil drought is a less common event, but when it happens, it can have serious consequences. An example of such an extreme phenomenon is the drought that began in April 2007. As a consequence of it is the damage of autumn crops in northwestern and northeastern Bulgaria. Often, drought

occurs in May. For example, in 2000, 2003, 2007 and 2015, in some regions of the country, the soil moisture was less than 70% FC in May.

June appears to be critical for soil water supplies in spring crops, as it was in 2000, 2002, 2003, 2010, 2015. The consequences of drought in these cases are the recorded damages in winter crops, vegetables and orchards. Soil drought in July was recorded in 2000, 2001, 2004 (only in separated regions), 2007 (soil water availability reach 23% of FC in Southern Bulgaria), 2008 (beginning of drought), 2011, 2015. In August, soil water supplies reach their lowest values, even in years that are considered wet. In two-thirds of the years under review (2000, 2001, 2003, 2004, 2006, 2007, 2008, 2009, 2014, 2015) soil drought was registered in August. In some years, the summer drought passes in autumn - 2003, 2004, 2008, 2009, 2015 when the September's soil water balance was decreased. (Hydro-meteorological Bulletins of NIMH).

Rainfalls in the area under consideration are between 85% (Pazardzhik) and 98% (Svilengrad) in the average of the country (Fig.2). Only in Haskovo annual rainfall exceeds the average of the country by 9%, but this is due to the autumn-winter rainfalls, since only 44% of them are in the vegetation period. The lowest rainfall sums are recorded in Plovdiv and Pazardzhik, but over 50% of them are in the vegetation season. The highest precipitation rate during the growth season is in Kazanlak (60%), and the smallest in Svilengrad (42%).

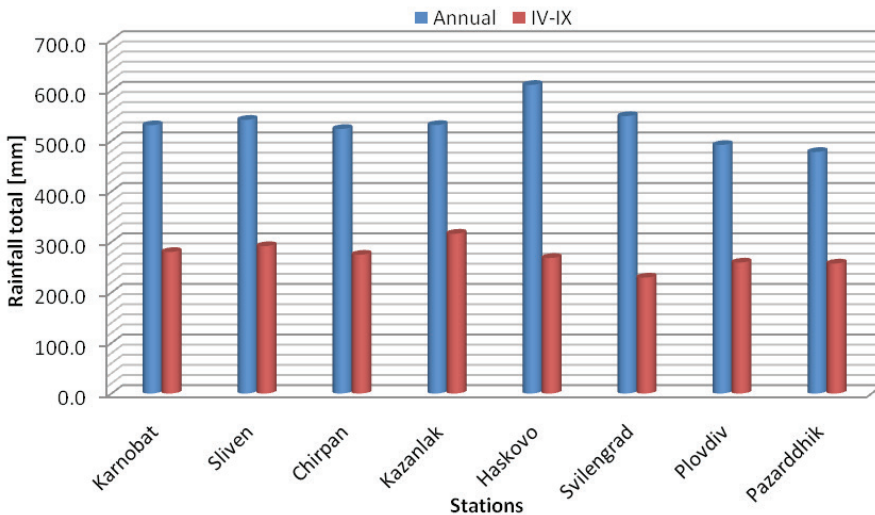


Fig.2. Long-term annual vegetation season precipitation sums (IV-IX)

SPI values were determined during the vegetation period for ten days (Fig.3). Half of the cases (between 49 and 55%) indicate atmospheric drought with moderate, severe and extreme intensity.

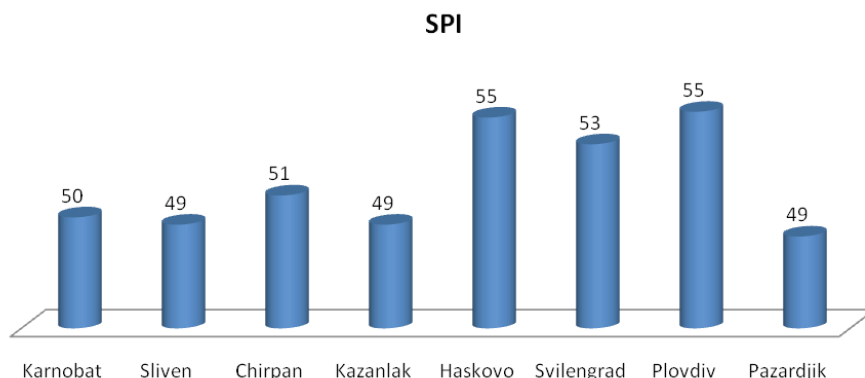


Fig. 3. Percentage of cases with extreme, severe, moderate and mild drought events according to SPI (ten days step for vegetation period)

Previous studies (Georgieva V., V. Kazandjiev, 2015) set the SMI values for which the quantities of soil moisture are less than 70% FC. It has been shown that danger for agriculture is increased, when the SMI values indicate strong and extreme drought.

The values of SMI for three soil layers - 0-30 cm, 0-50 cm and 0-100 cm for the ten-days periods have been determined and only the cases with a significant drought intensity for agriculture are selected (Fig. 4). The highest is the percentage of these cases in the upper soil layer (Fig. 5a), reaching up to 100% in Pazardzhik. In the deeper soil layers (Fig. 5 b, c) the percentage of cases decreases, but the difference is insignificant. In Karnobat the conditions of formation and utilization of water reserves in the soil differ from those in the other considered stations, because only the percentage of cases with soil drought is significantly lower than those indicated by SMI, respectively 34, 30 and 29% in the three soil layers. The remaining stations are between 56% and 100%.

The comparison between the drought cases reported by the SPI and the SMI indices shows that in a large percentage of cases, registered drought (according to SMI) is not indicated by the SPI, (Fig. 3 and Fig. 4).

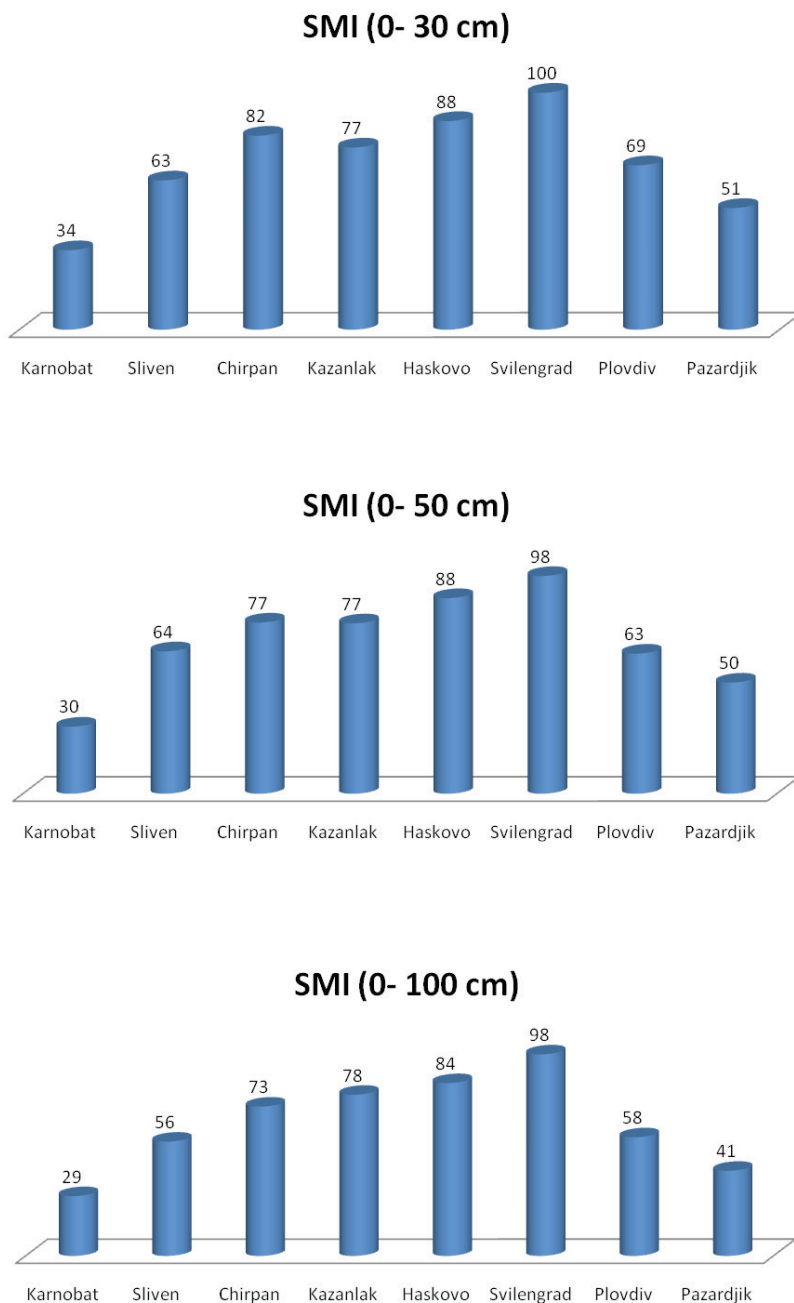


Fig. 4. Percentage of cases with increased drought (SMI) for three soil layers: a) 0-30 cm; b) 0-50 cm; c) 0-100 cm during the vegetation season

The distribution of the negative values of SPI reports atmospheric drought of varying intensity between 40 and 60% of the examined cases, evenly throughout the growth season, (Fig. 5). In each of the vegetation months, 50% of the ten-days periods have been reported as one of the degrees of extreme drought - extreme, severe, moderate and mild.

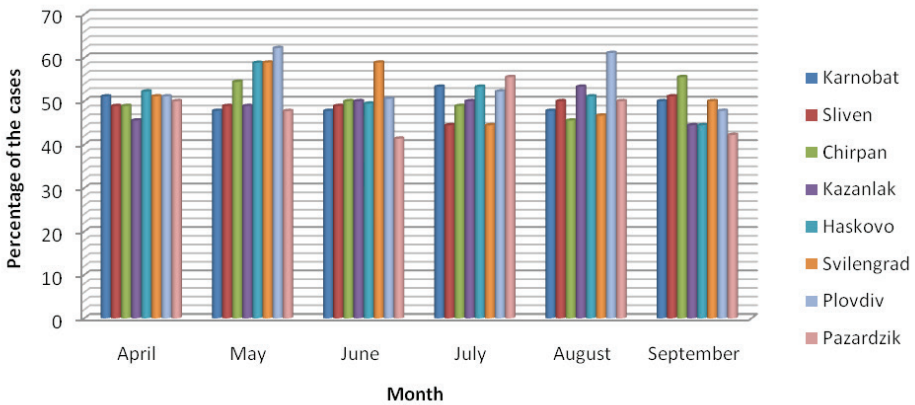


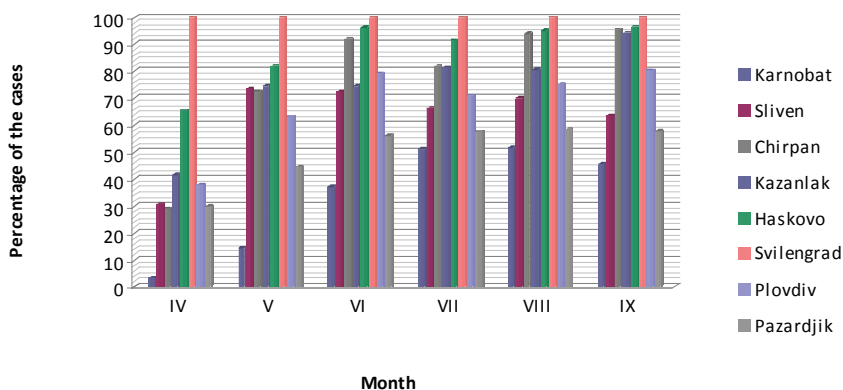
Fig. 5. Extreme, severe, moderate and mild drought distribution according to SPI during the vegetation season

Soil drought variations presented through the numbers of cases according to SMI are much higher. The largest in the 0-30 cm layer is in April (3-100%) and in May (14%-100%) – (Fig. 6), with the lowest number of droughts in April (Karnobat, Chirpan, Pazardzhik under 5%). In June, July, August and September, more than 50% of the occurrence of soil drought is observed, with the exception of region of Karnobat. The high percentage of cases of autumn drought in Chirpan, Kazanlak, Haskovo, Svilengrad and Plovdiv is noticeable. In the deeper soil layers in April and May, soil drought is not a common event, with the exception of Kazanlak, Haskovo, Plovdiv and Svilengrad stations.

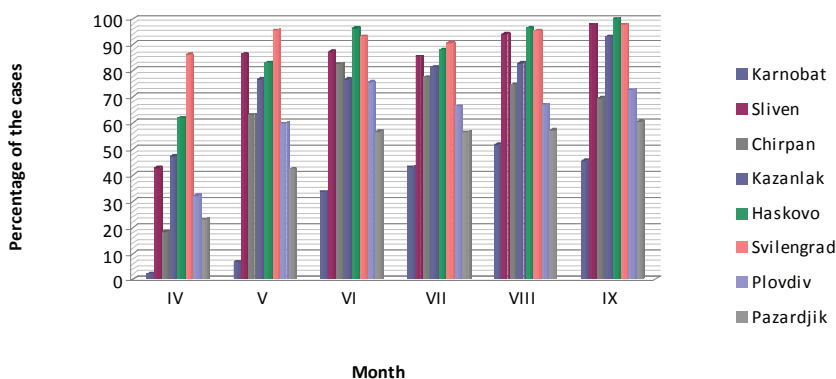
Only in April the cases of atmospheric drought exceed those with established soil drought. The soil water consumption in April is greatest, but at the beginning of the spring vegetation, soil water reserves usually reach to FC. This allows short droughts to be overcome without reaching moisture depletion below the optimum. The highest exceedance of the percentage of cases with soil drought is in August and September and at Svilengrad station, reaching 50%.

Different information is used to determine the two indices - rainfall SPI and soil humidity for SMI, which explains the insufficient relationship between them. Given that precipitation is the main resource for soil water supplies formation, we sought a correlation between the ranges of SPI and SMI for the three soil layers. Table 3 shows

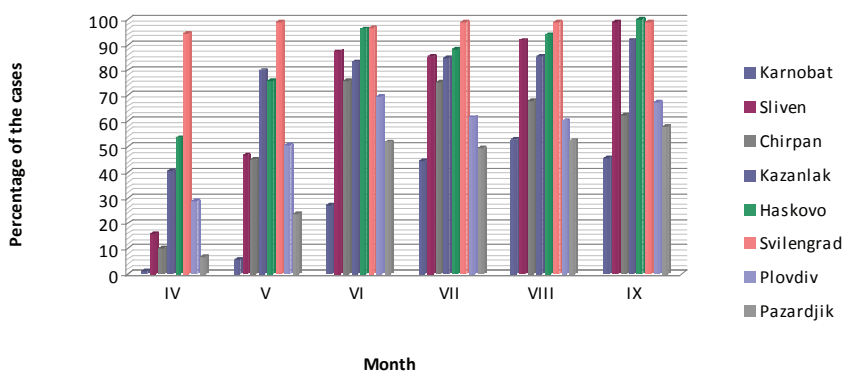
the correlation coefficients that indicate the absence of a significant relationship between the two indices.



a)

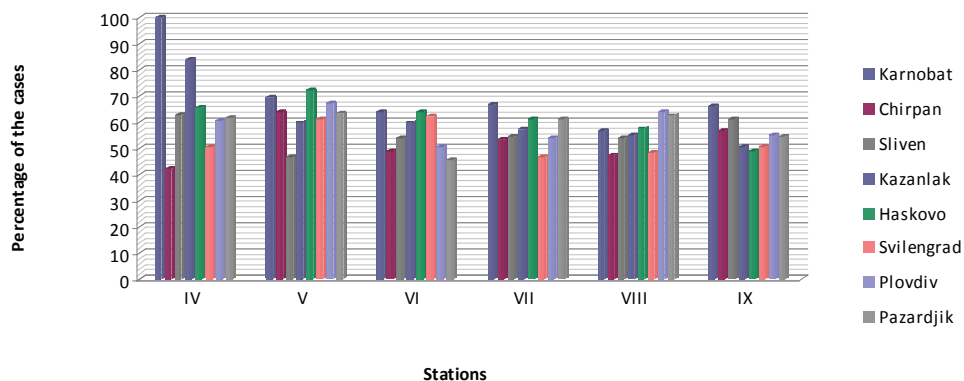


b)

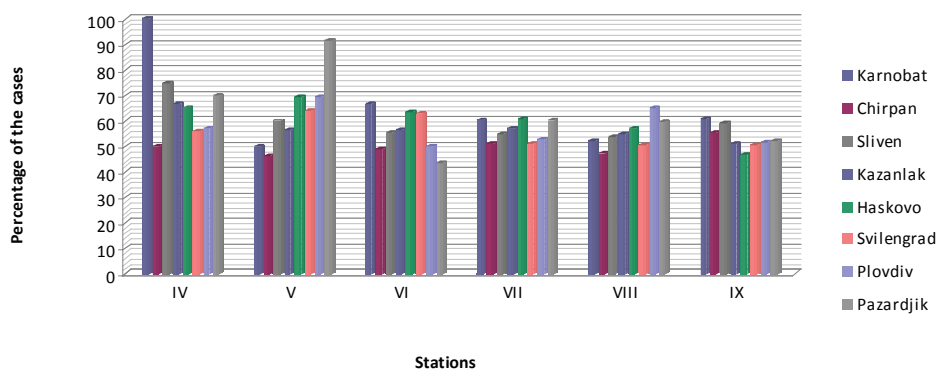


c)

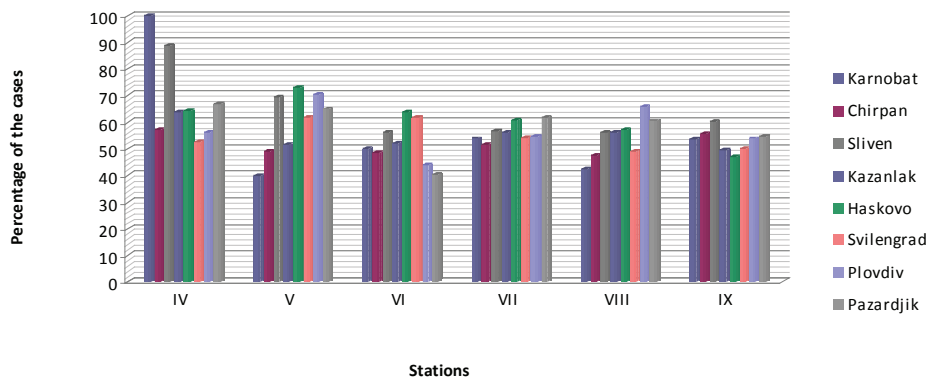
Fig. 6. Monthly distribution in (%) of cases with extreme, severe and high intense drought according SMI during the vegetation period in 3 soil layers: a) 0-30 cm; b) 0-50 cm; c) 0-100 cm



a)



b)



c)

Fig. 7. Coincidence of drought events: a) SPI and SMI 0-30 cm; b) SPI and SMI 0-50 cm; c) SPI and SMI 0-100 cm

Table 3 Correlation coefficient between SPI and SMI for 3 soil layers

Stations	0-30 cm	0-50 cm	0-100 cm
Karnobat	0.31	0.23	0.15
Sliven	0.22	0.29	0.24
Chirpan	0.15	0.11	0.07
Kazanlak	0.45	0.40	0.27
Haskovo	0.32	0.28	0.21
Svilengrad	0.25	0.26	0.20
Plovdiv	0.00	-0.01	-0.01
Pazardjik	0.04	0.04	0.01

The correlation between SPI and SMI-indicated droughts for the three layers by months during the vegetation period (Fig. 7) was analyzed. The highest coincidence rate is in April and May, but then, there are the least observed cases of soil drought. A higher incidence rate was observed in Karnobat, where the number of drought cases was the lowest. In 50-60% of the cases of soil drought, SPI values are negative, i.e. atmospheric drought is also reported. Conversely, in more than 40% of the SPI cases reported by the SMI does not indicate drought.

This result, as well as the low correlation coefficient between SPI and SMI, indicates that SPI alone can not be used to determine soil drought. For this purpose, it is necessary to use a quantitative indicator that takes into account the water deficit in the soil.

4. CONCLUSIONS

A parallel study of SPI and SMI over the period 1981-2010 was conducted. Summarizing the obtained results, following conclusions can be made:

1. During the period of investigation, the number of soil drought cases determined by the SMI value is significantly higher than that of atmospheric droughts according to the SPI value. That is because SPI gives an idea of precipitation deviation from the climate norm and does not take into account the losses of soil water by evaporation and transpiration;
2. The correlation between SPI and SMI during active vegetation period April – September is not significant;
3. It is found that both SPI and SMI indices are not always consistent. For example, when SMI indicates soil drought SPI does not always indicate atmospheric drought too;
4. SPI gives an inaccurate idea of soil drought. That is particularly true for the months of July and August. In relation to that, it is necessary to extend the study

on identification of an additional index connecting SPI and SMI in the case when the results of SPI deviate from that of SMI.

REFERENCES

- Alexandrov, V. 2011. Drought in Bulgaria. Sofia 2011, p.44.
- Georgieva V., V. Kazandjiev, 2015. Soil drought – degree and conditions of rise. Proc. Soil and agro technologies in the changing world, May, Sofia, Bulgaria (in Bulgarian).
- IPCC.2014. Impacts, Adaptation, and Vulnerability. http://www.ipcc.ch/pdf/assessment-report/ar5/wg2/ar5_wgII_spm_en.pdf
- Heim R. R., 2002. A review of twentieth-century drought indices used in United States. BAMS, vol. 83, 1149-1165.
- Hunt E., K. Hubbard, D. Wilhite, T. Arkebauer and A. Dutcher. 2008. The development and evaluation of a soil moisture index. International Journal Climatology v. 10.1002/joc.1749.
- Keyantash J., J. Dracup, 2002: The Quantification of Drought: An Evaluation of Drought Indices. Bull. Amer. Meteor. Soc., 83, 1167–1180.
- McKee, T.B., N. J. Doesken, and J. Kliest, 1993: The relationship of drought frequency and duration to time scales. In Proceedings of the 8th Conference of Applied Climatology, 17-22 January, Anaheim, CA. American Meteorological Society, Boston, MA. 179-18
- Palmer, W. C., 1965: Meteorological Drought. Weather Bureau, Research Paper No. 45, U.S. Dept. of Commerce, Washington, DC, 58 pp.
- Szezypta C., B. Deecharme, D. Carrer, J-C Calvet, S. Lafont, S. Somot, S. Farous and E. Marthin, 2012. Hydrology and Earth System Sciences, 16, 3351-3370.
- Wilhite, D.A. 2000. Drought, a global assessment. Natural Hazards and Disasters Series, vol. 1. Routledge, London, UK.
- ***Monthly Hydrometeorological Bulletin (IV-IX) 2000-2015.



Numerical study of meso-scale circulation specifics in the Sofia region under different large-scale conditions

Evgenia Egova^{1,2*}, Reneta Dimitrova¹, Ventsislav Danchevski¹

¹*Faculty of Physics, Department of Meteorology and Geophysics - Sofia University "St. Kliment Ohridski", 5 James Bourchier Blvd., 1164 Sofia, Bulgaria*

²*National Institute of Meteorology and Hydrology - BAS, 66 Tsarigradsko shose Blvd., 1784 Sofia, Bulgaria*

Abstract: Accurate airflow forecast over large urban areas in complex orography is very important problem and it is still a big challenge. Terrain and land-cover inhomogeneity cause thermal circulation domination under calm conditions, or significant modification of the large-scale synoptic flow. The Weather Research and Forecasting (WRF) model is used for numerical experiments with fine horizontal grid of 500 meters. The static terrestrial data are represented with very high resolution (1 arcsec for the orography and 3 arcsec for land-cover data). The purpose of this work is to assess the ability of WRF model to study the specifics of meso-scale circulation under various large-scale (synoptic) conditions for the Sofia region. Different model options (for microphysics and planetary boundary layer - PBL) are tested during the evaluation process based on comparison to measurements in order to determine the optimal configuration. Overall Lin et al. microphysics scheme shows the best performance. None of the PBL schemes is found to be superior, but all provide reasonable results. WRF model shows good performance and it is a very useful tool to study flow structure and variability. Different mesoscale phenomena are properly captured with numerical simulations.

Keywords: flow modification over complex orography, meso-scale phenomena, WRF, model sensitivity tests, evaluation for Sofia region.

1. INTRODUCTION

Several types of investigation (theory, numerical modelling and laboratory experiments) are used to study atmospheric dynamics and physics that play an important role in atmospheric processes. The analytical theory is limited to simplified equations

* evgenia.egova@abv.bg

that are unable to describe fully the atmosphere in its complexity. The advantages of laboratory experiments are their simplicity and directness, but not all major phenomena can be simulated (Tucker, 1989; Baines&Manins, 1988). Numerical modeling is a main tool for studying the phenomena in atmosphere and its potential is almost unlimited with fast improvement of computer resources during the last decade.

Meso-scale systems can be defined as those atmospheric systems that have a horizontal extent large enough for the hydrostatic approximation to the vertical pressure distribution to be valid, but small enough for the geostrophic and gradient winds to be inappropriate as approximations to the actual wind circulation above the planetary boundary layer (Pielke, 2013). Many different classifications are used in the literature. One of the most popular classifications (Orlanski, I., 1975) divides meso-scale systems into 3 sub-categories with horizontal scales for meso-gama between 2 and 20 km; meso-beta 20-200 km; and meso-alpha 200-2000 km. Some of the processes in the meso-alpha are at the edge of the synoptic systems which horizontal scales can start from 1000 km. This study investigates the atmospheric phenomena in meso-gama scale. Terrain and land-use inhomogeneity cause local thermally driven wind systems dominant under calm conditions (Zardi and Whiteman, 2012), or significant modification of the synoptic flow (Bretherton et al., 2009; Dixit&Chen, 2011).

Orography presents significant forcing on geophysical flows and induce substantial adjustment of the large-scale flow. The strong airflow under stratified conditions generates lee waves, propagating internal waves, rotors, flow separation or canalization and fascinating vortex structures. The part of the flow above the so-called dividing streamline goes over the mountain whilst the rest flows around the mountain (Snyder et al., 1985) producing upstream stagnation, the lee-side separation region and associated wake effects. The inhomogeneity of the flow, irregular protrusions from an obstacle in the direction of the approaching flow, slope angle, ground roughness lead to very complicated pattern. The varieties that incorporate slopes, valleys, canyons, escarpments, gorges and bluffs span different space-time scales contributing to innumerable phenomena that stymie the predictability of mountain weather.

Diurnal mountain winds develop typically under fair weather conditions, over complex topography of all scales, from small hills to large mountain massifs, and are characterized by a reversal of wind direction twice per day (Zardi&Whiteman, 2012). In the surface heated planetary boundary layer (PBL) landscape heterogeneities produce significant horizontal gradients in temperature that form phenomena like land and sea breezes. All these local thermally driven meso-scale circulations can be accelerated or suppressed by the large-scale flow. Urbanization in the post-industrial revolution era, especially the recent rapid urban growth, has brought about unprecedented anthropogenic stressors that may change the functioning and structure of the Earth system or a part thereof (Hunt et al., 2007). Intense modification of land surface occurs through urban development (Changnon, 1992), and the use of high heat capacity and water impermeable material for construction and roadways affects local microclimates. The differences in

energy balance, temperature, humidity, and storm runoff between urban areas and rural surfaces are substantial. A common urban effect is the urban heat island associated with the retention of heat in concrete and other material for longer times at night in urban compared to rural areas (Bornstein, 1987; Oke, 1988; Emmanuel&Fernando, 2007).

Sofia city is located in complex terrain in close proximity to Vitosha Mountain with highest peak Cherni vrah – 2286 m AGL (above ground level). All described factors above contribute to a very complicated flow pattern in Sofia valley that is difficult to predict. The purpose of this work is to investigate the abilities of the Weather Research and Forecasting (WRF) model to capture the specifics of the meso-scale circulation under different large-scale conditions for the Sofia region. Very high resolution static terrestrial fields (1 arcsec for the topography and 3 arcsec for land cover) are used in this study. Performance evaluation of different parameterization schemes (for both microphysics and PBL) is accomplished through comparison with observation.

2. DATA AND METHODOLOGY

The Advanced Research version of the Weather Research and Forecasting model (ARW-WRFv3.8.1.) is employed in this study. The ARW-WRF is a state-of-the art atmospheric meso-scale numerical weather prediction system, suitable for use in a broad range of applications (Skamarock et al., 2008; <http://www.mmm.ucar.edu/wrf/users>). The system solves fully compressible, Euler non-hydrostatic equations conservative for scalar variables, over terrain-following vertical coordinates with the possibility of vertical grid stretching. The upper boundary of the model is a constant pressure surface.

2.1. Domain set-up and initial conditions

A Lambert Projection is used with the center point for the modelling domain at 23.4°E, 42.68°N. Four nested domains with 32, 8, 2 and 0.5 km grid resolution are explored to perform meso-scale simulations, with the smallest one covers the Sofia valley. The model domains with an enlarged view of the most inner domain with 500 m resolution and 157x129 grid points (approximately 80x65 km) is shown Fig. 1.

Fifty terrain-following (η) levels are selected, with 21 levels between the surface and 500 m AGL to describe better the lowest part of the PBL. Meteorological initial and boundary conditions are provided to the coarsest meso-scale simulations from the National Centers for Environmental Prediction (NCEP) Final Analysis 0.25 degrees with outputs every 6 h (<http://rda.ucar.edu/datasets/ds083.2/>). Two new datasets have been implemented and adapted to the study domain - high resolution topography data (SRTM, NASA; <https://lta.cr.usgs.gov/SRTM1Arc>) with resolution 1 arcsec (approximately 30 m), and the Corine land-cover dataset (CLC2012, EEA; <http://land.copernicus.eu/pan-european/corine-land-cover/clc-2012>), with resolution 3 arcsec (approximately 90 m), which have been adopted to US Geological Survey land-use (USGS) classes.

More details regarding the procedure and new datasets implementation can be found in Vladimirov et al. (2018).

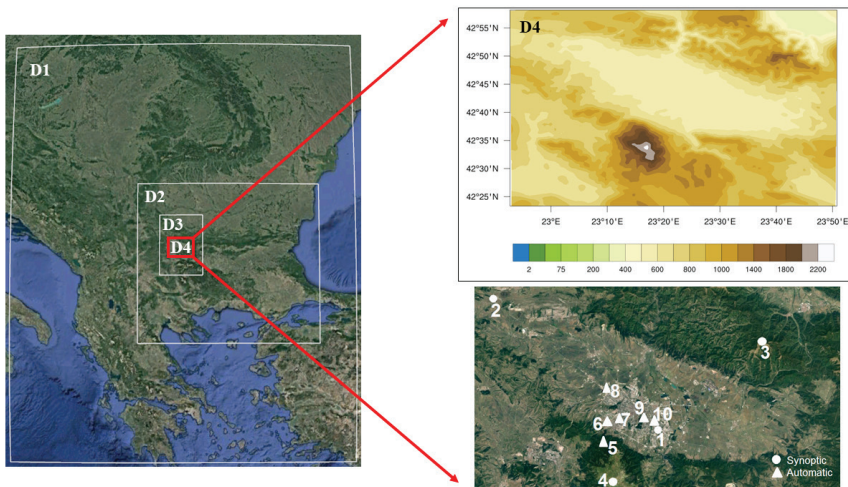


Fig. 1. Domain configuration (left panel); topography of the most inner domain (500 m grid) and location of the observational sites used for model validation (right panel).). SYNOP stations (circle symbol): 1. Sofia, 2. Dragoman, 3. Murgash, 4. Cherni vrah and Automatic stations (triangle symbol): 5. Kopitoto 6. Pavlovo 7. Hipodruma 8. Nadezhda 9. Borisova gradina and 10. Druzhba

2.2 Model options

The WRF physics package includes: the Rapid Radiative Transfer Model (RRTM) longwave radiation parameterization (Mlawer et al., 1997), Dudhia shortwave radiation parameterization (Dudhia, 1989), which computes radiation at fine time scales (every 10 min), and Grell-Devenyi (GD) ensemble scheme (Grell&Devenyi, 2002) for cumulus parameterization (only for the coarse meso-scale simulation with 32 and 8 km grids). Noah land surface model scheme (Chen&Dudhia, 2001) is chosen for this study. Four of the available in the model PBL schemes (with their corresponding surface schemes) are considered after preliminary comparison against observations in previous studies. The selected PBL schemes are: the Yonsei University scheme, YSU (Hong et al., 2006), the Asymmetric Convective Model, version 2 scheme, ACM2 (Pleim, 2007), the Bougeault and Lacarrere scheme, BouLac (Bougeault&Lacarrere, 1989), and the Quasi-Normal Scale Elimination scheme, QNSE (Sukoriansky et al., 2005). In addition comparison between model results for different microphysics schemes are conducted for one case with very high humidity (February 5th 2016). The YSU PBL scheme is used with four available microphysics options, all of them suitable for real-data high-resolution

simulations: a sophisticated scheme Lin et al. (Lin et al., 1983), WRF Single-Moment 6 (Hong&Lim, 2006), Goddard (Tao et al., 1989) and Thompson (Thompson et al., 2008).

2.3. Case studies selection

This study exemplifies the ability of WRF model to represent properly the meso-scale circulation in Sofia valley and study flow modification under different synoptic conditions. Nine cases between summer 2015 and summer 2016 are selected using weather maps for flow and temperature at 850 hPa and observational data from the radiosonding made once a day at 12 UTC at the National Institute of Meteorology and Hydrology (NIMH), Bulgarian Academy of Sciences (BAS). Sofia valley's orientation is Northwest-Southeast and flow directions along the axis (Northwest (NW) and Southeast (SE)) and across (Southwest (SW) and Northeast (NE)) are chosen for the simulations. The case studies are described in Table 1 - calm conditions (wind speed is lower than 5 m/s) and two classes depending on the wind speed – moderate (between 5 and 10 m/s) and strong (wind speed is higher than 10 m/s). Most of the cases, presented in Table 1, are associated with passage of atmospheric disturbance (cyclone or trough) over the Balkan Peninsula and with significant change in 850 hPa temperature. Due to the dynamics of the processes wind conditions are relatively fast changing. All simulations are run with spin-up of 24 hours before each of the selected cases.

Table 1. 9 cases (10 days) of simulations between August 2015 and August 2016.

Cases	Start (UTC)	End (UTC)	Wind Description	Wind Speed
Case 1	14/08/2016 00:00	16/08/2016 00:00	Calm	< 5 m/s
Case 2	04/01/2016 00:00	05/01/2016 00:00	Moderate SW	5 – 10 m/s
Case 3	06/08/2015 00:00	07/08/2015 00:00	Moderate NE	5 – 10 m/s
Case 4	11/11/2015 00:00	12/11/2015 00:00	Moderate NW	5 – 10 m/s
Case 5	22/10/2015 00:00	23/10/2015 00:00	Moderate SE	5 – 10 m/s
Case 6	22/11/2015 00:00	23/11/2015 00:00	Strong SW	> 10 m/s
Case 7	05/02/2016 00:00	06/02/2016 00:00	Strong NE	> 10 m/s
Case 8	25/05/2016 00:00	26/05/2016 00:00	Strong NW	> 10 m/s
Case 9	27/11/2015 00:00	28/11/2015 00:00	Strong SE	> 10 m/s

2.4. Observations

The observational data used for the model validation and sensitivity tests are based on data from ten surface stations, and vertical profiles from radiosonde at one site, National Institute of Meteorology and Hydrology (NIMH), once per day at 12 UTC. The surface stations are: four operational sites (SYNOP) in which data are recorded

every 3 hours: Sofia - NIMH (552 m AGL), Cherni Vrah (2286 m AGL), Murgash (1687 m AGL) and Dragoman (716 m AGL); five automatic stations operated by the Ministry of Environment and Water - Kopitoto (1321 m AGL), Sofia - Nadezhda (534 m AGL), Sofia - Pavlovo (615 m AGL), Sofia -Krasno selo (581 m AGL) and Sofia -Druzhba (548 m AGL), and additional automatic station operated by the Sofia University at Borisova Gradina (577 m AGL) provide hourly records of atmospheric parameters . Air temperatures and relative humidity from all stations are used in model validation. Simulated wind speed and direction are only verified against radiosonde data as all other wind measurements are strongly influenced by obstacles in station's surroundings. The location of observational sites used for model verification are presented in Fig. 1.

3. RESULTS AND DISCUSSION

3.1. Model validation

The model performance at surface level is assessed by comparison of modelled 2m temperature and relative humidity against measurements. Certain statistical accuracy metrics as standard deviation (*SD*), mean bias (*MB*), mean absolute error (*MAE*), root mean square error (*RMSE*), and correlation coefficient (*R*) are also estimated.

Two experiments have been conducted to find the best model configuration by varying PBL and microphysics parameterization schemes at fixed other options. Four different microphysics schemes are tested with the most widely used PBL scheme YSU for one case (Case 7, Table 1) with very high humidity. The selected microphysics option is used further to compare different PBL schemes for all considering cases.

The first experiment considers only Case 7 of Northeastern synoptic flow with high relative humidity (February 5th 2016). For all other selected cases the moisture level is low, relative humidity less than 50%, and the effect of the microphysics option can be ignored. Statistical metrics for two stations are presented - Sofia-NIMH (Table 2) and Borisova gradina (Table 3). The model performs well for both sites, with similar values for different statistical measures. WRF slightly overestimates the temperature with MB, MAE and RMSE values approximately 1°C. The relative humidity is underestimated with about 10% by all considering schemes. The RMSE is higher for the station Borisova gradina with maximum value 17%, than for Sofia-NIMH - 12%. The correlation coefficient is reasonable for all selected microphysics schemes, more than 0.6, as the temperature is better captured at Borisova gradina, the relative humidity at Sofia-NIMH. Overall the Lin scheme shows the best performance for both temperature and relative humidity and it has been selected to be used for the second experiment.

Table 2. Model microphysics evaluation metrics for air temperature and relative humidity in very humid Case 7 (February 5th 2016) at station Sofia-NIMH (number of measurements - 8).

Sofia-NIMH	<i>Mean</i>	<i>SD</i>	<i>MB</i>	<i>MAE</i>	<i>RMSE</i>	<i>R</i>
Temperature [°C]						
Observations	0.0	0.9				
Lin scheme	0.7	0.7	0.7	0.7	0.9	0.75
WRF Single moment 6 class scheme	0.7	0.6	0.7	0.7	1.0	0.65
Goddard scheme	0.5	0.6	0.5	0.5	0.8	0.63
Thompson scheme	0.8	0.6	0.7	0.8	1.0	0.60
Relative Humidity [%]						
Observations	89.6	5.5				
Lin scheme	77.9	6.9	-11.7	11.7	11.9	0.97
WRF Single moment 6 class scheme	79.9	7.9	-9.7	9.7	10.5	0.87
Goddard scheme	81.8	8.7	-7.8	7.8	9.0	0.90
Thompson scheme	78.9	10.1	-10.6	10.8	12.1	0.89

Table 3. Model microphysics evaluation metrics for air temperature and relative humidity in Case 7 (February 5th 2016) at station Borisova gradina (number of measurements - 24)

Borisova gradina	<i>Mean</i>	<i>SD</i>	<i>MB</i>	<i>MAE</i>	<i>RMSE</i>	<i>R</i>
Temperature [°C]						
Observations	-0.3	0.7				
Lin scheme	0.7	0.9	1.0	1.0	1.1	0.86
WRF Single moment 6 class scheme	0.9	0.7	1.1	1.1	1.2	0.69
Goddard scheme	0.5	0.8	0.8	0.8	0.9	0.84
Thompson scheme	0.6	0.8	0.9	0.9	1.0	0.81
Relative Humidity [%]						
Observations	93.5	0.6				
Lin scheme	78.7	8.1	-14.8	14.8	16.7	0.77
WRF Single moment 6 class scheme	79.3	9.8	-14.2	14.3	17.0	0.70
Goddard scheme	82.8	9.3	-10.7	11.0	13.9	0.82
Thompson scheme	82.1	8.7	-11.4	11.5	14.1	0.71

Four different PBL schemes are tested further for all selected study cases described in Table 1. Results of the calculated statistics are presented separately for automatic stations (Tables 4, 5) and SYNOP stations (Table 6). The reason for this separation is that the hourly data from the automatic stations represent more precisely diurnal cycle than data taken on every 3 hours. There is no substantial difference between performances

of the selected PBL schemes. WRF is in better agreement with observations for the cases with moderate (Table 4) than strong (Table 5) wind conditions. The tendency of overestimation of the temperature at 2 m with approximately 1-2°C (mean, *MB*, *MAE*, *RMSE*) is found in all PBL schemes for all study cases. The relative humidity is underestimated with approximately 7% for the moderate (Table 4) and 10% for strong (Table 5) wind conditions. The correlation coefficient differs between schemes and sometimes one scheme performs better for the temperature but worse for the humidity.

Table 4. Model PBL scheme evaluation metrics for air temperature and relative humidity, in cases with moderate wind (Cases 2, 3, 4 and 5) at Borisova gradina, Nadezhda, Pavlovo, Druzhba and Krasno selo (number of measurements - 480).

	<i>Mean</i>	<i>SD</i>	<i>MB</i>	<i>MAE</i>	<i>RMSE</i>	<i>R</i>
Temperature [°C]						
Observations	9.2	2.3				
QNSE	9.9	2.9	0.2	2.1	2.4	0.82
YSU	10.5	2.4	0.7	1.5	1.8	0.82
BouLac	12.9	2.5	1.1	1.9	2.2	0.76
ACM2	10.5	2.7	0.7	1.9	2.1	0.82
Relative Humidity [%]						
Observations	71.4	8.1				
QNSE	72.5	10.1	-1.2	7.9	9.5	0.71
YSU	70.2	8.4	-4.3	7.2	8.2	0.83
BouLac	67.4	8.1	-5.2	7.2	8.3	0.86
ACM2	70.9	8.7	-3.6	7.1	8.3	0.78

The summary of the surface statistics for two SYNOP stations – Sofia and Dragoman (Table 6) shows similar agreement with observations for temperature but worse correlation (less than 0.7) for the relative humidity in comparison with the automatic stations. The errors (*MAE*, *RMSE*) are in the same range – less than 2°C for the temperature and 11% for the relative humidity.

Vertical profiles of modeled atmospheric parameters at NIMH site are compared with derived ones from radiosonde in Fig.2. As an agreement indicator the coefficient of determination (R^2) is also shown. The radiosonde observations (at 12 UTC for all study cases) are interpolated to the model levels at corresponding time. All of the PBL schemes represent well temperature, u and v velocity components, and worse the wind speed and mixing ratio. The best correlation between observations and model data is observed for the temperature profile (R^2 approximately 0.98), the worst for the wind speed (R^2 approximately 0.8). Wind component across the axis (v) is better captured by the model than along the axis (u). Surprisingly much large differences are observed between different PBL schemes for the mixing ratio. The best correlation is achieved using QNSE ($R^2=0.88$), the worst correlation for ACM2 ($R^2=0.75$). In general the

vertical profile evaluation shows the same weakness that is found for the surface relative humidity – WRF underestimate the mixing ratio.

Table 5. Model PBL scheme evaluation metrics for air temperature and relative humidity, in cases with strong wind (Cases 6, 7, 8 and 9) at Borisova gradina, Nadezhda, Pavlovo, Druzhba and Krasno selo (number of measurements - 480).

	<i>Mean</i>	<i>SD</i>	<i>MB</i>	<i>MAE</i>	<i>RMSE</i>	<i>R</i>
Temperature [°C]						
Observations	7.4	1.6				
QNSE	8.2	1.8	0.3	1.6	1.9	0.68
YSU	11.8	2.0	-0.1	1.9	2.2	0.69
BouLac	9.2	1.4	1.2	1.6	1.8	0.73
ACM2	8.6	1.7	0.7	1.6	1.8	0.69
Relative Humidity [%]						
Observations	75.2	9.1				
QNSE	75.9	9.1	-2.4	10.2	11.9	0.67
YSU	71.0	8.5	-3.7	9.2	10.4	0.71
BouLac	70.9	7.6	-7.5	10.3	12.1	0.69
ACM2	73.4	9.3	-4.4	10.4	11.7	0.71

Table 6. Model PBL scheme evaluation metrics for air temperature and relative humidity for 8 cases (from case 2 to 9), at SYNOP stations Dragoman and Sofia (number of measurements - 480).

	<i>Mean</i>	<i>St. Dev</i>	<i>MB</i>	<i>MAE</i>	<i>RMSE</i>	<i>R</i>
Temperature [°C]						
Observations	9.3	2.0				
QNSE	9.2	2.3	-0.1	1.6	1.9	0.80
YSU	9.6	2.0	0.3	1.2	1.4	0.82
BouLac	10.1	1.9	0.8	1.3	1.5	0.83
ACM2	9.9	2.3	0.2	1.4	1.7	0.82
Relative Humidity [%]						
Observations	71.1	10.0				
QNSE	71.2	10.6	0.1	11.2	13.2	0.58
YSU	68.5	8.9	-2.6	9.3	10.4	0.64
BouLac	66.3	7.9	-4.8	9.8	11.7	0.62
ACM2	68.9	9.6	-2.2	10.1	11.7	0.62

A number of studies on PBL sensitivity tests (Zhang & Zhang, 2004; Cheng and Steenburgh, 2005; de Meij et al., 2009; Gilliam & Pleim, 2010; Mass and Ovens, 2011; Jiménez and Dudhia, 2013; Gómez-Navarro et al., 2015; Dimitrova et al., 2016) are published for diverse domains and various combinations of model's options. Despite of all these efforts it is hard to select the best and universal PBL scheme as performance of different schemes is highly influenced by large variety of local conditions.

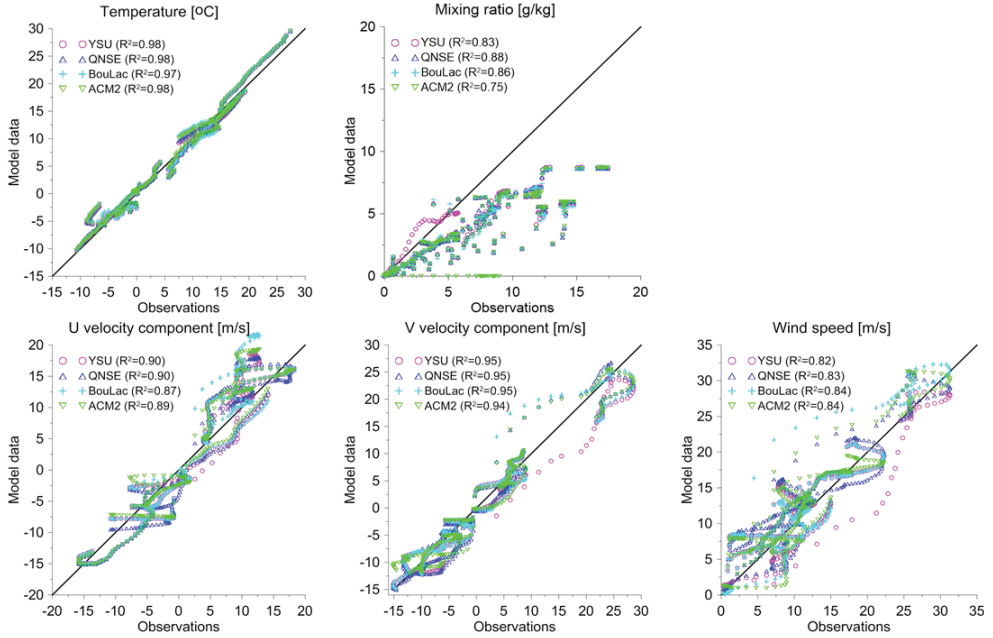


Fig. 2. Scatter plot of the vertical profiles of temperature, mixing ratio, wind speed and u and v wind components.

The choice of microphysics schemes highly affects the model's results for precipitation (Queen and Zhang, 2008), since microphysics includes explicitly resolved water vapor, cloud, and precipitation processes. Comparisons between different microphysics schemes are made for severe rainfall events (ElTahan M. and Magooda M., 2017) or different meteorological condition during summer and winter months (Borge et. al., 2008).

Several studies are carried out for the Sofia region during the recent years covering different aspects. Kirova & Batchvarova (2013) estimate the model abilities to perform convective conditions with one specific configuration using radiosonde profiles for 5 days on every 2 hours. Penchev & Peneva (2013) validate WRF model for icing conditions for one day and demonstrate very good correlation coefficient between the model and sounding data ($r = 0.91$ for the temperature and $r = 0.7-0.8$ for humidity). The YSU PBL and Double-Moment 6 class schemes are used in this study and the

results are similar to outcomes found here. The authors however show that for the wind the correlation is not so good especially in the low atmospheric layers. Manafov I. (2017) focus on improving the model performance for fog conditions at the Sofia airport comparing five PBL schemes for 18 cases and 6 microphysics schemes for 2 cases. The author found that QNSE is the best performing PBL scheme (one of the best in our study also) and Thompson for microphysics (Lin scheme is the best in our study). Test with various land surface models are performed in Manafov I. (2017) and Georgieva I. (2017), showing contradictory results regarding Noah LSM, which is used in this study.

3.2. Meso-scale circulation under different large-scale conditions

As already has been mentioned above, the purpose of this study is to model the specifics of the meso-scale circulation under different large-scale conditions for the Sofia region. All numerical results have been analyzed qualitatively by looking at the flow field plotted at 10 m and at 700 hPa level (undisturbed synoptic flow), and at the vertical cross sections along and across the valley axis. One example for the cases with strong wind (>10 m/s) is shown in Figs. 3 (cases 8 and 9) and 4 (cases 6 and 7). The Northwesterly synoptic current is slightly changed, and flows along the valley floor. Modification of the stream is significant mainly around the Vitosha Mountain. Tunnel effects following the gorges between Vitosha and surrounding mountains, stagnation at the windward and acceleration of the flow on the leeward slope are easily discernible.

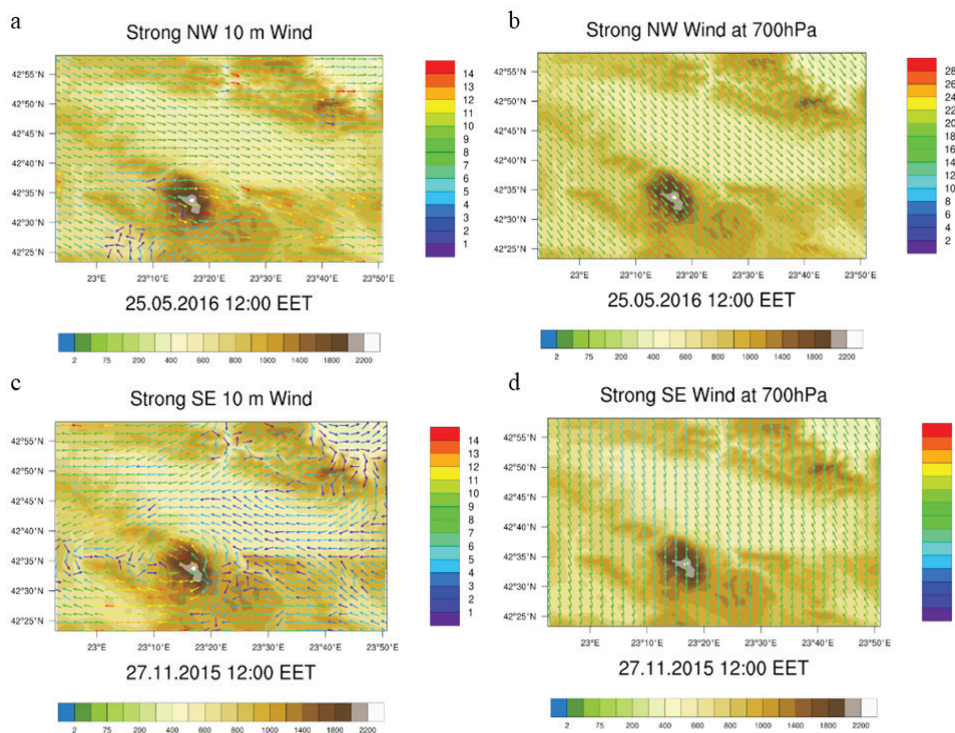


Fig. 3. Modification of the surface wind in Sofia valley (a, c) during synoptic flows along the valley axes – case 8 of northwesterly (b) and case 9 of southeasterly winds (d). The color bar (right) indicates weed speed in m/s; the bar (below) the model terrain height in meters.

This is the most common invasion for the Sofia valley (Blaskova et. al., 1983). The Southeasterly large scale flow is variable in the domain changing to Southern flow above the Vitosha Mountain. The collision with the obstacle makes the near surface flow pattern more complicated. The wind speed is significantly reduced inside the valley and the flow turns around the Vitosha Mountain forming lee vortex and stagnation region west of the obstacle. The observed flow pattern is in agreement with the laboratory experiment (Tucker, 1989).

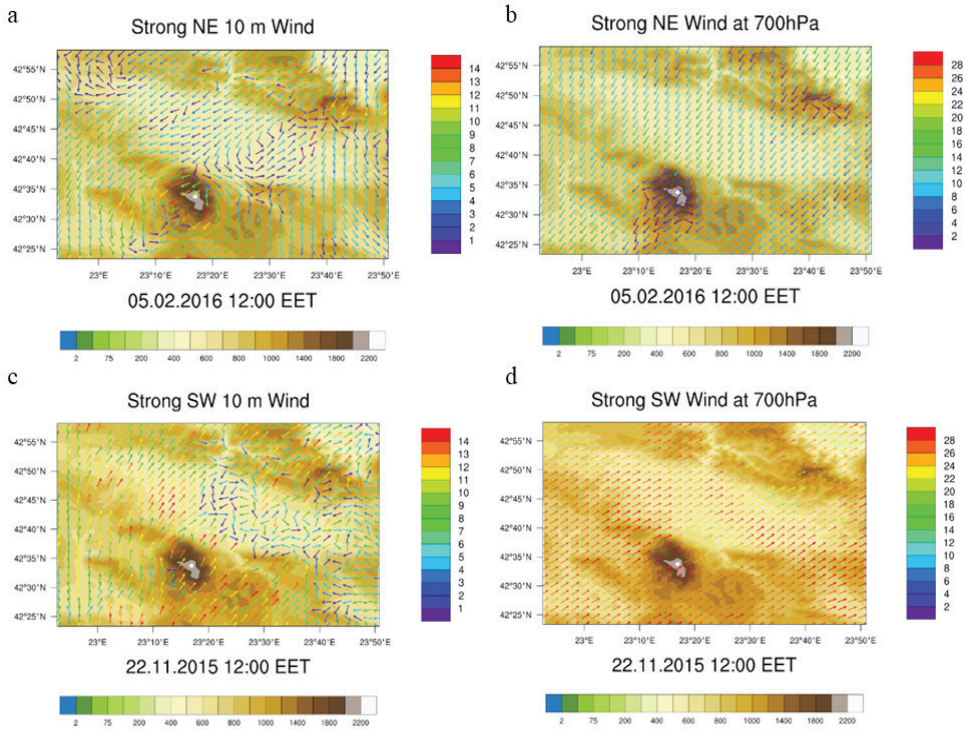


Fig. 4. Modification of the surface wind in Sofia valley during synoptic flows across the valley axes - Northeasterly flow and Southwesterly flow. The color bar (right) indicates weed speed in m/s; the bar (below) the model terrain height in meters.

More interesting is modification of the synoptic airflow when the direction is perpendicular to the main obstacles Stara Planina and Vitosha mountains. The Northeasterly synoptic flow collide with the Vitosha Mountain, some of the air is blocked, part of the flow splits around the obstacle forming stagnant area within the wake behind the mountain. Another part of the flow overturns against the main current, forming large vortex in the eastern part of the valley. The Southwesterly synoptic flow is the case with the highest wind speed more than 25 m/s at 700 hPa. The current has enough energy to overcome the Vitosha Mountain making large stagnation area in the wake behind the obstacle with weak return flow.

Vertical slides of the interpolated horizontal wind vectors over the chosen cross-section across the valley axis are shown for both interesting cases (cases 6 and 7), which

have been described in Fig. 4, and for the case with calm conditions. Fig. 5 corresponds to case 7 with strong Northeasterly synoptic wind (see fig. 4a, b), which hit the Vitosha Mountain. Three layers, with reverse flow in the middle, are simulated during the stable nocturnal conditions (fig. 5a, b).

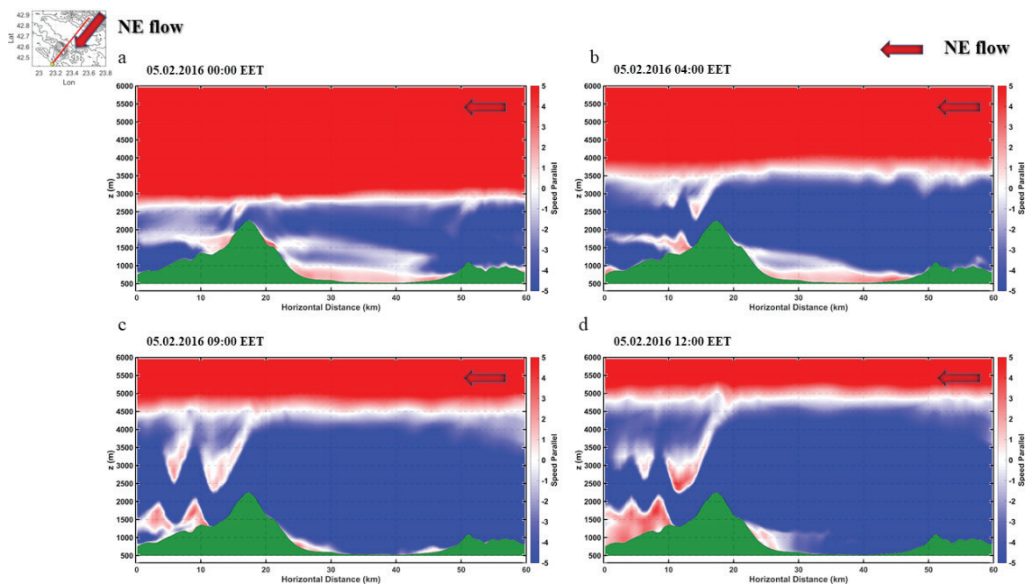


Fig. 5. Vertical slides of wind over the chosen cross-section (shown at the left upper corner) for YSU PBL scheme for the Case 7 - strong NE flow at different times.

The reversal flow depth increases with time and strong wind shear produces flow propagation behind the obstacle and large vortexes formation on the leeward slop of the Vitosha Mountain. Secondary return flow is observed inside the valley close to the ground. The disturbances grow with time forming lee-waves with maximum in amplitude before the sunrise (fig. 5c). After the sun rise the stable nocturnal layer becomes weaker, the magnitude of the lee-waves decreases, and they disappear at 12 EET (fig. 5d).

Fig. 6 corresponds to case 6 with very strong Southeasterly synoptic wind with speed more than 25 m/s (see fig. 4c, d). The airflow has enough energy to pass over the mountain forming patchy regions with reverse flow inside the wake of the obstacle. The disturbance mostly due to increase in roughness above the urban area leading to development of very complicated layered structure during the stable night conditions.

The slop flow formation can be observed in presence of weak synoptic flow – Case1 (fig. 7). During the night due to surface cooling thin layer colder than environment run downslope forming a downslope flow (fig. 7a) which strengthen with the increase in stability (fig. 7b). After the sun raise the ground heating reverse the process and after the morning transition (fig. 7c) well displayed anabatic flow inside the valley can be seen (fig. 7d).

*Numerical study of meso-scale circulation specifics in the Sofia region
under different large-scale conditions*

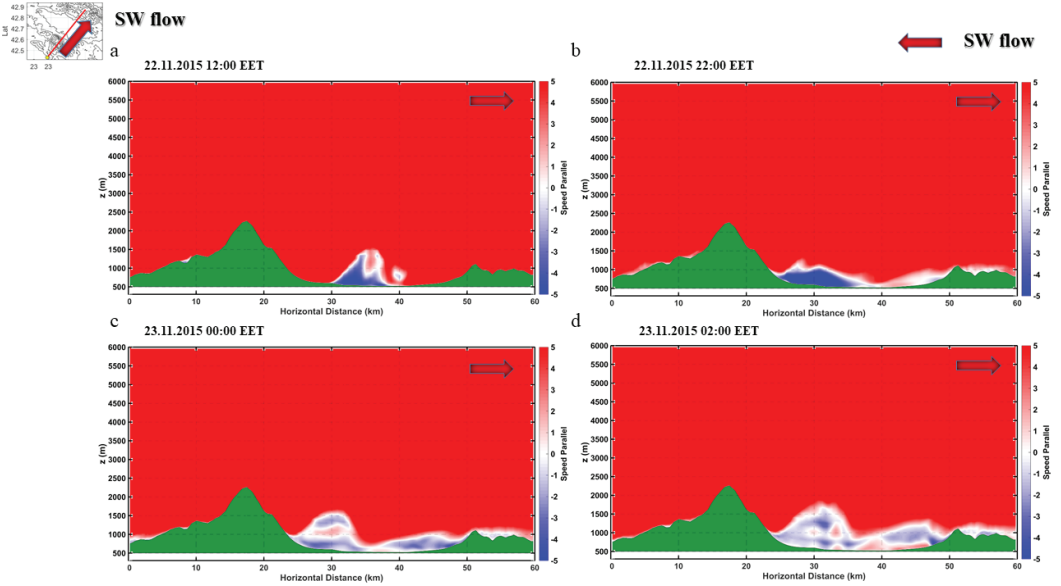


Fig. 6. Vertical slides of wind over the chosen cross-section (shown at the left upper corner) for YSU PBL scheme for Case 6 - strong SW flow at different times.

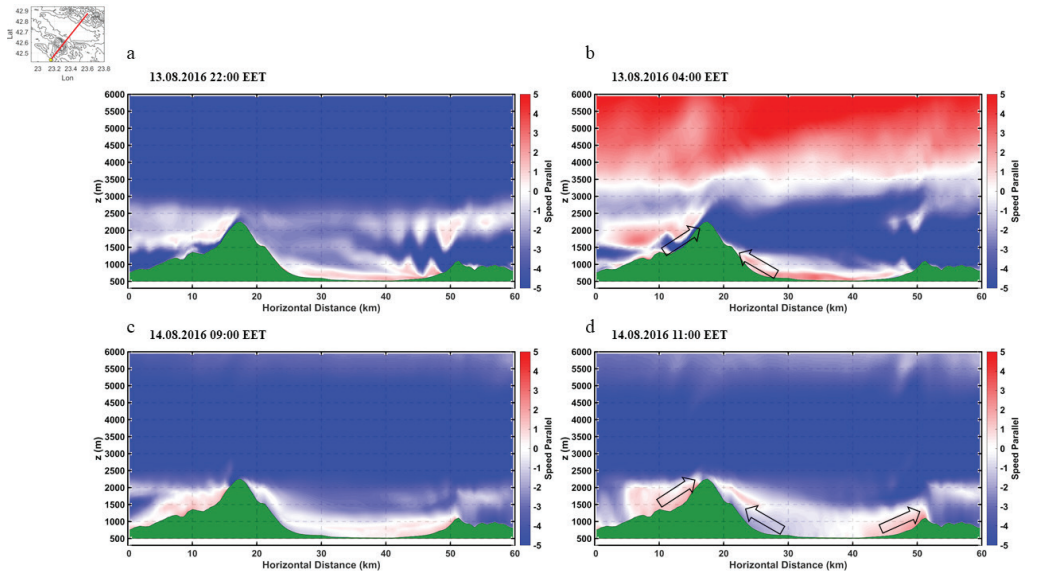


Fig. 7. Vertical slides of wind over the chosen cross-section (shown at the left upper corner) for YSU PBL scheme for Case 1 - calm conditions at different times.

5. CONCLUSIONS

Different PBL and microphysics schemes available in WRF model are evaluated in this study. Experimental data from 2 surface SYNOP sites, 6 automatic stations and daily radiosounding (at 12 UTC) are used to assess the model performance. Simple statistics for surface parameters (only temperature and relative humidity) and vertical profiles of temperature, mixing ratio and wind, show good model ability to describe the study cases. The model shows better agreement for the cases with moderate wind (cases 2, 3, 4 and 5) conditions in comparison to the strong synoptic winds (cases 6, 7, 8 and 9). The agreement between model data and observations is very good for the temperature and moderate for the wind speed and relative humidity. Two experiments have been conducted to estimate the best model performance using various schemes for microphysics and PBL with constant other options. Overall the Lin et al. scheme shows the best performance and it has been selected to be used for the PBL experiment. None of the PBL schemes is found to be superior, but all provide reasonable results. There is no significant difference in the horizontal flow pattern, but the main variations between different PBL schemes appears in the vertical wind speed profiles, with some cases of large over or underestimation of the observed values.

The modification of the synoptic flow within PBL due to the complex orography in Sofia region is substantial and Vitosha Mountain plays a significant role in this process. The large-scale flow remains unaffected above 700 hPa. Different mesoscale phenomena are captured with numerical simulations such as mountain lee waves, vortex shedding, stagnant area within the wake behind the obstacle, and nocturnal jet formation. Due to the downslope flows with different density coming from the surrounding mountains during nocturnal stable conditions several layers appear inside the valley. The diurnal evaluation of well mixed convective layer during the day and decrease of the PBL height during the night within the valley is also captured well by the model.

WRF model shows good performance and it is a very useful tool to study flow structure and variability. All of the meso-scale phenomena play significant role on the local PBL structure and microclimate. Due to the complex orography and the presence of huge urban area inside the valley it is difficult to separate the influence of different factors. Further investigation is needed to increase and analyse the number of events (days) inside the defined large scale conditions in order to get statistically significant representativeness of the specific meso-scale circulation in the Sofia valley.

ACKNOWLEDGEMENTS

This research is developed within the scope of the project DN4/7 (Study of the PBL structure and dynamics over complex terrain and urban area), funded by Research Fund at the Bulgarian Ministry of Education and Science.

REFERENCES

- Baines, P. G. and P. C. Manins, (1988), The principles of laboratory modelling of atmospheric flow over complex terrain. Manuscript. CSIRO Division of Atmospheric Research, Mordialloc, 3195, Australia.
- Blaskova D., L. Zlatkova, S. Lingova, Zh. Modeva, L. Subev, M. Teneva (1983), Climate and microclimate of Sofia. BAS, Sofia. (in Bulgarian).
- Borge, R., V. Alexandrov, J. del Vas, J. Lumbreras, and E. Rodríguez, (2008), A comprehensive sensitivity analysis of the WRF model for air quality applications over the Iberian Peninsula, *Atmos. Environ.*, 42, 8560–8574.
- Bornstein, R. F., D. R. Leone, D. J. Galley, (1987), The generalizability of subliminal mere exposure effects: Influence of stimuli perceived without awareness on social behaviour. *Journal of Personality and Social Psychology*, 53, 1070-1079.
- Bougeault, P., P. Lacarrere, (1989), Parametrization of orography-induced turbulence in a mesobeta-scale model. *Mon Weather Rev* 117(8):1872–1890.
- Bretherton, S. Christopher and Sungsu Park, (2009), A new moist turbulence parameterization in the Community Atmosphere Model. *J. Climate*, 22, 3422–3448.
- Chen, F., and J. Dudhia, (2001), Coupling an advanced land surface-hydrology model with the Penn State-NCAR MM5 modelling system. Part I: Model implementation and sensitivity. *Mon Weather Rev* 129:569–585.
- Cheng, W. Y. Y. and Steenburgh, W. J., (2005), Evaluation of Surface Sensible Weather Forecasts by the WRF and the Eta Models over the Western United States, *Weather Forecast.*, 20, 812–821, doi:10.1175/WAF885.1.
- De Meij, A., A. Gizella, C. Cuvelier, P. Thunis, B. Bessagnet, J. F. Vinuesa, L. Minut, and H. M. Kelder, (2009), The impact of MM5 and WRF meteorology over complex terrain on CHIMERE model calculations, *Atmos. Chem. Phys.*, 9, 6611–6632.
- Dimitrova R., Silver Z., Zsedrovits T., Hocut C., Leo L. S., Di Sabatino S., Fernando H. J. S., (2016), Assessment of Planetary Boundary-Layer Schemes in the Weather Research and Forecasting Mesoscale Model Using MATERHORN Field Data, *Boundary-Layer Meteorol*, 159, 589–609, doi 10.1007/s10546-015-0095-8.
- Dixit, P. N., and D. Chen, (2011), Effect of topography on farm-scale spatial variation in extreme temperatures in the Southern Mallee of Victoria, Australia. *Theor. Appl. Climatol.*, 103, 533-542.
- Dudhia, J., (1989), Numerical study of convection observed during the winter monsoon experiment using a mesoscale two-dimensional model. *J Atmos Sci* 46:3077–3107.
- ElTahan, M. and M. Magooda, 2017, Evaluation of different WRF microphysics schemes: severe rainfall over Egypt case study, *Physics - Atmospheric and Oceanic Physics*.
- Emmanuel, R. & H. J. S. Fernando, (2007), Urban heat islands and arid climates: role of urban form and thermal properties in Colombo, Sri Lanka and Phoenix, USA, *Climate Research* 34 (3), 241.
- Gilliam, R., and J. Pleim, (2010), Performance assessment of the Pleim-Xiu LSM, Pleim surface-layer and ACM PBL Physics in version 3.0 of WRF-ARW (accepted by *Journal of Applied Meteorology and Climate*).
- Gómez-Navarro, J. J., Raible, C., C. and Dierer S., Sensitivity of the WRF model to PBL parametrisations and nesting techniques: evaluation of wind storms over complex terrain, *Geosci. Model Dev.*, 8, 3349–3363, 2015.

- Georgieva, I., (2017), Local transport and chemical transformations in the atmosphere, PhD thesis, (in Bulgarian).
- Grell, G. A. and D. Devenyi, (2002), A generalized approach to parameterizing convection combining ensemble and data assimilation techniques. *Geophys. Res. Lett.* 29(1693).
- Hong, S., Y. Noh, J. Dudhia, (2006), A new vertical diffusion package with an explicit treatment of entrainment processes. *Mon Weather Rev* 134(9):2318–2341.
- Hong, S. Y. and J. O. J. Lim, (2006), The WRF single-moment 6-class microphysics scheme (WSM6). *J. Korean Meteor. Soc.*, 42, 129–151.
- Hunt, J. C. R., M. Maslin, T. Killean, P. Backlund, J. Schellnhuber, (2007), Introduction: Climate change and urban areas; Research dialog in a policy framework. *Phil. Trans. Roy. Soc. (London)* DOI: 10.1098/ersta.1007.2089.
- Jiménez, P. A. and Dudhia, J., Improving the Representation of Resolved and Unresolved Topographic Effects on Surface Wind in the WRF Model, *J. Appl. Meteorol. Clim.*, 51, 300–316, doi:10.1175/JAMC-D-11-084.1, 2012.
- Jiménez, P. A. and Dudhia, J., (2013), On the Ability of the WRF Model to Reproduce the Surface Wind Direction over Complex Terrain, *J. Appl. Meteorol. Clim.*, 52, 1610–1617, doi:10.1175/JAMC-D-12-0266.1.
- Kirova H. and E. Batchvarova, (2013), Verification of meso-meteorological model using aerological data from the Sofia experiment 2003, Proceedings of the 2nd National Congress in Physical Sciences, 25- 29 September 2013, Sofia, Bulgaria (in Bulgarian).
- Lin, Y. L., R. D. Farley, H. D. Orville, (1983), Bulk parametrization of the snow field in a cloud model. *J Appl Meteorol* 22:1065–1092.
- Manafov, I., (2017), Fog forecast for Sofia airport, PhD thesis, (in Bulgarian).
- Mass, C. and Ovens, D., (2011), Fixing WRF's high speed wind bias: A new subgrid scale drag parameterization and the role of detailed verification, in: 24th Conf. on Weather and Forecasting/20th Conf. on Numerical Weather Prediction, Vol. 9B.6, available at: <http://ams.confex.com/ams/91Annual/webprogram/Paper180011.html> (last access: 21 October 2015), *Amer. Meteor. Soc.*
- Mlawer, E. J., S. J. Taubman, P. D. Brown, M. J. Iacono, S. A. Clough, (1997), Radiative transfer for inhomogeneous atmospheres: RRTM, a validated correlated-k model for the longwave. *J Geophys Res Atmos* 102(14):16,663–16,682.
- Oke, T. R., (1988), Street design and urban canopy layer climate. *Energy and Buildings*, 11, 103–113.
- Penchev R. and E. Peneva, (2013), Numerical simulation of extreme convective events during 2012 in Bulgaria using the weather forecast model WRF, Proceedings of the 2nd National Congress in Physical Sciences, 25-29 September 2013, Sofia, Bulgaria (in Bulgarian).
- Pielke, R. A., (2013), *Mesoscale Meteorological Modelling*, Academic Press is an imprint of Elsevier, Third Edition, p. 716.
- Pleim, J. E., (2007), A combined local and nonlocal closure model for the atmospheric boundary layer. Part I: Model description and testing. *J Appl Meteorol Clim* 46(9):1383–1395 .
- Queen, A.N., Zhang, Y, 2008. Examining the sensitivity of MM5-CMAQ predictions to explicit microphysics schemes and horizontal grid resolutions. Part II - PM concentration and wet deposition predictions. *Atmospheric Environment*. doi:10.1016/j.atmosenv.2007.12.066.
- Snyder, W. H. and Coauthors, (1985), The structure of strongly stratified flow over hills: dividing-740 streamline concept. *J. Fluid Mech.*, 152, 249-288.

- Sukoriansky, S., B. Galperin, V. Perov, (2005), Application of a new spectral theory of stably stratified turbulence to the atmospheric boundary layer over sea ice. *Boundary-Layer Meteorol* 117(2):231–257.
- Tao, Wei-Kuo, J. Simpson, M. McCumber, (1989), An Ice–Water Saturation Adjustment. *Mon. Wea. Rev.*, 117, 231–235.
- Thompson, G., P. R. Field, R. M. Rasmussen, W. D. Hall, (2008), Explicit Forecasts of Winter Precipitation Using an Improved Bulk Microphysics Scheme. Part II: Implementation of a New Snow Parameterization. *Mon. Wea. Rev.*, 136, 5095–5115.
- Tucker, G. B., (1989), Laboratory modelling of air flow in the Sofia valley Bulg. *Geophys. J.* 15, 92-100, [pp. 450, 453].
- Vladimirov, E., R. Dimitrova and V. Danchevski, Sensitivity of the WRF model results to topography and land cover: study for the Sofia region, *Annuaire de l'Université de Sofia "St. Kliment Ohridski"*, Faculté de Physique - accepted for publication.
- Zardi, D. and C. D. Whiteman, (2012), *Mountain weather research and forecasting*, Chapter 2, p. 74.
- Zhang, D.-L., and W.-Z. Zhang, 2004. Diurnal cycles of surface winds and temperatures as simulated by five boundary layer parameterizations, *J. App. Meteor.*, 114, 157–169.



The Operative System ProData—Part One: Current Stage and Recent Improvements

**Hristo Chervenkov*, Valery Spiridonov, Eram Artinyan, Plamen Neytchev,
Kiril Slavov, Minka Stoyanova**

*National Institute of Meteorology and Hydrology- BAS,
Tsarigradsko shose 66, 1784 Sofia, Bulgaria*

Abstract. The present article, which is part one of several common works, describes the operative system ProData—the reasons and motivation for its creation, the embedded processing technique, the input/output data flow, as well as its strengths. The possibility of the system to adopt further improvements and some achievements in this direction are described and visualized. The main conclusion is that the system is a reliable source of consistent meteorological information with high spatial and temporal resolution with minimal latency from the input data acquisition time.

Keywords: Operative System, Meteorological Data Processing, Automatic Weather Station, Satellite-derived Data, SWEEP Operator

1. INTRODUCTION

The modern applied meteorology is faced with the challenge of the growing demand on reliable data, available in high resolution, both in time and space. Numerous mesoscale geophysical tasks and applications need such data: practically all spatially distributed hydrological and ecological models need certain meteorological information, most frequently formatted as initial data set, containing the values of some input parameters. Thus, for instance, they use air temperature to drive processes such as evapotranspiration, snowmelt, soil water and temperature evolution, and plant productivity. As fundamental meteorological variable, rainfall is primary input for hydrological models, specifically distributed hydrological ones. The regional climate and weather prediction models also rely on such data for verification and tuning. In the common case all near-surface

* hristo.tchervenkov@meteo.bg

weather observations are collected at irregularly spaced point locations (for example the network of the measurement stations) rather than over continuous surfaces. Although the synoptic records are considered to be relatively accurate and reliable at the point where the station locates, the density of the measurement network and frequency of observations are generally not high enough to describe the spatial and temporal distribution of the considered meteorological variables. Often, in many environmental studies, it is impossible to use directly such information or this can lead to serious biases in the results. Consequently, different methods for estimation of spatially and temporally distributed near-surface meteorological variables are developed. They can be pure mathematical, for example inverse-distance weighting (IDW), kriging, 2-dimensional splines, and trend-surface regression (Myers, 1994) or, alternatively, combined-mathematical based on physical assumptions (Chervenkov, 2016). As stated in Dodson and Marks, 1997, these methods often work well over relatively flat, homogeneous terrain. The weather conditions in local scales, however, are partially influenced by the topography of the area. Extensive research was carried out worldwide, partly using the modern GIS technologies, aiming at the accurate visualization and digitization of various climate variables (see Feidas et al 2014 for detailed review). Many efforts are dedicated on developing of appropriate methods for estimating climatic elements using topographical and geographical parameters as independent variables. Such models are able to estimate climate variables in sites that observational data are not available, giving a relatively reliable solution to the old problem of insufficient climatic data. Common weakness of many of these, product of purely geographical approach, is the utilization of only topographical parameters as regressors. Most of the existing solutions work as climate hindcast, i.e. usually the output is produced months after the data acquisition time. Overall, the incorporated techniques are quite sophisticated, the implementation of such methods demands significant computational power and increased amount of input data, making the overall procedure quite difficult. In the group of products from such systems it is worthy to outline the Pan-European gridded dataset on daily basis E-OBS of the European Climate Assessment&Dataset (ECA&D). This dataset is periodically updated, well known in the meteorological community, and widely used for many tasks, extensively as reference in model verification studies (Haylock et al, 2008). As will be commented in the next section, however, the need for operative work of the system is a very significant constraint and has to be always kept in mind.

The paper is structured as follows: Hence this is the first publication, dedicated on ProData, the general description of the system is placed in second section. The most significant recent improvements are concisely reported in the third and fourth section. The main conclusions as well as short outlook of the planned future work are described in the conclusion.

2. SHORT DESCRIPTION OF THE CURRENT STAGE OF PRODATA

The operative system (OS) ProData was created in NIMH-BAS in the period 2012-2015 by the team under the leadership of prof. V. Spiridonov. The basic concept was to combine in methodologically consistent way all available on hourly basis meteorological and auxiliary data in order to produce high-quality gridded time-series, of the most significant meteorological variables. These time-series, or digital maps, have to be with 1 hour time resolution and at least national coverage. The horizontal resolution has to be also adequate, which, according to the modern requirements for the considered scale, is below 10 km. Thus, the current implementation of the system runs on grid with $0.045^\circ \times 0.045^\circ$ spacing, which corresponds approximately of $4 \text{ km} \times 4 \text{ km}$. The model domain, which is shown on Figure 1, covers entirely Bulgaria and consists of $147 \times 73 = 10731$ grid-cells.

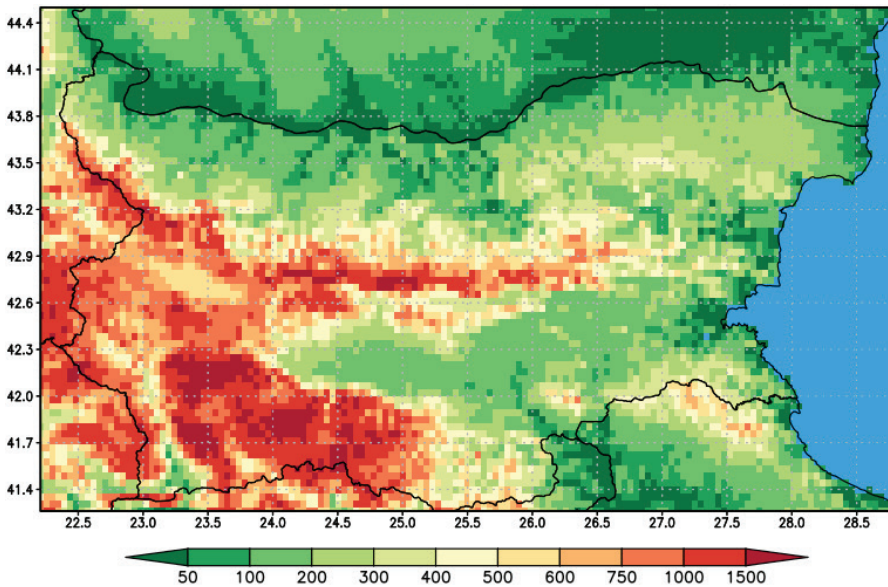


Fig. 1. Model domain and elevation (unit: m) of the grid-cells over land

The specific need of various scientific and other experts was additional motivation. Thus, for example, the operative hydrology needs such data for calculation of the total precipitation amount over a certain river basin; the electricity companies used it for evaluation of the energy consumption, and many more. The requirement for one hour time resolution is a very serious constraint - it narrows significantly the number of potential input data sources. Neither of the traditional (i.e. synoptic and climatic) observational networks measures the meteorological variables in intervals shorter than 3 hours, our radar is currently also disabled. It is necessary in such situation to rely on data, collected and transmitted from *in situ* platforms for environmental monitoring, as

automatic weather and hydrological stations (AWS/AHS) as well as satellite-derived data, mainly from the services of the European Organisation for the Exploitation of Meteorological Satellites (EUMETSAT).

The network of AWS and AHS was built gradually following the needs of particular projects directed primarily toward streamflow analysis and forecasting as “Flood forecasting and early warning system for Maritsa and Tundzha rivers” (Roelevink et al., 2010), “Flood warning system in Arda river basin - Ardaforecast” (Artinyan et al., 2016), “Danube Water” (Nedkov et al., 2015), etc. The automatic stations measuring hourly precipitation rate over the country are about 140 but only 80 of them have also combined air temperature and relative humidity sensors and 40 of them have solar radiation sensors. These stations are spread irregularly over the country as the above projects covered partially Southern Bulgaria but didn’t cover Black Sea river basins for instance. Stations data is collected at hourly basis (Naldzhiyan, 2017) and is exported as ASCII files to be used from ProData system.

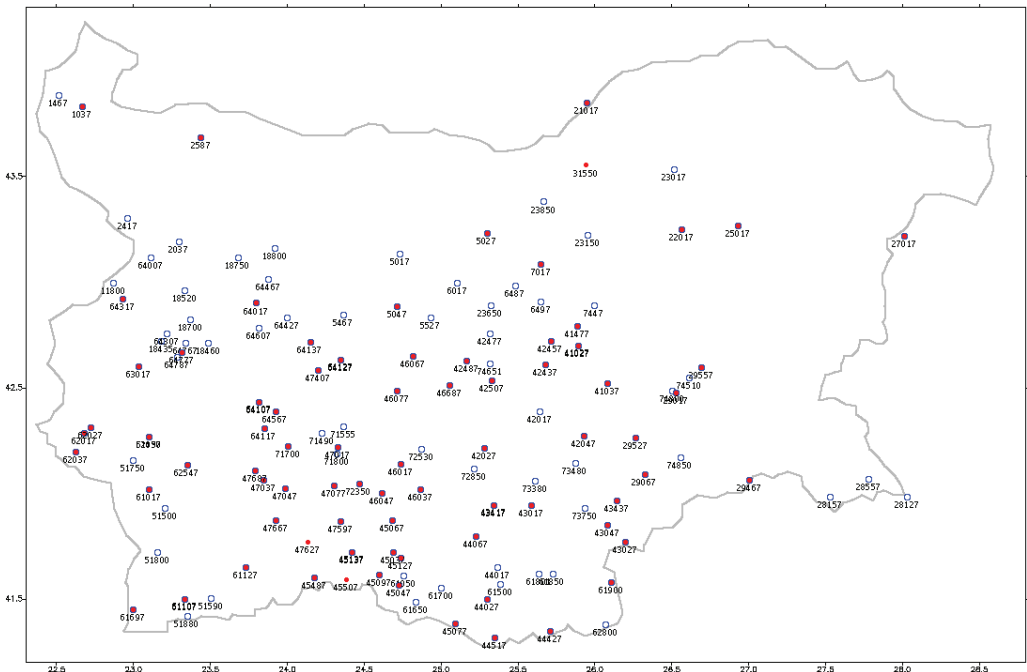


Fig. 2. Network of AWS/AHS, measuring the temperature and relative humidity at 2 m above the ground (red dots) and precipitation amount (blue circles) at every hour.

Being the Bulgarian National Hydromet Service, NIMH-BAS uses widely and decades-long the services and products of EUMETSAT. Since 2014, however, as Bulgaria became a member of the organization, the quantity and variety of the available information, both raw and processed data, have increased remarkably. Consequently,

the possibilities for implementation of such data have risen significantly. As will be commented further, the satellite retrievals, more specially these in the infrared (IR) channel of the Meteosat second generation (MSG), are the primary source for the input information for ProData. Currently, gridded estimates for the following 11 variables are routinely produced in the frame of the system every hour:

- temperature and relative humidity at 2m above the surface
- precipitation amount
- cloud coverage
- wind speed and direction
- solar shortwave incoming radiation downwards
- presence of fog, precipitation of hail and thunderstorm
- snow water equivalent (SWE)

Hence the analyzed variables are fairly different and each one has specifics, which have to be taken into account, there is no common procedure for the processing of the input data and, respectively, the preparation of the final product. The wind speed and direction are directly taken from the output of the ALADIN-BG (Bubnova et al., 1995), which is the Bulgarian short-range operational weather forecast model. Many issues have to be addressed intending to combine the information from the geostationary satellite and the network of AWS/AHS. Most of the problems are rooted in the principle differences of the two observation concepts, respectively platforms. Thus, for example, the satellite data have to undergo georeferencing, consequently mapped onto the grid of the system, the error, caused from the parallax and synchronization have also to be taken into account. All corresponding procedures inherently introduce biases, the cumulative effect of which leads to unavoidable limitation of the final product accuracy (for more details see http://www.hydro.bg/mapValej/metodika_za_satelitni_nazemni.pdf).

The core of the system is the objective analysis of the variables. It is done by statistical means, using the well-known multiple linear regression technique (MLR, see appendix). It is widely and successfully implemented in geophysics, partly in climatology (see Feidas et al., 2014 again). The independent variables used are functions of the brightness temperature and also derivatives of the topography, which are calculated prior the MLR. Elevation, exposure, and convexity, which are proportional to the Laplacian of the elevation, belong to the last group. The conceptual scheme and the stepwise data flow processing within ProData are shown on Figure 3. Data from AWS/AHS are used as dependent variables; i. e. the model is forced to mimic the spatial distribution as established from these data. The residual value is the bias between the AWS/AHS-measurements and the final output value. Some authors, in an attempt to refine the estimated values, propose residual correction using different local interpolation methods. The validity of these models is checked through cross-validation error statistics against an independent (test) subset of station data. The benefit of such second step is often questionable: Feidas et al. (2014) finds that the correction of the developed regression models using residuals improved though not significantly the interpolation accuracy.

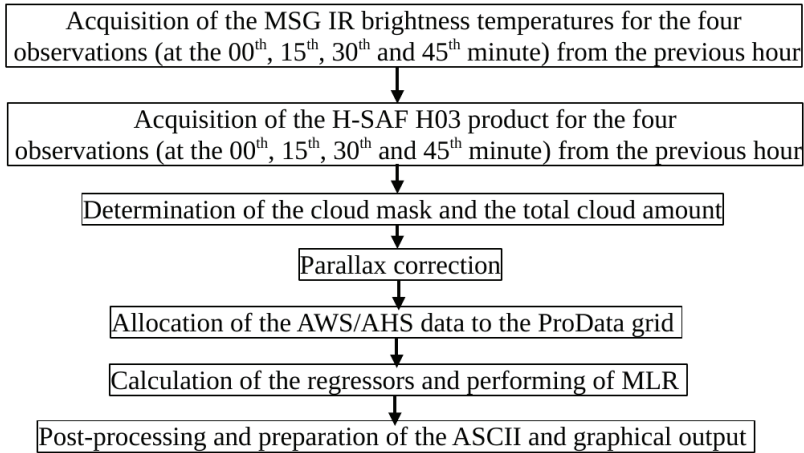


Fig.3. Data flow and processing steps within ProData

The modules for estimation of fog presence, precipitation of hail and thunderstorm, are similar. All of them use the threshold approach, calculating in advance some criterion quantities. The fog, hail and thunderstorms are determined in two degrees of likelihood of their occurrence depending on the number of conditions fulfilled. For fog the satellite information used follows the criteria, proposed by Barbosa (2012) modified for the Bulgarian conditions. Additional criteria are limitations on wind speed, air temperature, dew point and rainfall. The probability of hail follows the criteria described in Siewert et al. (2010). In the snow module, the snow is accumulated from the precipitation by negative temperatures. The quantitative description of snow pack evolution, including the snow depth determination and SWE, is performed using the methodology, described in the Engineer Manual of the U.S. Army Corps of Engineers (see references).

Concluding this section, we would like to emphasize the main features of the system ProData, on which its success is based:

- The system works in operational (i.e. with minimal latency from the data acquisition time, as a rule approximately 1 hour and 30 minutes) and fully automatic (i.e. unattended from personnel) regime.
- A native computational procedure, coded by the ProData-team, which relies on efficient and transparent statistical technique
- Freely accessible (from within NIMH-BAS private network) through a web-page.

The basic output products, hourly data sets of all 11 analyzed variables for each grid cell, are available at <https://users.meteo.bg/ProData/> in convenient ASCII csv-type format. This site is designed as single point access - it contains also many secondary products, tailored for the specific needs of the different end-users as well as explanatory descriptions and auxiliary data.

3. SOME RECENT IMPROVEMENTS OF THE SYSTEM PRODATA

Significant merit of the system is its flexibility, expressed mainly in the possibility for further enhancement and development. As far as the mathematical approach seems a reasonable choice, it appears to be most perspective to experiment with, and eventually to adopt, new sources of input data as independent variables in the MLR.

A vast quantity of high-quality and reliable environmental data is exchanged nowadays through the scientific networks or is free-of-charge for non-commercial use. It is expected that this stream, due to the implementation of new methods and platforms on one hand and the increased international cooperation on the other, will rise steadily. This fact is a favorable prerequisite for such experiments. As emphasized before, the requirement for the data acquisition frequency and the transmission latency appear as a principle constraint. Some of the products of the eight satellite application facilities (SAFs) of the EUMETSAT seem promising and especially these, which are directly linked with some of the analyzed within ProData parameters. So far, we have performed an extensive test with the H-SAF PR OBS 3-H03 product. It is worth to emphasize, however, that the other precipitation-linked H-SAF products, despite their advantages over H03, are not suitable due to the timelines constraint: All others are with latency significantly longer than the one-hour limitation.

The primary goal of the Satellite Application Facility in Support to Operational Hydrology and Water Management (H-SAF) is to provide satellite-derived products from existing and future satellites with sufficient time and space resolution to satisfy the needs of operational hydrology. Five of the H-SAF operational products are targeted to the precipitation, and due to the minimal latency, the H-SAF PR OBS 3-H03 one, as stated before, is the single one suitable. Core of the product is the “Rapid Update” technique, which allows computing of instantaneous rain intensities at the ground at the geostationary time-space scale (Turk et al. 2000). It is based on a blended micro-wave (MW)-IR technique that correlates, by means of the statistical probability matching, to brightness temperatures measured by the IR geostationary sensors and passive MW-estimated precipitation rates at the ground. Hence the method suffers from many issues (see the listed in the references Product User Manual for details), this product cannot be used as dependent variable in the MLR, as the data from the AWS/AHS.

The raw ProData output can be preprocessed in order to respond more adequately to the specific needs of the end-users. As a result, various secondary, both numerical and graphical, products could be offered. The biggest share of the ProData web-page content consists already of such data. Maps of the most analyzed parameters in 3-hour interval from 12 UTC of the previous day until the current hour are available on-line on <http://hydro.bg>. Our intent is to enrich this approach, proposing new figures. The leading idea is to combine optimally clarity and information in as small as possible number of new items. Thus, the collated maps, shown on Figure 4, are specially tailored for quick-view of the meteorological situation in the previous day.

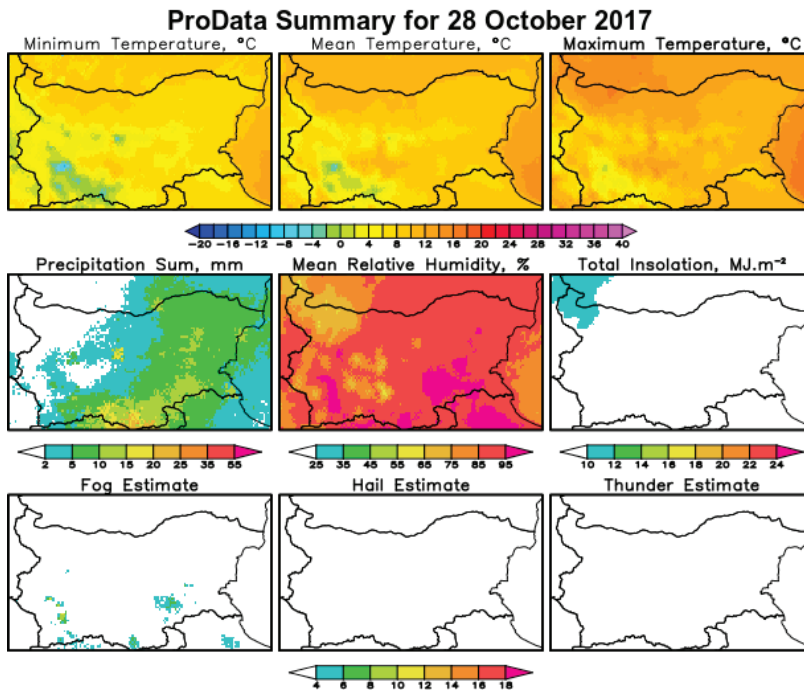


Fig. 4. Quick-view of the meteorological situation

It is worth to emphasize, that the daily minimum, mean, and maximum temperature are calculated a posteriori, using the hourly values of the temperature. These three parameters, together with the daily precipitation amount are most frequently used for estimation of climate extremes and, respectively, they form the standard input data set for the calculation of the climate indices (see, for example, the STARDEX project <https://crudata.uea.ac.uk/projects/stardex/>)

In some cases and for certain users, as for example representatives of national and municipal authorities, figures with the values in concrete points (i. e. grid cells) of interest, are more suitable rather than color-coded maps. Such figures, for the temperature in the main synoptic terms and the precipitation for four equal intervals, are already automatically generated. Thus far, data for the 27 province centers (i.e. first level administrative subdivisions of the country) are plotted. The possibility however to change easily the list of the considered places, without modification of the main procedure, is already foreseen. Examples of such figures are shown on Figure 5 and Figure 6.

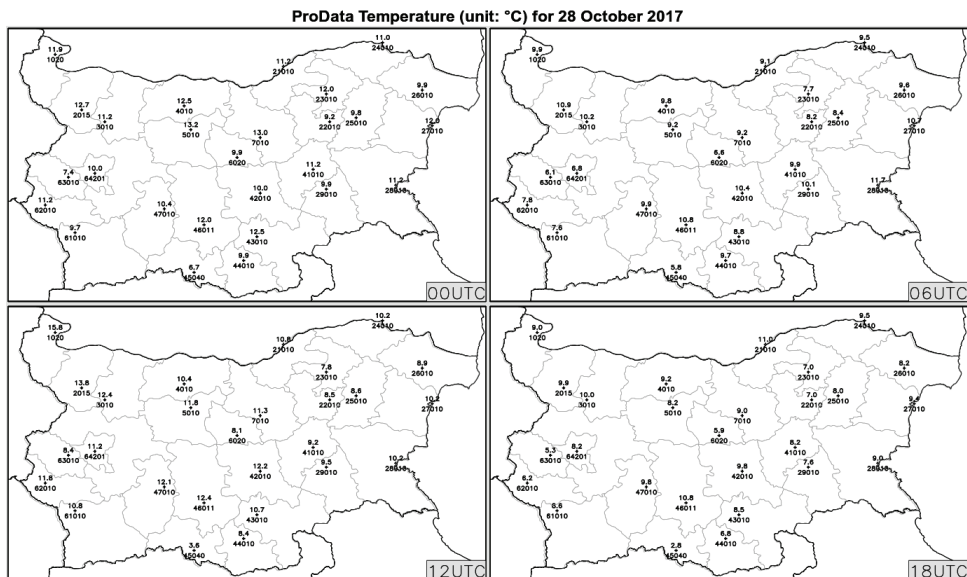


Fig. 5. Temperature in the 27 province centers

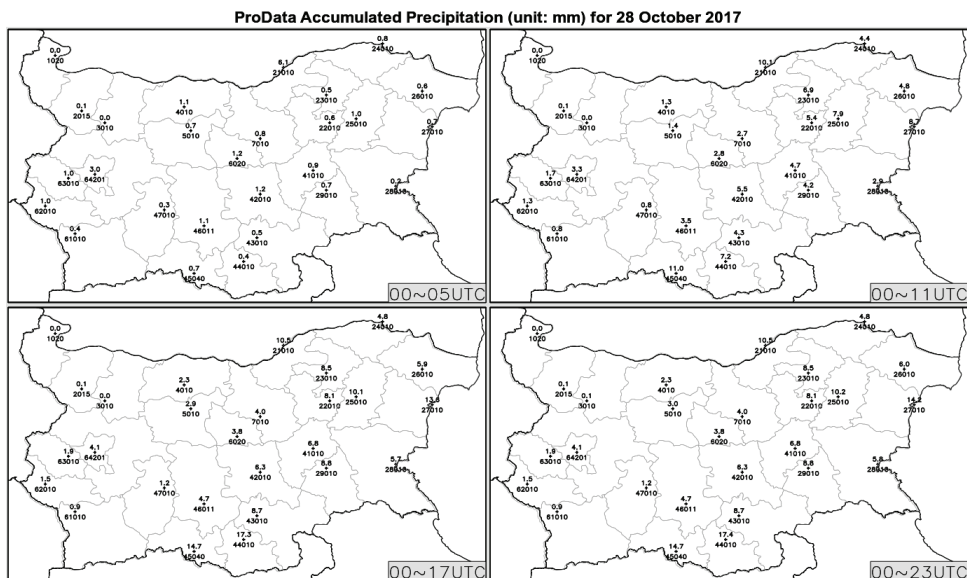


Fig. 6. Precipitation amount in the 27 province centers

The system ProData is also a very convenient source for synoptical and climatological analysis in retrospective manner, including for conducting of hindcast studies. Maps of

the day-by-day mean temperature and precipitation amount, as shown on Figure 7 and Figure 8, are very useful in this sense.

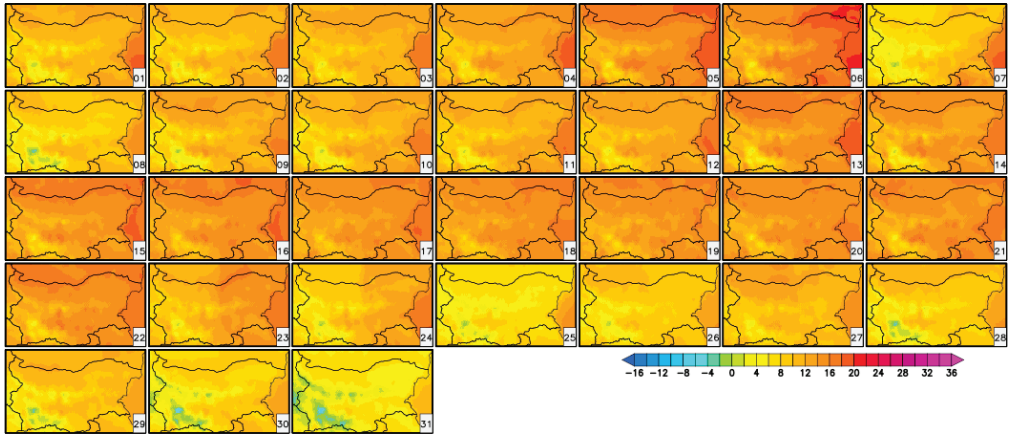


Fig. 7. Daily average temperature for October 2017 (unit: °C)

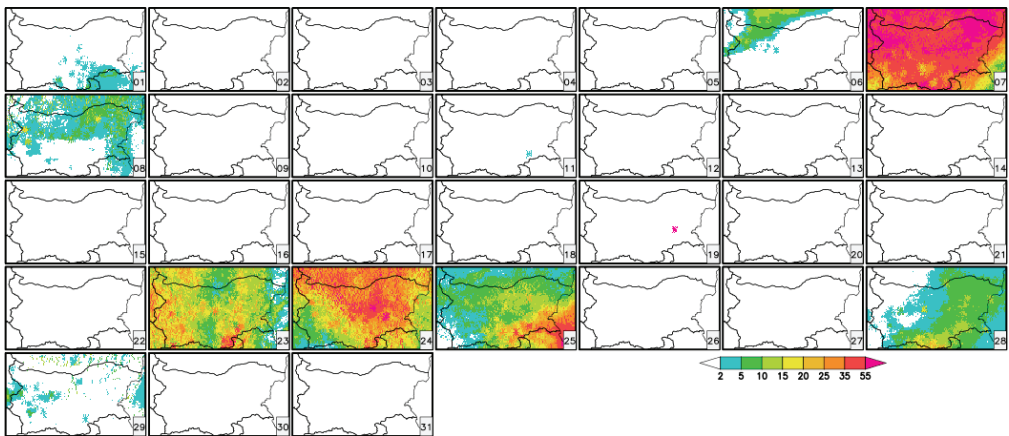


Fig. 8. Daily precipitation amount October 2017 (unit: mm)

A key point in many hindcast studies is to assess the dynamics of the meteorological situation for a certain period of interest. The well-known in the community Grid Analysis and Display System (GrADS), which is used as main graphical pre-processor, provides rich set of built-in functions for spatial and temporal analysis. Thus, with GrADS it is easy to estimate and plot the areal average (AA) of a certain variable as shown on Figure 9.

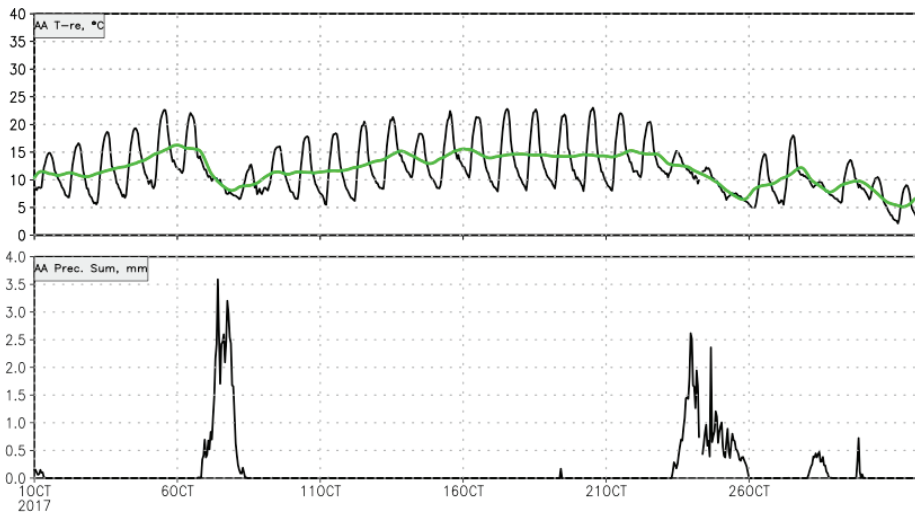


Fig. 9. Monthly chronograms of the AA temperature and precipitation for October 2017

Hence the AA characterizes the domain as a whole, its evolution, unlike the change in a single grid-cell, can be caused only by mesoscale or synoptic reasons. This can be used, in particular, for quick detection of fronts, as illustrated on figure 9: the rapid decrease of the temperature around the 7th October in conjunction with the heavy precipitations over the whole domain, together with the corresponding subplots on figures 8 and 7, suggest passing of a cold front.

It is obvious that the type and quantity of such secondary products can be extended practically with no limits. From at least technical point of view, however, it is reasonable to keep this in certain limits. The authors of the system remain open for any feedback and advice from the community of the end-users.

CONCLUSION

Combining methodological consistency, easy maintenance, transparency and last but not least quick availability of plenty of output data-sets and products, the operative system ProData proves itself as a reliable source of high-quality meteorological information. It is designed as convenient versatile for all, who need single point access of meteorological data in operational mode. Thus, it is used extensively in NIMH-BAS for hydrological short-range forecasts, eventually issuing of warnings. It could be used also in many nowcasting routines for weather forecast activities. Last but not least, ProData is proven to be very robust - practically all cases of failure could be explained with data transfer issues, which are caused by communication problems outside the

system. ProData fills in the gap of information in this time and spatial scale and satisfies the needs of various end-users and experts. The necessary next step in our work is to perform in-depth comparison with independent data, which could be treated as reference. This is expected to be the subject of the second part of this article.

ACKNOWLEDGEMENTS

As far as the study is based on free of charge data and open source software, the authors would like to express their deep gratitude to all institutions (EUMETSAT, H-SAF, Unidata, and all others) and individual enthusiasts. This study would not be possible without their innovative data services and tools.

APPENDIX

Multiple linear regression (MLR) is natural generalization of the simple linear one-dimensional model in case of more than one independent variables. MLR attempts to model the relationship between two or more explanatory variables (“regressors”) and a response variable by fitting a linear equation to observed data. Formally, the model for MLR, given n observations, is:

$$y_i = \beta_0 + \beta_1 x_{i1} + \beta_2 x_{i2} + \dots + \beta_p x_{ip} + \varepsilon_i \quad \text{for } i = 1, 2, \dots, n, \quad (1)$$

where $x_i, i = 1, 2, \dots, p$ are the independent variables. The term ε is called a disturbance term or error variable - an unobserved random variable that adds noise to the linear relationship between the dependent variable and regressors. The $p+1$ parameters $\beta_i, i = 0, 1, \dots, p$ are referred to as partial regression coefficients, which have to be estimated. Equation (1), which is a system of n equations for $p+1$ unknown coefficients, can be rewritten in matrix form as follows:

$$y = X\beta + \varepsilon, \quad (2)$$

where X is a $n \times p$ matrix of the explanatory variables, y is a $n \times 1$ vector of the observations and β is a $p \times 1$ vector of the unknown parameters to be estimated. As far as $p+1 < n$, the linear system in Eq.(2) is overdetermined (i.e. more constraints than variables). Ordinary least squares (OLS) is the simplest and thus most common estimator. It is conceptually simple and computationally straightforward. OLS minimizes the error

$S(\hat{\beta}) = \|y - X\hat{\beta}\|^2$ in meeting the constraint and leads to:

$$\beta = (X^T X)^{-1} X^T y, \quad (3)$$

where β are the estimated regression coefficients. The linear system in Eq. (3) can be solved by means of different methods (e.g. QR- or Cholesky decomposition) including the SWEEP operator as shown in Goodnight (1979) and Neytchev (1995).

REFERENCES

- Artinyan, E. et al., (2016): Flood forecasting and alert system for Arda River basin. *Journal of Hydrology*, 2016, ISSN: 0022-1694
- Barbosa, H. (2012) Usefulness of METEOSAT-9 information for fog top detection in Brazil: first measurements, *Proceedings of WMO/WWRP International Symposium on Nowcasting and Very Short Range Forecasting*
- Bubnová, R., Hello, G., Bénard, P., & Geleyn, J. F. (1995). Integration of the fully elastic equations cast in the hydrostatic pressure terrain-following coordinate in the framework of the ARPEGE/Aladin NWP system. *Monthly Weather Review*, 123(2), 515-535
- Chervenkov, H. (2016) Simple Postprocessing Method for Vertical Correction of Stratified Near-surface Atmospheric Parameters. *Bulgarian Geophysical Journal*, 40, ISSN:1311-753X, 14-22
- Dodson, R., Marks, D., (1997) Daily air temperature interpolated at high spatial resolution over a large mountainous region *Clim Res Vol. 8: 1-20*.
- Engineer Manual 1110-2-1406, Department of the U.S. Army Corps of Engineers. Washington DC, 20314-1000 RUNOFF FROM SNOWMELT, March 1998. (available on-line at http://www.publications.usace.army.mil/Portals/76/Publications/EngineerManuals/EM_1110-2-1406.pdf?ver=2013-09-04-070756-610)
- Goodnight, J. H. (1979) A Tutorial on the SWEEP Operator *The American Statistician Vol. 33, No. 3 (Aug., 1979), pp. 149-158*
- Feidas, H., Karagiannidis, A., Keppas, S. et al. *Theor Appl Climatol* (2014) 118: 133. <https://doi.org/10.1007/s00704-013-1052-4>
- Haylock, M. R., N. Hofstra, A. M. G. Klein Tank, E. J. Klok, P. D. Jones, and M. New (2008), A European daily high-resolution gridded dataset of surface temperature and precipitation for 1950 – 2006, *J. Geophys. Res.*, 113, D20119, doi:10.1029/2008JD010201
- Myers DE (1994) Spatial interpolation. An overview. *Geoderma* 62(1):17-28
- Naldzhyan A., Georguiev O., Artinyan E., (2017): From the sensors to the models, integrated hydro-meteorological systems in NIMH – BAS, Bulgaria, *International Conference on Automatic Weather Stations (ICAWS-2017)*, 24 – 26 October 2017, Offenbach am Main, Germany
- Nedkov, N., et al., (2015): NIMH BG PP10 contribution for the BG - RO common water monitoring and flow forecasting in the CBC region. On-line report. http://danube-water.eu/wp-content/uploads/2015/09/NIMH_4.pdf
- Neytchev, Pl. (1995) SWEEP operator for least-squares subject to linear constraints, *Computational Statistics & Data Analysis*, Vol. 20, Issue 6, 1995, pp. 599-609, ISSN 0167-9473, [https://doi.org/10.1016/0167-9473\(94\)00067-8](https://doi.org/10.1016/0167-9473(94)00067-8).

- Product User Manual-PUM – 03A (Product H03A-PR-OBS-3A) Doc.No: SAF/HSAF/PUM-03A Issue/Revision Index: 1.2 Date: 10/04 /2015 Page: 1/19
available on-line at http://hsaf.meteoam.it/documents/PUM/SAF_HSAF_PUM-03A_1_2.pdf
- Roelevink A., Udo J., Koshinchanov G., Balabanova S., (2010): Flood forecasting system for the Maritsa and Tundzha Rivers, Proceedings of BALWOIS (2010) – Ohrid, Republic of Macedonia – 25, 29 May 2010
- Siewert, C. W., Koenig M., Mecikalski J. R. (2010) Application of Meteosat second generation data towards improving the nowcasting of convective initiation, Meteorol. Appl., 17 pp. 442 - 451 DOI: 10.1002/met.176.
- Turk J.F., G. Rohaly, J. Hawkins, E.A. Smith, F.S. Marzano, A. Mugnai and V. Levizzani, (2000): “Analysis and assimilation of rainfall from blended SSMI, TRMM and geostationary satellite data”. Proc. 10th AMS Conf. Sat. Meteor. and Ocean., 9, 66-69.



Applicability of Gaussian dispersion models for accidental releases in urban environment – results of the “Michelstadt” test case in COST Action ES1006

**Anton Petrov^{1*}, Joana Valente², Kathrin Baumann-Stantzer³,
Ekaterina Batchvarova¹**

¹*National Institute of Meteorology and Hydrology – Bulgarian Academy of Sciences, Sofia, Bulgaria;*
²*CESAM & DAO, University of Aveiro, 3810-193, Aveiro, Portugal.;* ³*Central Institute for Meteorology and Geodynamics (ZAMG) – Vienna, Austria*

Abstract. One of the main research tasks of COST Action ES1006 was testing available dispersion models in order to evaluate their applicability in real situations of accidental gas releases in urban environment. For that purpose, model inter-comparison as well as comparison against test data from wind-tunnel experiments was performed.

Because of the characteristics of the wind flow in urban conditions, such as recirculation and/or blowing through the street canyons, the influence of high buildings and the relatively higher overheating at the surface, the use of more complex models is necessary. When it comes to complexity however, some questions are to be considered:

- What computer resource does the chosen model demand? For emergency response, minimum time for processing the input data combined with maximum output resolution of the pollution field would be a decision for a part of the problem.
- Is the model adequate enough to handle, and to what degree could it represent, the situation of emergency: input/output issues – meteorology, number of sources and receptors, specifics of the pollutant etc.

When Gaussian models were applied for the “Michelstadt” experiment, namely AERMOD, TRACE and ALOHA for the sake of emergency response, a very simplified output was achieved at minimum input requirements. TRACE and ALOHA showed similar sensitivity to wind direction, due to the relatively narrow plume simulated by both models. The best concentration predictions for continuous releases were observed when the wind flow direction was rotated -5°

* anton.petrov@meteo.bg

(5° counter-clockwise in relation to 0° direction). The tests with varying surface roughness (0.5, 0.8, 1.0 and 1.25 m) gave negligible differences both with ALOHA and TRACE.

Being an integrated system, the AERMOD dispersion model is more complex. So, besides the sensitivity to surface roughness, the sensitivity of AERMOD to flow direction and friction velocity values was investigated. Changing the wind direction with -5° and -10° improved the prediction at the near source receptors. Reducing the friction velocity by 71% ($u_* = 0.4$ m/s) compared to the initial one ($u_{*0} = 0.566$ m/s) improved the concentration prediction at the near source receptors and at some distant receptors.

Keywords: air pollution, model evaluation, Gaussian models, accidental releases, wind-tunnel data, sensitivity test.

1. INTRODUCTION

With the process of industry development and urban area spreading, some corresponding changes in the factors that influence dispersion of air pollutants take place. An example for a typical city evolution scenario and its concomitant air pollution problems, is an industrial facility which in a distant time in the past had been situated out of the populated area, but with the city expansion it fell into it. The transition from a rural to an urban canopy with its newly constructed buildings, streets, fittings and installations, modifies the physical conditions which heavily affect the wind speed and especially the wind direction around these obstacles (Britter and Hanna, 2003; Oke, 1996; Venegas et al., 2014). As a result, conditions for downwashing and trapping of pollutants into the so called “street canyons” are created. Furthermore, the modified urban canopy yields micro-climate changes – not only in the examined domain, but in its neighboring areas as well.

Nowadays, an increasing interest in studies and discussions over scenarios involving accidental releases in urban environments takes place (COST ES1006, 2012). The source of such releases could be an industrial accident, fire, explosion or a toxic chemical spill. Buildings and other obstacles disturbing the wind flow are better described by CFD (computational fluid dynamics) and Lagrangian coupled with CFD models which consume larger computational power and time resources, and which are still not practical for use as emergency response tools. On the other hand, Gaussian dispersion models requirements are low, but at the expense of accuracy. In this paper, three Gaussian models – AERMOD, ALOHA and TRACE are examined for emergency response applicability by comparison between model output data and wind-tunnel data.

2. DESCRIPTION OF WIND TUNNEL EXPERIMENT

Within the scope of COST Action ES1006, the large boundary layer wind tunnel facility “WOTAN” at the Environmental Wind Tunnel Laboratory of Hamburg University was used for the experiments. A neutrally stratified model boundary layer flow was generated by a carefully optimized combination of turbulence generators (so-called “spires”) at the inlet of the test section, and a compatible floor roughness.

The extended “Michelstadt” wind tunnel experiment (Fischer et al., 2010) was designed as the first application-specific test case for the validation of local scale emergency response models. The building structure named “Michelstadt” represents an idealized Central-European urban environment. Figure 1 indicates the urban layout that was developed and used for model evaluation. Flow and concentration measurements were carried out in selected relevant locations with a higher density of data close to the ground. Measurements were collected for seven release scenarios corresponding to different point source locations and two different wind directions. Both continuous and short-term (puff) releases were carried out. Flow and concentration data were made available in a first “open” test case for the modeling exercise. In a second “blind” test, only minimum information on inflow data and the emission description were provided to the modelers. For the sake of brevity and for clarity, only the “non-blind” test with continuous releases from one point source (with ID “S2”) is described here.



Fig. 1. “Michelstadt” urban layout developed in the wind tunnel “WOTAN” and used for model evaluation.

3. MODEL RUNS

3.1. Used input data

The input used for ALOHA, TRACE and AERMOD models is given in Table 1. Sensitivity tests with changing of the wind direction (+ / - 5°) were made. The main difficulties with ALOHA and TRACE data assimilation were, that the receptor data could only be entered manually (no batch allowed), which was time consuming.

Table 1. Used input for ALOHA, TRACE and AERMOD

<i>Source input – continuous release</i>	
Type of pollutant	C ₂ H ₆ (ethane)
Source locations (x, y, z)	Source “S2” at (0.0, 0.0) m for ALOHA and TRACE, and (-361.9, 125.1) m for AERMOD
Source diameter	1.575 m (TRACE, AERMOD)
Source volume flow rate	0.4 m ³ s ⁻¹ (ALOHA, AERMOD)
Source mass flow rate	0.5 kgs ⁻¹ (TRACE, AERMOD)
Temperature of the source’s exit gas, T	293.15K
<i>Receptor input</i>	
Discrete receptor locations	Taken from database and transformed to meet the source locations (ALOHA, TRACE) or left as they are (AERMOD)
Receptors flagpole height	7.5 m for TRACE and AERMOD and 0.0 m for ALOHA
Receptor grid origin	ALOHA and TRACE: Coincides with the source; AERMOD: (x,y) = (0.0, 0.0) m – the center of Michelstadt domain
<i>Meteorological input</i>	
Wind velocity at 9 m height	2,7 ms ⁻¹
Wind direction at 9 m height	270.0° (sensitivity tests: -5°, +5° – counter-clockwise and clockwise rotation in relation to 270° direction accordingly)
Ambient temperature at 2 m height	293.15 K
Relative humidity	50 %
Surface roughness length	0.8 m (sensitivity tests in the 0.8 – 1.2 m interval show almost no change in output)
Pasquill stability class	D (Neutral)(ALOHA, TRACE)
Inversion height options	Set to “No inversion” (ALOHA, TRACE)
Monin-Obukhov similarity (AERMOD)	u _* = 0.35, 0.4 , 0.45, 0.5 and 0.566 ms ⁻¹

TRACE always sets the x coordinate axis downwind the source, so in order to make wind change sensitivity tests in absolute coordinates, the rotation matrix (Eq. 1) had to be applied:

$$\begin{pmatrix} x' \\ y' \end{pmatrix} = \begin{pmatrix} \cos \theta & -\sin \theta \\ \sin \theta & \cos \theta \end{pmatrix} \begin{pmatrix} x \\ y \end{pmatrix} \quad (1)$$

where $\theta = +/ - 5^\circ$ is the angle of rotation. As a result, any change of coordinates in that manner yields the need of additional receptor input for the TRACE model.

Neither ALOHA nor TRACE need vertical wind profiles for the meteorological input (Reynolds, 1992; Thoman et al, 2006). The wind speed value of 2.7 ms^{-1} (at 9 m reference height, in full scale) was taken from the vertical wind profile database, situated in Michelstadt domain at coordinates $(-450, 112.5)$ – see “Profile 2” location on Figure 2). This point would be the most representative for the meteorological input, since it was within the domain, and the wind direction at that point was not directly influenced by any situated buildings in the vicinity. Another advantage was, that the point was close to the source “S2”, (coordinates $-361.9, 125.1$).

AERMOD requires vertical wind and temperature profile data in a separate file (e.g. “aermod.pfl”). The profile may be consisted of data which is limited to as little as one layer (e.g. the temperature and wind at 2 m height only), but the more detailed the data is (if available), the more accurate the output results would be. The sensitivity tests made were more extended: -10° , -5° , $+5^\circ$, and $+10^\circ$ for the wind direction, 0.566 ms^{-1} (100% u_{*0} – the approach flow friction velocity scale), 0.5 ms^{-1} (88% u_{*0}), 0.45 ms^{-1} (80% u_{*0}), 0.4 ms^{-1} (71% u_{*0}), and 0.35 ms^{-1} (62% u_{*0}) for the friction velocity scale, and 0.5, 0.8, 1.0, 1.25 and 1.5 m for the surface roughness z_0 . Here, only the cases with $u_{*0} = 0.4 \text{ ms}^{-1}$ and $z_0 = 0.8 \text{ m}$ are shown, since they have the best match with the wind tunnel measured data.

3.2. Performance of the models

Developed for emergency response, both ALOHA and TRACE had almost instantaneous output for an arbitrary receptor when run under Windows 7 OS on a i3 dual core machine with 4GB RAM. The only impediment was when larger number of receptors were needed for examination. For TRACE, there is limitation to 20 receptors for a model run. One very good feature of the model is the option to perform sensitivity tests for various parameters (surface roughness, stability, etc.), except for wind direction variations. For ALOHA, coordinates for only one receptor can be given as an input for a model run. However, there is an option to see the concentration of the pollutant at any point interactively.

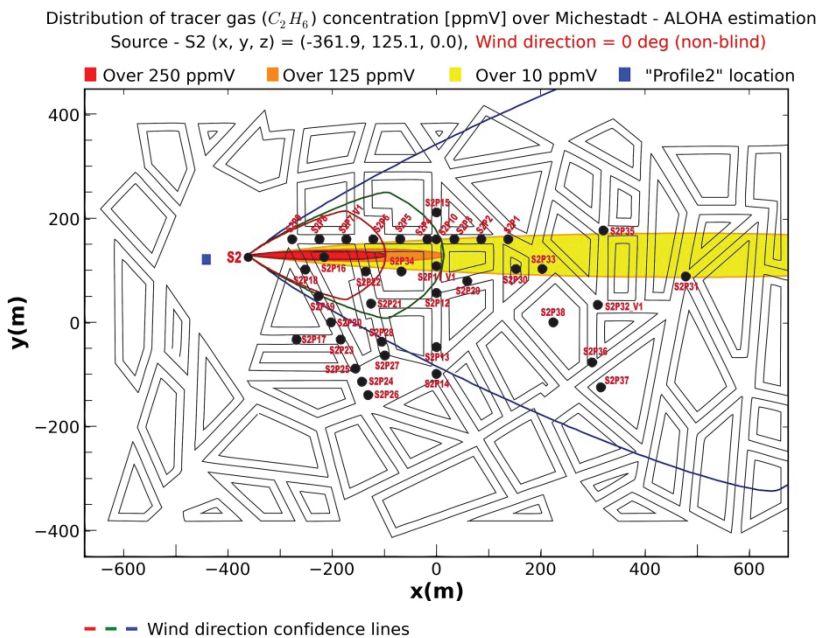
AERMOD has instantaneous output as well, with the difference that the model allows setting of receptor grid with an arbitrary resolution, and the number of discrete

receptors to be defined could be practically unlimited. AERMOD is an open source model. It could run on any Windows or Linux machine. Since the model is intended for regulatory purposes it has some limitations in its use as an emergency response tool: it cannot handle short term (“puff”) releases, as its minimal temporal resolution is 1 hour, and the input data files preparation is time consuming.

4. OUTPUT RESULTS, DATA COMPARISON AND STATISTICS

4.1. ALOHA

On Fig. 2 ALOHA’s outputs for continuous releases are shown for three cases. Figure 2 (top) shows the “ordinary” (0°) non-blind scenario, Fig. 2 (middle and bottom) – the wind direction change sensitivity (-5° and $+5^\circ$) test outputs. The contour lines colored in red, green and blue are the wind direction confidence lines. They show the possible mean concentration of the pollutant within the area enclosed by them in case, that wind direction fluctuations in the $\pm 30^\circ$ interval occur.



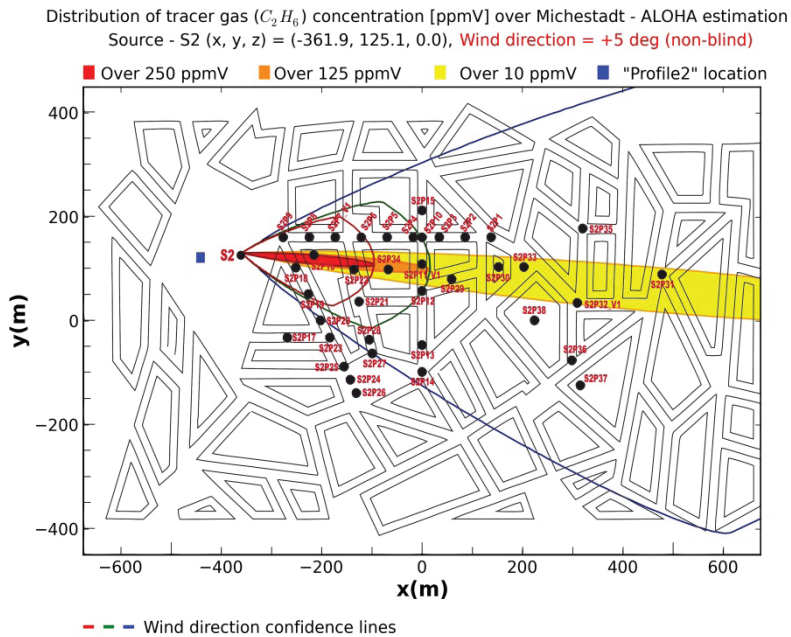
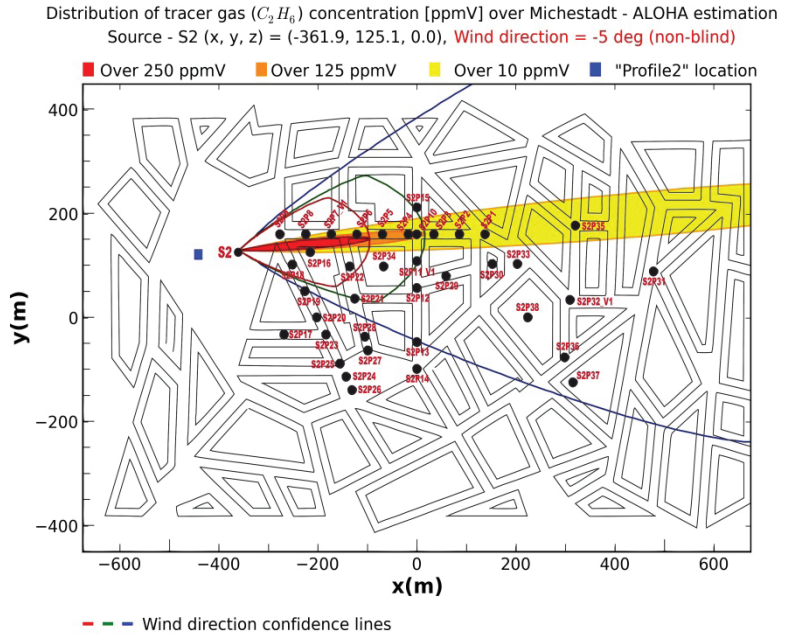


Fig. 2. Wind direction sensitivity of ALOHA; top is for 0° ; middle for -5° ; and bottom for $+5^\circ$

For the puff releases, the picture would be the same with the reservation that the displayed values of the concentration of the pollutant are relevant to the *peak* concentration.

The comparison between the images which show the distribution of the pollutant reveals very high sensitivity of the model to wind direction change. This becomes even more obvious if we take a look at the graphical expression of the comparison between the three specific cases on Fig. 3:

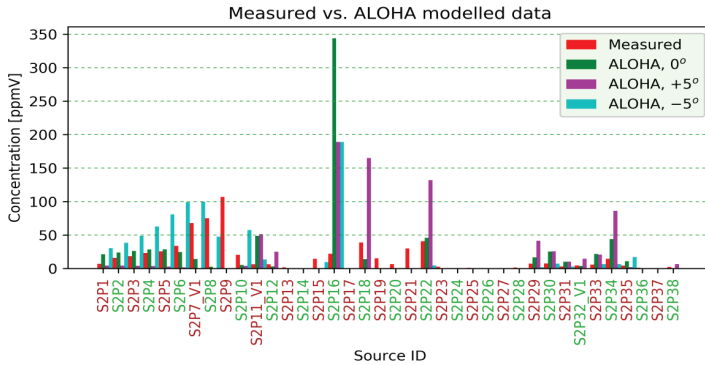


Fig. 3. Comparison between ALOHA’s estimated (0°, +5° and -5°) and wind tunnel measured concentrations [ppmV] for source S2

Interesting situation occurs at point S2P16. It is located exactly downwind the source S2, at the centerline of the plume, and therefore the highest pollutant concentration is observed there. The +5° and the -5° wind direction sensitivity tests show identical results due to distribution symmetry. The estimate concentrations for the receptor point S2P9 which is the closest to the source S2, show values near to zero. If we look at Fig. 2, we could see that the width of the plume is very small, hence the receptor point S2P9 is very weakly affected by the source. The same goes for the points S2P2 to S2P10, in the case when the wind direction is slightly rotated clockwise (+5°), and for S2P18, S2P19, S2P21, and S2P22 in the counter-clockwise rotation (-5°) case. Only the results of S2 receptor set are discussed here, for the reason that it involves the largest number of receptors and covers the largest area of the Michelstadt domain.

One of the best ALOHA model’s output features that come in handy, are the wind direction confidence lines. Even though not directly, they can show that the point S2P9 mentioned above could get into a zone with pollutant concentration exceeding 250 ppmV.

The statistical performance measures (SPM) used in the comparison were:

$$FB = \bar{c}_0 - \bar{c}_p / 0.5(\bar{c}_0 + \bar{c}_p) \quad (2)$$

$$\text{NMSE} = \overline{(c_0 - c_p)^2} / \overline{c_0 c_p} \quad (3)$$

$$R = \overline{(c_0 - \bar{c}_0)(c_p - \bar{c}_p)} / \sigma_{c_0} \sigma_{c_p} \quad (4)$$

$$\text{FAC2} : 0.5 \leq c_0 / c_p \leq 2.0 \quad (5)$$

where FB is the fractional bias, NMSE – the normalized mean square error, R – the correlation coefficient, FAC2 – the fraction of predictions within a factor of two of observations, c_o and c_p are the wind tunnel and modeled concentrations respectively, and σ_{c_o} and σ_{c_p} – their corresponding standard deviations. The four SPM for ALOHA are shown in Table 2:

Table 2. ALOHA statistics for continuous releases

SPM	Wind direction	0°	-5°	+5°
NMSE		10.23	4.22	6.62
R		0.06	0.32	0.14
FB		-0.19	-0.27	-0.23
FAC2 (%)		21.05	15.79	2.63

According to statistics, the best match between measured and modeled data for the source S2 is observed in the case of wind direction shifted with -5° (counter-clockwise rotation).

4.2. TRACE

On Fig. 4. the graphical output for a continuous release provided by the TRACE model is shown, and on Fig. 4 - for the three cases involving wind direction sensitivity tests (plotted with Python 2.7.5 Matplotlib library; Tosi, 2009). TRACE supports pollution dispersion modeling for a horizontal plane, situated at any arbitrary height (ALOHA makes this only at ground level $z = 0.0$ m). For that reason, the statistical analysis for S2 includes the receptors situated on different flagpole heights (S2P7_V2 – S2P7_V7, S2P11_V2 – S2P11_V7, S2P32_V2 – S2P32_V5).

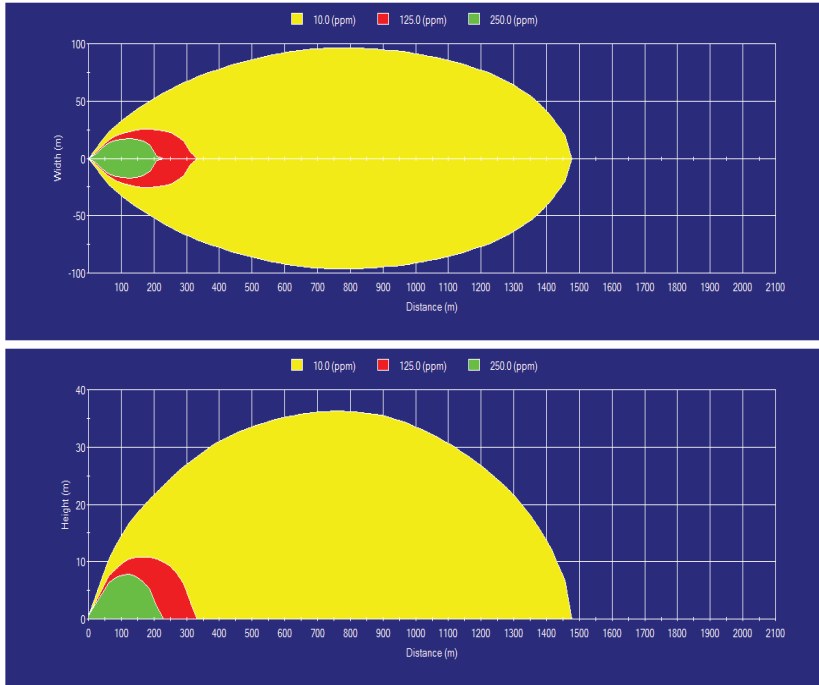
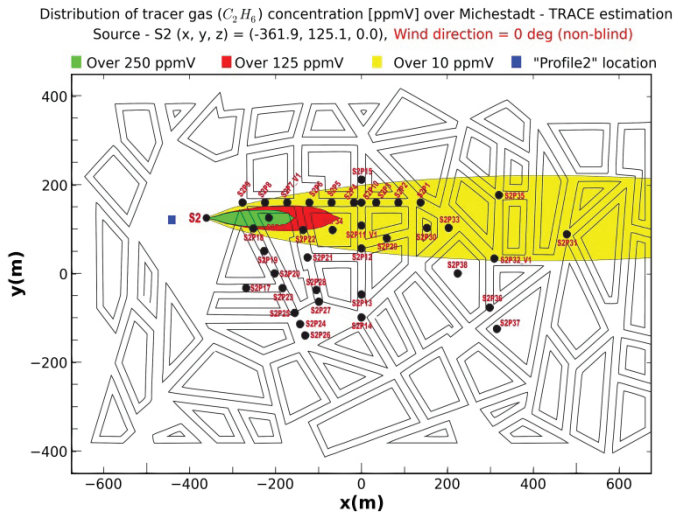


Fig. 4. TRACE direct graphical output (horizontal and vertical plane)



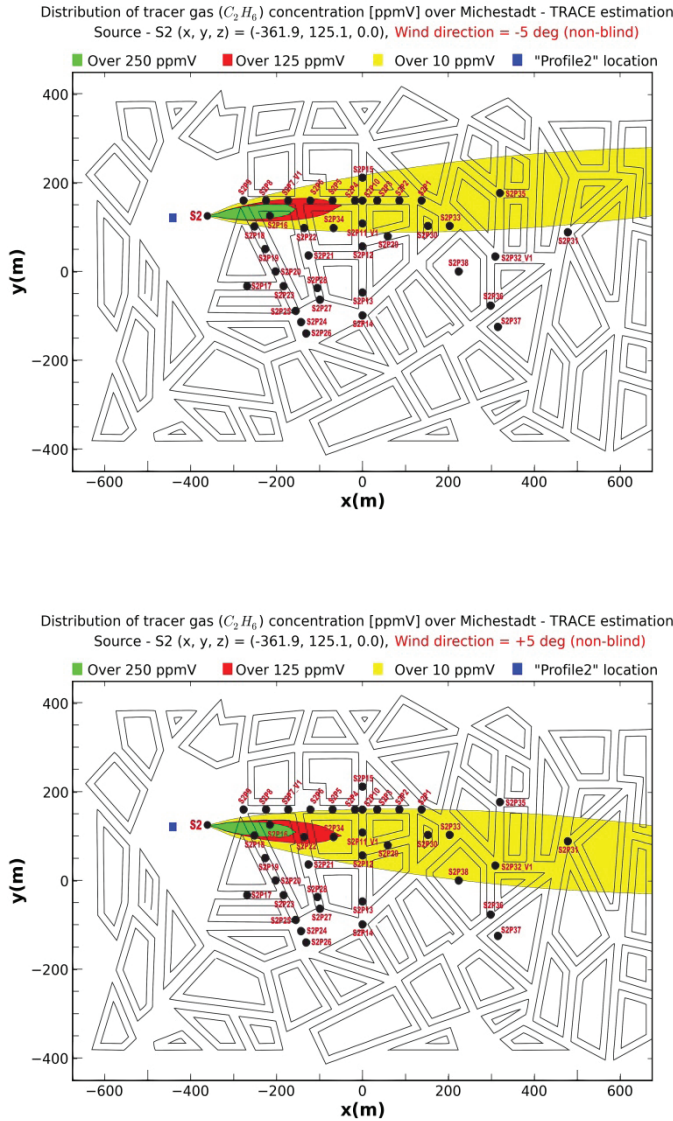


Fig. 5. Wind direction sensitivity of TRACE; top is for 0° ; middle for -5° ; and bottom for $+5^\circ$

As seen on Fig. 5 the path of the plume generated by TRACE is slightly wider than the one by ALOHA. On the comparison chart (Fig. 6), however, almost the same pattern of the estimated concentrations is observed. The receptor point S2P9 stays away from the direct influence of the plume, with concentrations of pollutant close to 0 ppmV, and a maximum of the concentration is observed at S2P16 for wind direction 0° . At the latter point, the pollution level estimates for wind directions $+5^\circ$ and -5° are equal, i.e.

we have the same distribution symmetry as with ALOHA. Generally, for the S2 source-receptor set, the best match between measured and estimated concentrations, has the case with the -5° wind direction. It has the highest correlation coefficient (R) (Table 3) and the lowest normalized mean square error (NMSE). Even though the fractional bias (FB) is the highest (-0.47), the difference of its values between the cases is not that big judging by their distance from the ideal value – zero.

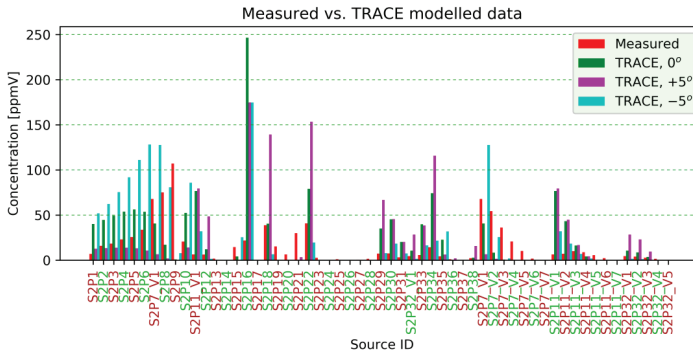


Fig. 6. Comparison between TRACE’s estimated (0° , $+5^\circ$ and -5°) and wind tunnel measured concentrations [ppmV] for source S2

Table 3. TRACE statistics for continuous releases

SPM	Wind direction	0°	-5°	$+5^\circ$
NMSE		4.83	3.77	5.71
R		0.17	0.47	0.09
FB		-0.41	-0.47	-0.35
FAC2 (%)		15.79	12.28	17.54

TRACE provides outputs for dosage and puff duration (ALOHA v5.4.4 provides dosage output only in the version intended for work under the MacOS).

4.3. AERMOD

The surface friction velocity u_* of the wind tunnel’s approach flow is calculated from its mean kinematic turbulent flow data and it appears to be 0.566 ms^{-1} . However, over the Michelstadt domain, due to presence of buildings, the surface roughness z_0 and therefore u_* undergo some modifications. As a result, the approach flow vertical wind profile does not correspond to the one observed over Michelstadt. This is the reason for

the additional sensitivity tests made with AERMOD for varying values of u_* and z_0 for the urban area.

A picture of the pollution field over Michelstadt according to AERMOD model estimations is shown below (Fig. 7). Since the source of tracer gas is situated at ground level ($z = 0.0$ m) and the receptor grid flagpole height is 7.5 m, there is a white spot observed at the source location – an absence of pollutant, due to the specifics of the AERMOD concentration distribution, a vertical section of which can be seen on Fig. 8.

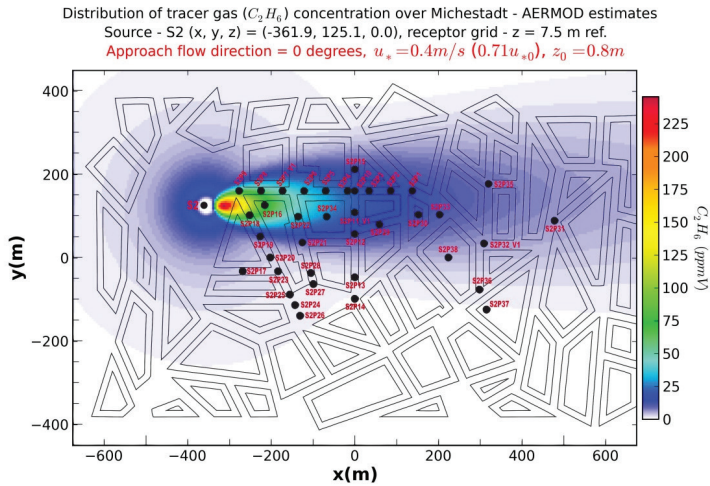


Fig. 7. AERMOD estimated concentration distribution of ethane over Michelstadt

The difference between the pollution distributions modeled by AERMOD and the other two models could be easily noticed. In the represented by AERMOD concentration field on Fig. 7, the pollutant tends not only to spread in the direction of the wind, but to disperse in all directions as well. The drag generated by the surface disturbs and slows down the transport of the pollutant near the ground, resulting in a plume with irregular shape in the vertical plane (Fig. 8). The bar graph (Fig. 9) shows very good match between observed and modeled concentrations, especially for the case with -5° (counter-clock rotated) wind direction, which is as well confirmed by the statistical performance measures (Table 4).

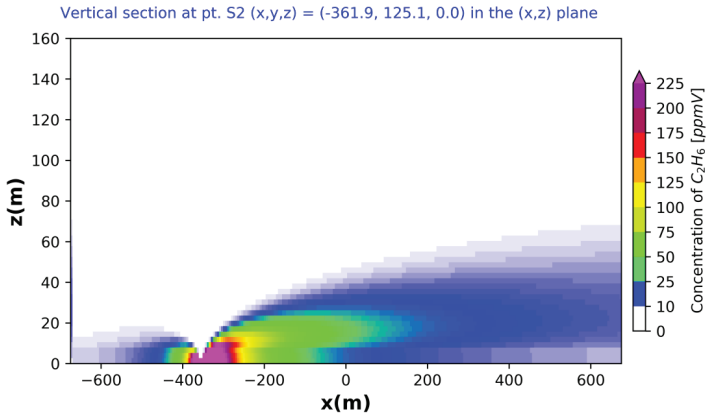


Fig. 8. AERMOD estimated concentration distribution of ethane – a vertical section.

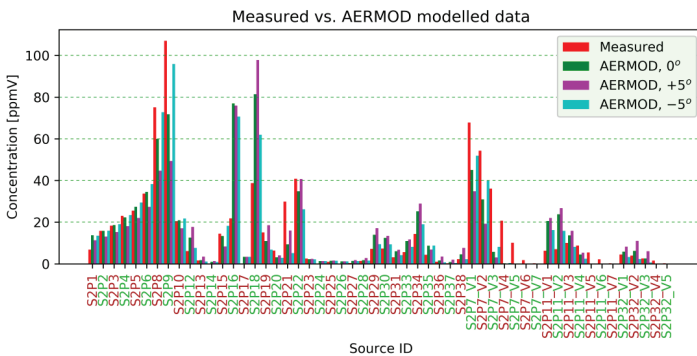


Fig. 9. Comparison between AERMOD's estimated (0°, +5° and -5°) and wind tunnel measured concentrations [ppmV] for source S2

Compared to ALOHA and TRACE AERMOD shows significantly lower sensitivity towards wind direction change. An obvious reason for that could be the wider plume path modeled.

Table 4. AERMOD statistics for continuous releases

SPM	Wind direction	0°	-5°	+5°
NMSE		0.88	0.85	1.45
R		0.76	0.86	0.61
FB		0.01	0.05	0.04
FAC2 (%)		51.85	55.56	40.74

5. CONCLUSIONS.

Gaussian models are still in use despite their simple output. Moreover, some of them are perfected to a degree at which they can be used for urban air pollution modeling where buildings are to some extent taken into account. AERMOD for example has the PRIME algorithm implemented which handles the building downwash effects. ALOHA is designed to calculate the indoor pollution, and handles heavy gas dispersion. Both ALOHA and TRACE include an intuitive user friendly GUI wizard which leads the user step by step to a successful scenario setup in a very short time. From a statistical point of view however, the performance of ALOHA and TRACE confronted with the measured data was very poor. Nevertheless, these two models, with some reservations, could be used as emergency response tools in densely built environments, especially in the cases when they are applied in areas where the count of one to three story buildings is predominant.

AERMOD showed very good results in this particular study. Some GUI wrapped commercial versions of the model could decrease the input data preparation time to an extent at which it could be used as an emergency response model though it is a regulatory one. The open source version of the model armed with the suitable script and batch processing inventory could shrink the preparation time as well.

ACKNOWLEDGEMENTS

This research was supported by COST Action ES1006. We thank our colleagues from the workgroups who provided insight and expertise that greatly assisted the research, although they may not agree with all of the interpretations and conclusions of this paper. We are grateful to all of those with whom we have had the pleasure to work during this and other related projects. The final results and publication are supported by “Urban Air Pollution Modeling” project, sponsored by the Program for Young Scientists and Scholars - 2017 of the Bulgarian Academy of Sciences.

REFERENCES

- Britter, R.E., Hanna, S.E. (2003): Flow and dispersion in urban areas. *Annual Rev. Fluid Mech.* 35, 469-496.
- COST ES1006 (2012): Background and Justification Document, COST Action ES1006, May 2012, University of Hamburg, Meteorological Institute, Bundesstraße 55, D – 20146 Hamburg, Germany. ISBN: 3-00-018312-X.
- Fischer, R., Bastigkeit, I., Leidl, B., Schatzmann, M. (2010): Generation of spatio-temporally high resolved datasets for the validation of LES-models simulating flow and dispersion phenomena within the lower atmospheric boundary layer. *Proc. 5th International Symposium on Computational Wind Engineering (CWE2010)*, Chapel Hill, North Carolina, USA.
- Oke, T.R. (1996) : *Boundary Layer Climates*, second ed. Routledge, London.
- Reynolds, M.R. (1992): ALOHA TM (Areal Locations of Hazardous Atmospheres) 5.0 Theoretical Description, Seattle Washington 98115
- Thoman, D. C., O’Kula, K. R., Davis, M. W., Knecht, K. D. (2006): Comparison of ALOHA and EPIcode for Safety Applications, Washington Safety Management Solutions, LLCWSMS-TR-05-0020 / LA-UR-05-8594
- Tosi, Sandro (2009): *Matplotlib for Python Developers*, Packt Publishing Ltd., 32 Lincoln Road, Olton Birmingham, B27 6PA, UK. ISBN 978-1-847197-90-0
- Venegas, L.E., Mazzeo, N.A., Dezzutti, M.C. (2014): A simple model for calculating air pollution within street canyons. *Atmospheric Environment* 87 (2014) 77 – 86, Elsevier Ltd., 2014.



In remembrance of

George Djolov

(05.08.1940 – 07.11.2017)



On 7 November 2017, the Bulgarian meteorological community lost a respected and beloved colleague – Prof. George Djolov.

George Dimitrov Djolov was born on 5th August 1940 in Sofia. He graduated in physics, specialization meteorology at the Faculty of Physics, Sofia University. For his studies in USSR (Leningrad) and Canada (Waterloo), he received two doctoral degrees, first one in Physics and Mathematics, and second one in Mechanical Engineering. Since 1969, he was working for more than 15 years at the Institute of Hydrology and Meteorology at the Bulgarian Academy of Sciences (BAS).

He was the founder and first Director of the Institute of Ecology at BAS in 1989. During 1990 he was Senior Advisor to the Commission for Conservation and Reproduction of the Natural Environment in Bulgaria and was Chair of the World Federation of Engineering Organizations (WFEO's) Committee on Engineering and Environment. During this period G. Djolov had a close working relationship with the Energy and Climate Task Force of the International Institute for Applied Systems Analysis (IIASA). Later, he left Bulgaria and settled in Africa where he first served as co-ordinator of the Bachelor of Technology Programme in Applied Physics at the University of Zimbabwe. In 1996 G. Djolov was appointed as Professor and Chair of Physics, and thereafter Dean of the School of Mathematics and Natural Sciences at the University of Venda. In 2003, the University of the North (now Limpopo) appointed him as Professor and Director of the Faculty of Physical and Mineral Sciences. For two years thereafter, ending in 2006, he served as chief executive officer of the National Community Water and Sanitation Training Institute in Polokwane (then Pietersburg).

After his formal retirement in 2007, Professor George Djolov joined the University of Pretoria as a meteorologist and Extraordinary Professor in the Department of Geography, Geoinformatics and Meteorology. In his final three years he managed the University of Pretoria's Laboratory for Atmospheric Studies, with the primary role to support research and student supervision in the field of air quality management.

In 2015, the International Eurasian Academy of Sciences honoured Prof. George Djolov for his distinguished career and contribution to science.

The scientific interests of Prof. G. Djolov were in the fields of: atmospheric boundary layer and turbulent diffusion; modeling of air pollution; transport of radioactive and chemical compounds in the atmosphere at long, meso- and local scales; different aspects of ecological issues. He published more than 100 scientific articles in Bulgarian and international journals and conferences, and was coauthor of several books. He was also a member of the Editorial Board of the international journal of Urban Climate.

During his career in Bulgaria Prof. G. Djolov was a scientific consultant and supervisor of many colleagues-meteorologists from the Institute of Hydrology and Meteorology and the Institute of Geophysics at BAS. He was known for his restless and searching spirit in scientific development and readiness to give advice. We will remember him with his cheerful and open character, sense of humor and teasing.

A deep bow to his bright memory!



Ekaterina Batchvarova
Tatiana Spassova